MANNED SPACE-FLIGHT EXPERIMENTS

INTERIM REPORT

GEMINI IX MISSION

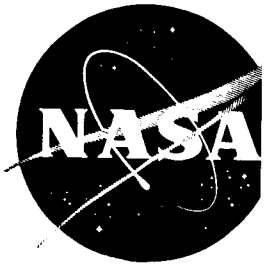

NATIONAL AERONAUTICS AND SPACE ADMINISTRATION

WASHINGTON, D. C.

November 1, 1966

FOREWORD

This compilation of papers constitutes an interim report on the results of experiments conducted during the Gemini IX manned space flight. The results of experiments conducted on earlier flights have been published in similar interim reports which are available on request from the MSC Experiments Program Office, Houston, Texas (Code EX).

Seven experiments were scheduled on this mission. Four were designed to obtain basic scientific knowledge, one was medical in nature, and two were of technological import. Four of the experiments had been flown on previous flights; three were scheduled for the first time. The results of the experiments are presented in the following papers with comments on the effects of the unforeseen fatigue factors of extravehicular activity and the limitations incurred by the failure of the augmented target-docking adapter shroud to jettison.

It should be noted that this report is published to provide an early report and quick dissemination of Gemini IX experiment results, even though some of the results are tentative and incomplete. Some data have not been analyzed, and some experiments depend on a summation of data from other flights with the data from this flight. The purpose of this report, as stated, is to provide interim information.

CONTENTS

1. EXPERIMENT S-1, ZODIACAL LIGHT PHOTOGRAPHY

By E. P. Ney, Ph. D., and W. F. Huch, Ph. D.
University of Minnesota

OBJECTIVES

The purpose of Experiment S-1, Zodiacal Light Photography, was to obtain 30-second exposures at f/1 of several objects of astronomical interest. These include the airglow (viewed in profile from above), the zodiacal light, and the Milky Way.

EQUIPMENT

The camera was designed to view a wide-angle field (approximately 50° by 130°). Mechanically, it was the same kind of camera as the one flown on the Gemini V and Gemini VIII missions. The exposure sequence was automatic, and it alternated 30-second exposures with 10-second off-periods. During the off-periods, thrusters could be fired without exposing the film. The film was 35-mm black and white with a speed of 400 ASA.

PROCEDURE

The original flight plan called for the camera to be handheld during extravehicular activity and to be used on the nightside pass just before ingress. However, because of the visor fogging difficulties, the extravehicular operation of the camera was abandoned. Subsequently, the crew carried out the experiment from inside the spacecraft, photographing through the pilot's window. The pilot held the camera in the window during the exposures, sighting past the camera and directing the command pilot to maneuver to the appropriate position. The pilot turned the camera off between successive exposures. The astronomical objects were not in the command pilot's view, and his role was to null the spacecraft rates.

RESULTS

The procedure adopted by the crew resulted in obtaining 17 very good photographs. They are listed as follows:

Exposure number	Orientation	Object
1	North	Horizon airglow
2, 3	West	Horizon airglow
4, 5	South	Horizon airglow and aurora
6, 7	East	Horizon airglow
8, 9, 10, 11	Northeast	Milky Way
12, 13, 14	East	Horizon airglow
15, 16, 17	East	Airglow, zodiacal light, twilight

Exposure 9 is shown in figure 1-1. This figure is a copy of a photograph of the Milky Way with Cygnus in the center. The airglow layer shows to the right of the spacecraft. The bright spot at the upper right was caused by moonlight. Exposure 15 is shown in figure 1-2. This figure is a copy of an overexposed print to emphasize the zodiacal light, airglow, and stars.

CONCLUDING REMARKS

The negatives are being studied using an isodensitracer to produce intensity isophotes. The following data will be obtained:

(1) Intensity distribution of the zodiacal light, both morning and evening

(2) The height and intensity of the airglow at various geographic positions

(3) Intensity distribution of the Milky Way in the region of the sky near Cygnus.

In addition, a previously unreported phenomenon was discovered. This phenomenon appears as an upward extension of the normal 90-kilometer airglow layer. The extension is in the form of wisps or plumes about 5° wide and extending upward about 5°. The plumes appear in the east and are almost certainly not due to aurora. The phenomenon is believed to be truly in the sky, but a number of tests will be made to determine this point.

The experiment is considered an unqualified success, and the crew must be given credit for making an excellent program for the experiment after the extravehicular performance was terminated.

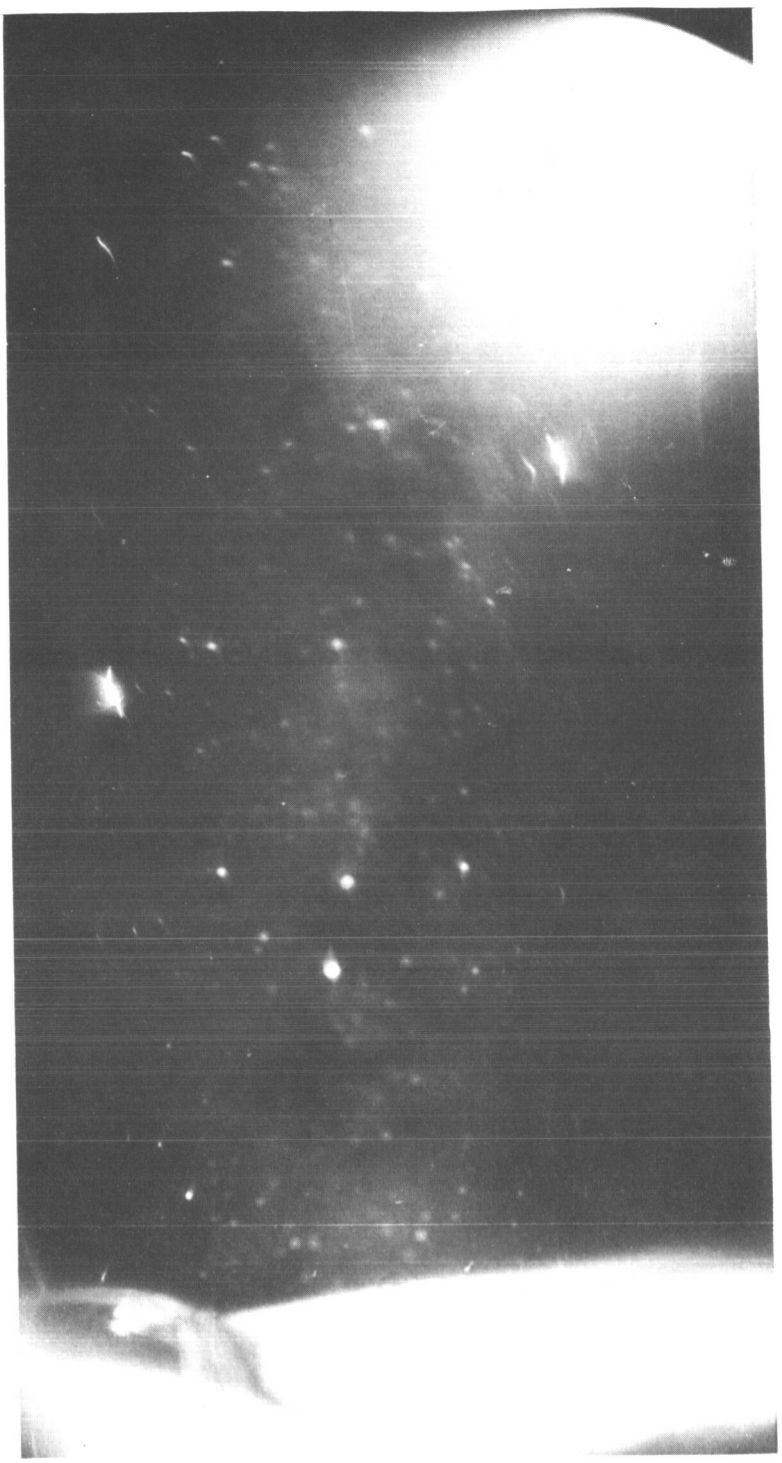

Figure 1-1.- Experiment S-1, photograph of Milky Way.

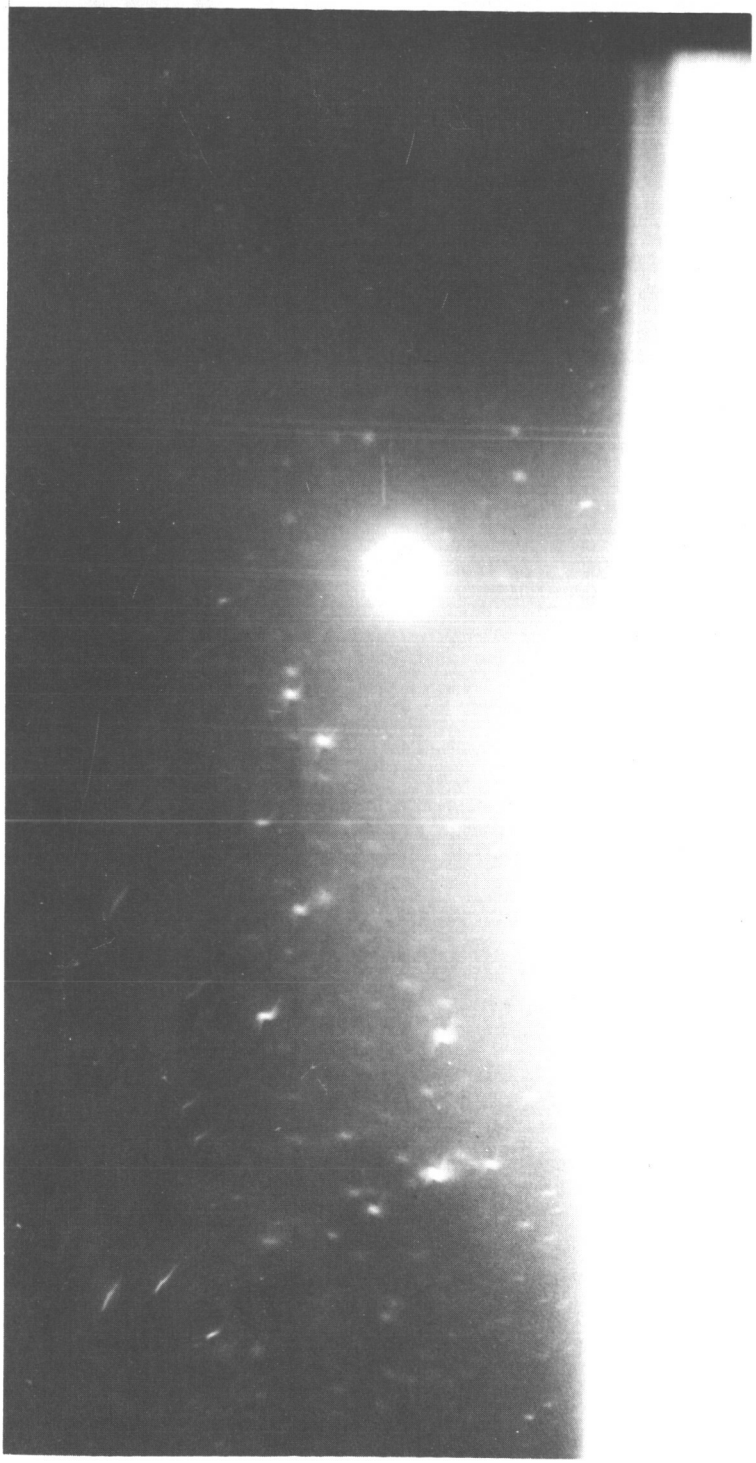

Figure 1-2.- Experiment S-1, photograph of zodiacal light.

2. EXPERIMENT S-10, AGENA MICROMETEORITE COLLECTION

By Curtis L. Hemenway, Ph. D.
Dudley Observatory

OBJECTIVE

The S-10 experiment was designed to provide, with a 2- to 4-month space exposure, the following data:

(1) Micrometeorite cratering effects on selected highly polished surfaces

(2) Collection of small micrometeorites at orbital altitudes by various thin films and soft plastics

(3) Lethal effects of the space environment on selected micro-organisms.

EQUIPMENT

The S-10 micrometeorite collector is illustrated in figure 2-1. The four outer cratering surfaces are visible on the top of the unit. The hardware measures 5-1/2 by 6-1/4 by 1 inches and weighs approximately 4 pounds loaded for flight. The surfaces are of highly polished stainless steel with six small circular depressions cut in one plate for seeding and space exposure of micro-organisms. The micro-organisms used on the outside of the package were T_1-bacteriophage, Penicillium roqueforti spores, and Bacillus stearcthermophilus spores. The experiment hardware was located on the target-docking adapter (TDA) of the target vehicle as shown in figure 2-2.

PROCEDURE

The loaded experiment hardware was hand-carried to Kennedy Space Center and mounted on the TDA at approximately T-24 hours. The protective plastic-film cover was removed at T-6 hours, just prior to removal of the access tower. After launch, the Atlas vehicle malfunctioned, and the Agena target vehicle did not achieve orbit. The experiment hardware was, therefore, lost.

Another S-10 unit was prepared, hand-carried to Kennedy Space Center, and mounted on the augmented target-docking adapter (ATDA) for the Gemini IX-A mission. The unit was mounted at T-24 hours and the protective cover was removed at T-6 hours.

After completion of the rendezvous maneuver, it was determined that extravehicular activity to the ATDA would not be possible because of the failure of the ATDA shroud to jettison. Figure 3-3 is an in-flight photo showing the S-10 unit in place on the ATDA.

RESULTS

The outer surfaces visible on the S-10 unit in figure 2-3 appear to be in good condition. However, since they could not be returned for study, no results were obtained from the S-10 experiment during Gemini IX.

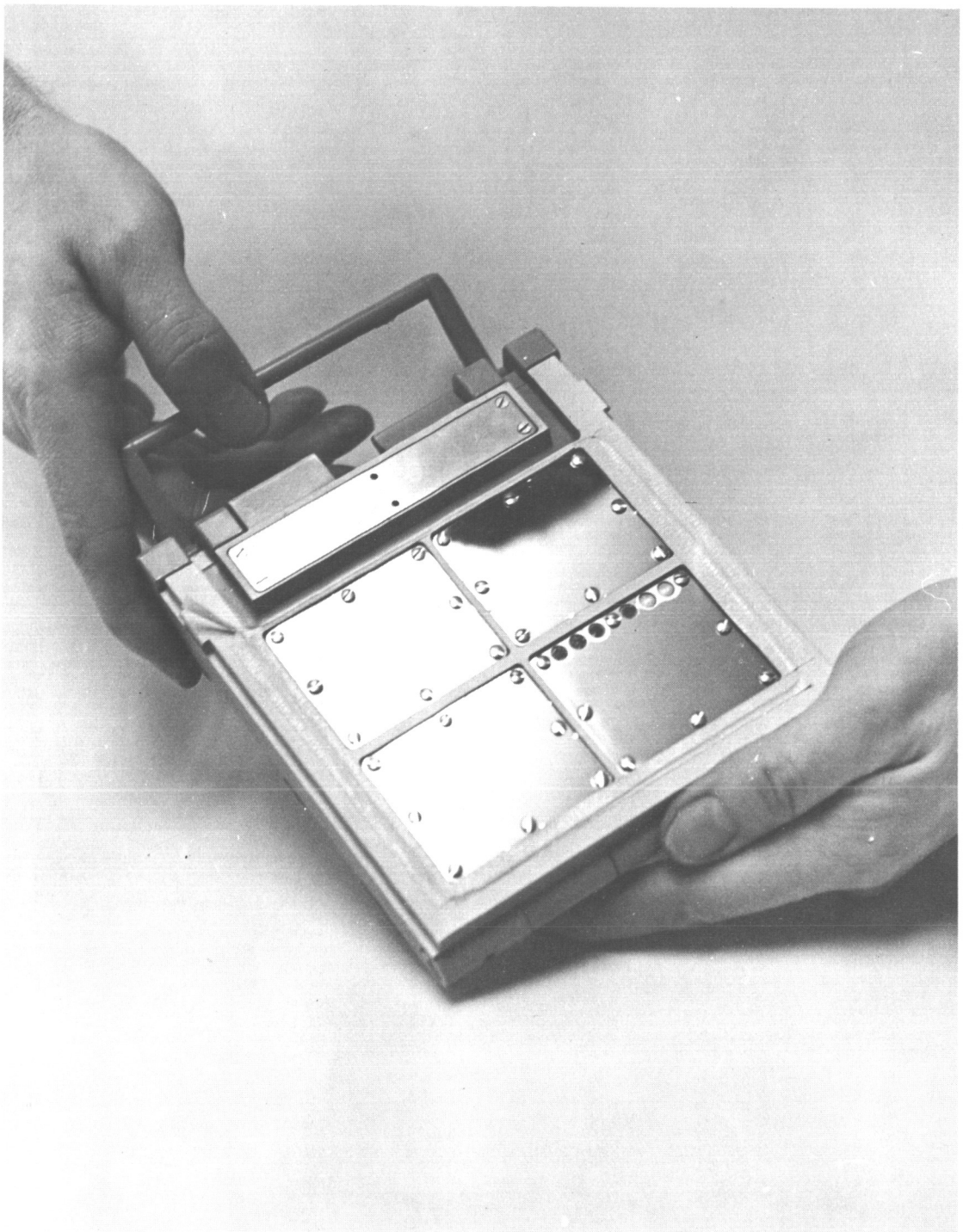

Figure 2-1.- S-10 micrometeorite collector.

NASA-S-65-9617

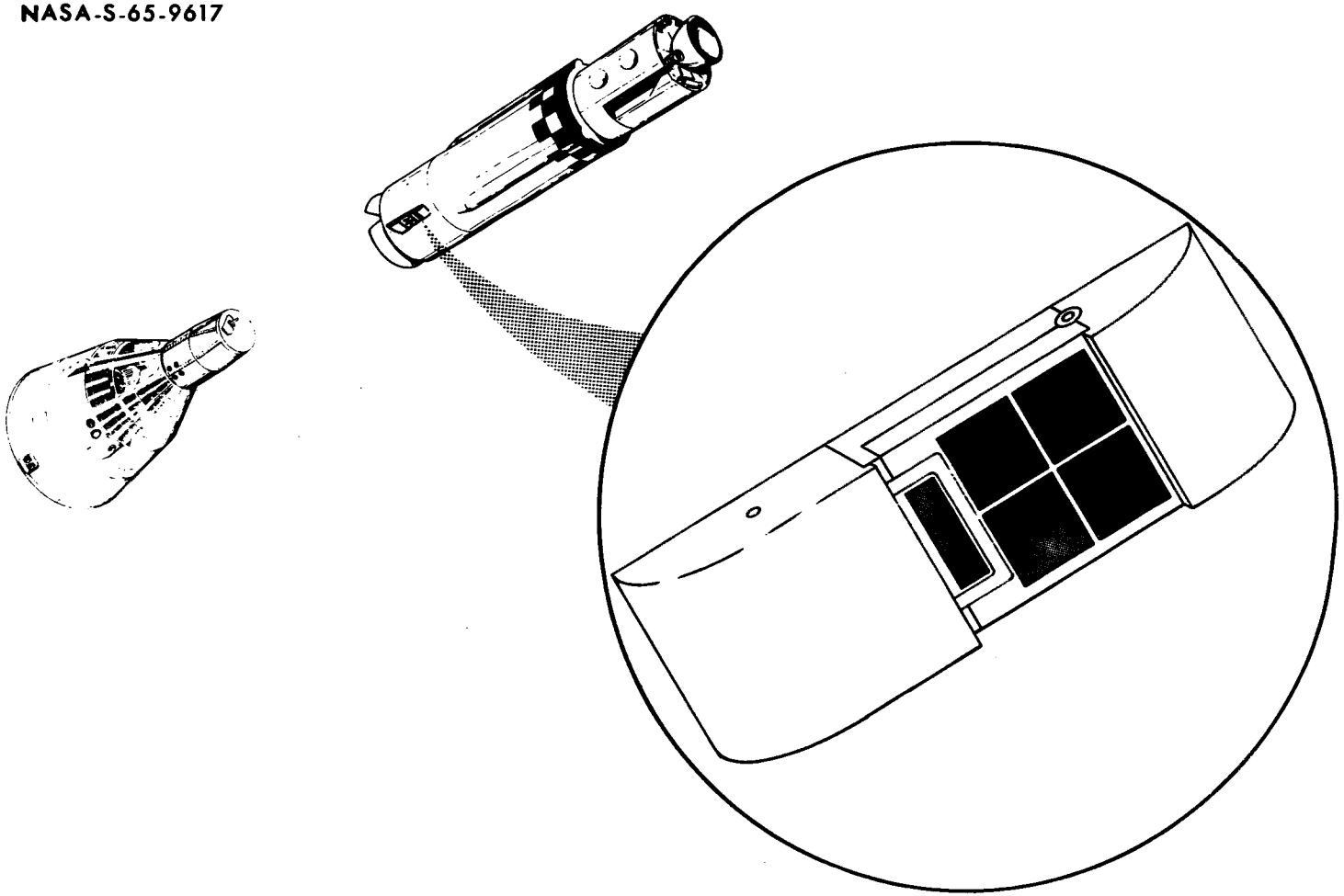

Figure 2-2.- Location of S-10 micrometeorite collector.

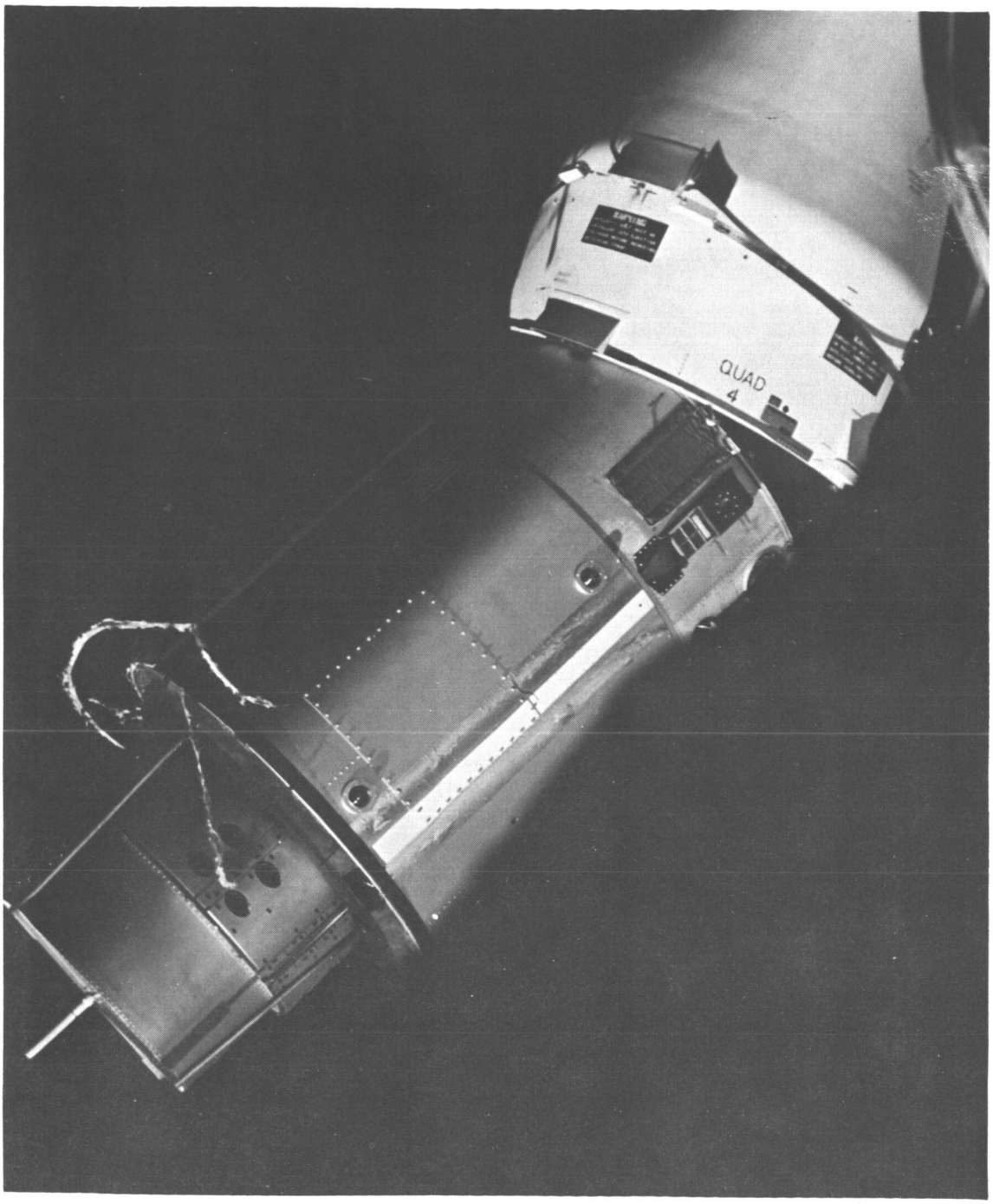

Figure 2-3.- Collector on augmented target-docking adapter.

3. EXPERIMENT S-11, AIRGLOW HORIZON PHOTOGRAPHY

By M. J. Koomen and R. T. Seal, Jr.
U.S. Naval Research Laboratory

SUMMARY

Forty photographs of night airglow and four photographs of twilight airglow were obtained on June 4, 1966, from the window of the spacecraft during the Gemini IX mission. An f/0.95, 50-mm focal length camera was optically filtered to photograph airglows in visible bands centered at 5577 Å and 5893 Å, where prominent airglow emissions occur due to atomic oxygen and atomic sodium, respectively. Filter combinations with broader spectral coverage were also used. Exposure times were between 2 and 20 seconds, and fine-pointing of the camera was required during exposure. An illuminated camera sight and an adjustable camera mount were used. The photographs show variations in the altitude and intensity of the airglow emissions. Data reduction is still in progress.

OBJECTIVE

Experiment S-11, Airglow Horizon Photography, was designed to study the night airglow which lies in a thin layer 70 to 100 kilometers (40 to 60 miles) above the earth. Although the surface brightness is low when one looks through this layer from below, its brightness is enhanced by a factor of approximately 35 when viewed tangentially from the vantage point of the Gemini orbit. This enhancement phenomenon, which makes the airglow easily observable, plus the worldwide coverage provided by orbiting vehicles, offers a highly attractive means for synoptic airglow study.

The Mercury and Gemini crews have had no difficulty in observing the night airglow as a relatively bright band lying above the nighttime horizon. During the Mercury-Atlas 9 mission, the pilot was able to photograph the layer with high-speed color film and an f/1.0 handheld camera, using 10- and 30-second exposures (refs. 1 and 2). The photographs revealed geographical variations in altitude and intensity.

The objective of the S-11 experiment during the Gemini IX mission was to extend and refine the photographic method as follows:

(1) The camera was filtered to photograph the two prominent line emissions at 5577 Å and 5893 Å which are due to atomic oxygen and sodium, respectively.

(2) An illuminated camera sight and an aiming camera mount were provided in an attempt to reduce the number of blurred photographs which occurred during the longer exposures. The S-11 experiment during the Gemini IX mission was, therefore, a feasibility test for these components.

(3) The number of photographs taken and amount of the earth photographed were as large as possible. The experiment is scheduled to be repeated on later Gemini missions to collect as much data as possible.

(4) Attempts were made to photograph the twilight horizon to reveal a sunlit dayglow layer.

EQUIPMENT DESCRIPTION

The equipment may be described as follows:

(1) Camera: The experiment used the Maurer 70-mm general purpose camera in the configuration employing an f/0.95, 50-mm lens and focal plane filter. This configuration was designed especially for airglow and other dim-light photography.

(2) Film: Eastman 103-D emulsion on 2-1/2 mil Estar base was used to provide maximum film speed in the 5577 Å to 5893 Å region. Development was for 6 minutes in Eastman D-19.

(3) Additional equipment: Additional equipment was as follows:

(a) Camera filters: A camera lens filter and a focal plane filter were provided to perform the function shown schematically in figure 3-1. The lens filter was of the multilayer interference type and had a steep-sided bandpass which admitted 5577 Å and 5893 Å, respectively, at short and long wavelength ends of the band. The focal plane filters, mounted side by side over the film, divided this band into two bands centered at 5577 Å and 5893 Å. Band half-widths (HW) were, respectively, 270 Å and 380 Å. Thus, light in these two wavelength bands was photographed side by side in the picture plane, in a split-field arrangement with a vertical dividing line. The extreme edges

of the focal plane filter were of clear glass to admit the entire band of the lens filter. The system represented an attempt to detect small altitude differences in the airglow emission wavelengths. The effect of the above filter combination could not be achieved by narrow-band filters in the focal plane alone, since these would not perform in the convergent light of the f/0.95 lens.

It may be mentioned that the filter bands were rather wide and admitted considerable contamination in addition to the wanted lines. The condition was most unfavorable for the sodium filter which admitted a large amount of OH radiation. However, it was believed that the photographs could yield significant results which would indicate the direction of refinements for later missions.

(b) Camera sight: The camera sight was designed and built especially for the experiment, and it contained a reflex element molded in the shape of a parabolic toroid. The camera operator could look through this element at the horizon and could see superimposed on it, by reflection, the images of three small penlights arranged in a horizontal line. The reflex element folded down for storage. Figure 3-2 shows the camera with lens filter and focal plane filter. The sight is shown in folded position. The cable release with event timer was not used.

(c) Camera bracket: Because relatively long exposure times were required, the camera could not be handheld. A bracket, adjustable in pitch, held the camera to the right-hand spacecraft window. Figure 3-3 shows the bracket configuration. The two fluted knobs fastened the bracket to the lower part of the window frame. Turning the large knob adjusted the camera aim in the elevation (pitch) direction; the limits of motion were somewhat more than 6° in either direction from its center position. This center position was marked with a visible groove in the knob shaft, and the groove could also be felt with the fingers when the cabin was dark. When not in use, the bracket could be removed from the window and folded into the storage configuration shown in figure 3-4.

PROCEDURE

Camera components, including the window bracket, were stored in the spacecraft cabin and assembled onto the right-hand window during revolution 19. The camera axis was essentially perpendicular to the spacecraft window and was, therefore, not boresighted to the spacecraft. To acquire the horizon at any particular azimuth, the entire spacecraft was adjusted in attitude until the appropriate part of the horizon

appeared "right side up" in the camera sight. This required activity by both the command pilot and pilot. Spacecraft drift rates were then damped as much as possible and the exposure was begun. The pilot compensated for drifts in pitch during exposure by fine-pointing the camera at the horizon with the aid of the camera sight and adjustable bracket. The spacecraft thrusters were not used during the exposure since they produced a large amount of light.

During spacecraft night, a set of horizon exposures was taken successively to the east, north, west, and south. Each set consisted of a 20-second exposure with all filters in place, plus a 2- and a 5-second exposure with the lens filter removed. Exposures were timed by the spacecraft clock. As the spacecraft entered the twilight zone, exposures of 5 and 10 seconds, with all filters in place, were made of the eastern horizon in an attempt to record the sunlit airglow. The entire sequence was repeated in revolutions 20 and 21.

RESULTS AND CONCLUSIONS

Forty-four photographs of the horizon airglow layer were obtained. Four of these were of the sunlit airglow on the eastern horizon, and they represented the first photographic record of the dayglow.

Figures 3-5, 3-6, and 3-7 show typical examples of the night photographs. In figure 3-5, the strip to the left of the central vertical line is recorded in the sodium wavelength band (Na D) centered at 5893 Å with a 380 Å half-width. The strip to the right of the central dividing line is recorded in the oxygen green-emission band at 5577 Å with a 270 Å half-width. Areas of the photograph at the extreme right and left were exposed with the broadband filter to include both 5893 Å and 5577 Å. Streaks in the sky are stars which were rising while the camera was kept centered on the horizon. The most prominent streak above the airglow is α Ophiuchus. Figures 3-6 and 3-7 are 5-second and 2-second exposures, each made with the broadband (5893 Å to 5577 Å) filter removed from the camera lens. The strip to the left of center records transmission through an orange filter (Corning No. 3480) of wavelengths at 5577 Å and longer, while the strip to the right records transmission through didymium glass and includes most of the visible spectrum except Na D. Areas at the extreme right and left were exposed with no filter. The bright stars in and below the airglow in figures 3-6 and 3-7 are γ and β Ursa Minor.

The moonlit earth is visible in all the photographs. Since data reduction is still in progress, no interpretation of the photographs will be made at this time, except to state that they show global

variations in altitude and intensity of the airglow. The crewmembers reported variations in thickness and sharpness of the layer. The photographs confirm this observation.

Some of the photographs contained rich star fields, and stars were recorded to approximately the 7th magnitude. These stars were sometimes recorded through the airglow layer. This suggests that the layer is essentially transparent and does not contain dust as originally suggested by Link (ref. 3).

Data reduction has thus far shown no evidence that the moon, which was full at the time of the flight, contributed light to the airglow layer. This also suggests that the layer contains no scattering material.

The experiment has produced some practical conclusions which may be mentioned. First, the mounting of the camera axis perpendicular to the window, while desirable from an optical standpoint, produced an awkward angle with respect to the spacecraft attitude control system. The crew found it difficult and time consuming to aim the camera at the horizon because the yaw, roll, and pitch thrusters had to be coupled to achieve the correct attitude. They reported that boresighting the camera to the spacecraft roll axis would have made the maneuver much easier. Nevertheless, the attitude control and camera pointing were remarkably good.

The camera position also required the pilot to move partly out of his seat to use the camera sight. Therefore, the restraint normally provided by his seat belt was lost, and the pilot found himself constantly floating away from the camera during the sighting time. The pilot recommended that the sight and camera be placed where they could be used from the normal seat position if possible.

The results from this experiment indicate a promising future for airglow and astronomical measurements from manned spacecraft.

ACKNOWLEDGMENTS

The authors wish to acknowledge the cooperation of the National Aeronautics and Space Administration and, particularly, the cooperation of astronauts Thomas Stafford and Eugene Cernan. The authors are indebted also to John Lintott, Roy Stokes, and George Laski of the Optics Branch of the Manned Spacecraft Center; to John Brinkmann, T. Brahm, R. Gray, and Fred Southard of the MSC Photographic Laboratory; to Robert O. Piland of the MSC Experiments Program Office; and to Dr. Jocelyn Gill of NASA Headquarters.

REFERENCES

1. Mercury Project Summary. NASA SP-45, National Aeronautics and Space Administration, Washington, D.C., October 1963.

2. Gillett, F. C.; Huch, W. F.; Ney, E. P.; and Cooper, G.: Photographic Observations of the Airglow Layer. J. Geophys. Res., vol. 69, no. 13, 1964, pp. 2827-2834.

3. Link, F.: Thèorie photomètrique des èclipses de Lune. Comp. Rend., vol. 196, Jan. 23, 1933, pp. 251-253.

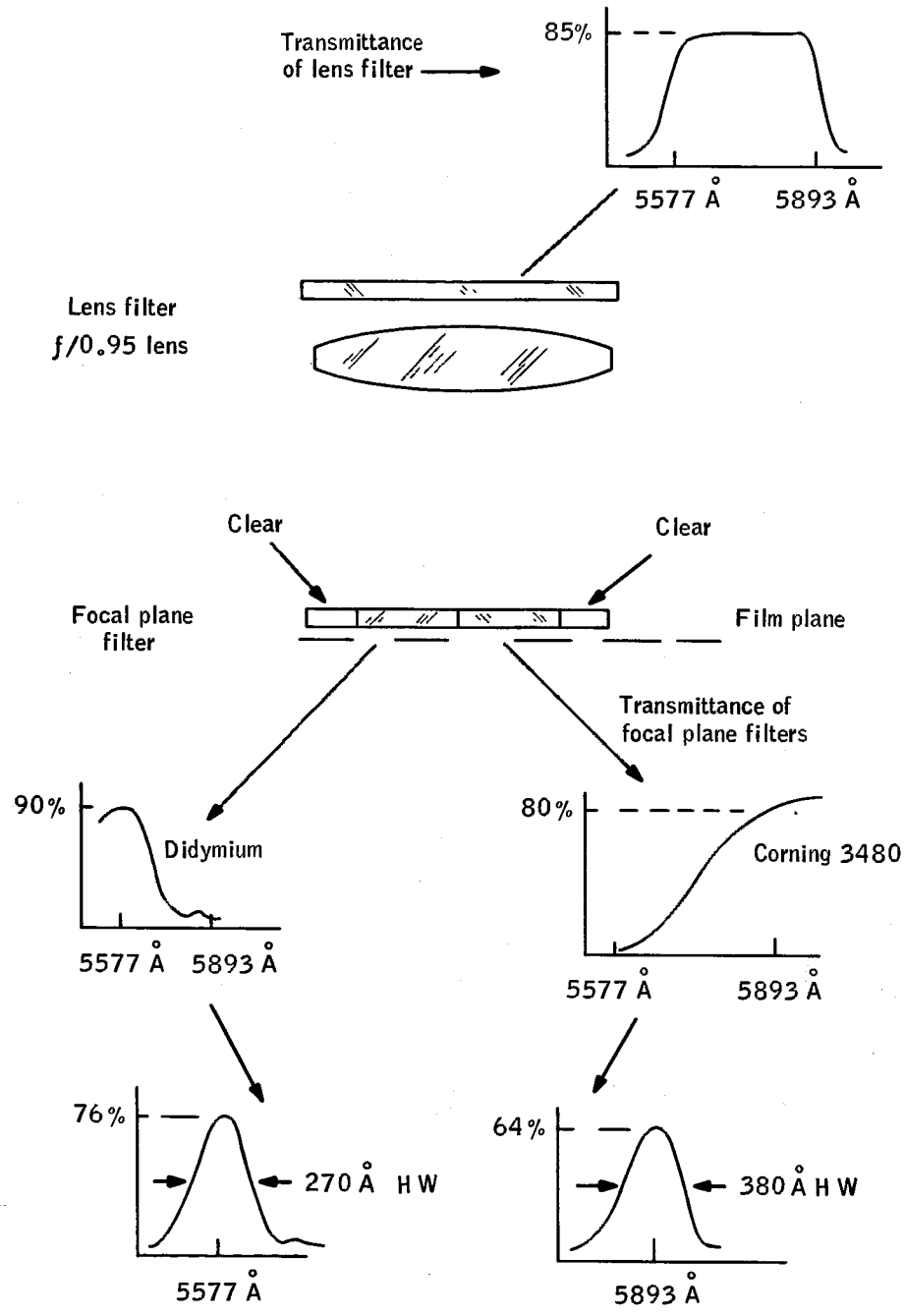

Figure 3-1.- Combined transmittance, lens, and focal plane filters.

NASA-S-66-2604 MAR 22

EXPERIMENT S-11 CAMERA SYSTEM

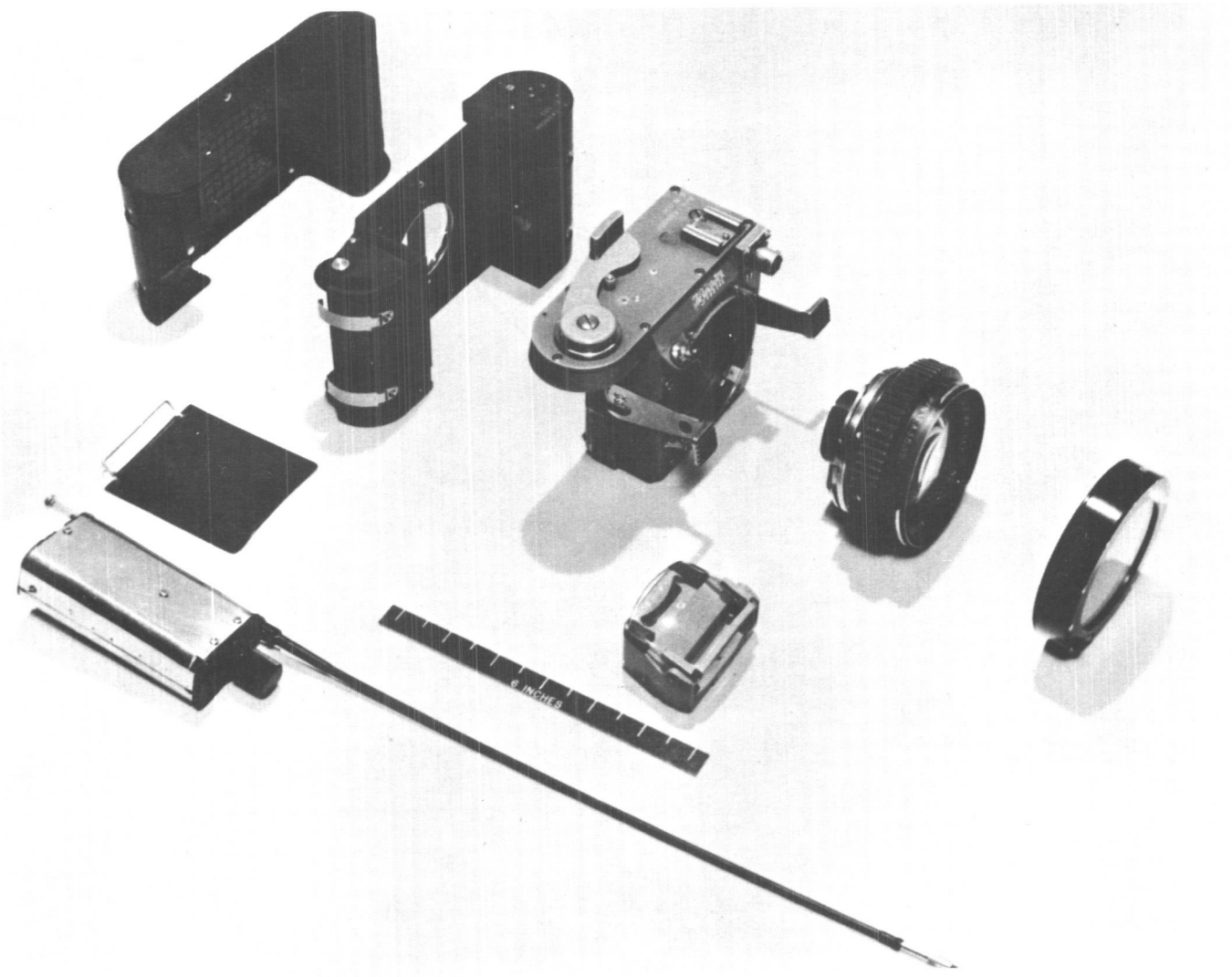

Figure 3-2.- Camera system used in experiment S-11.

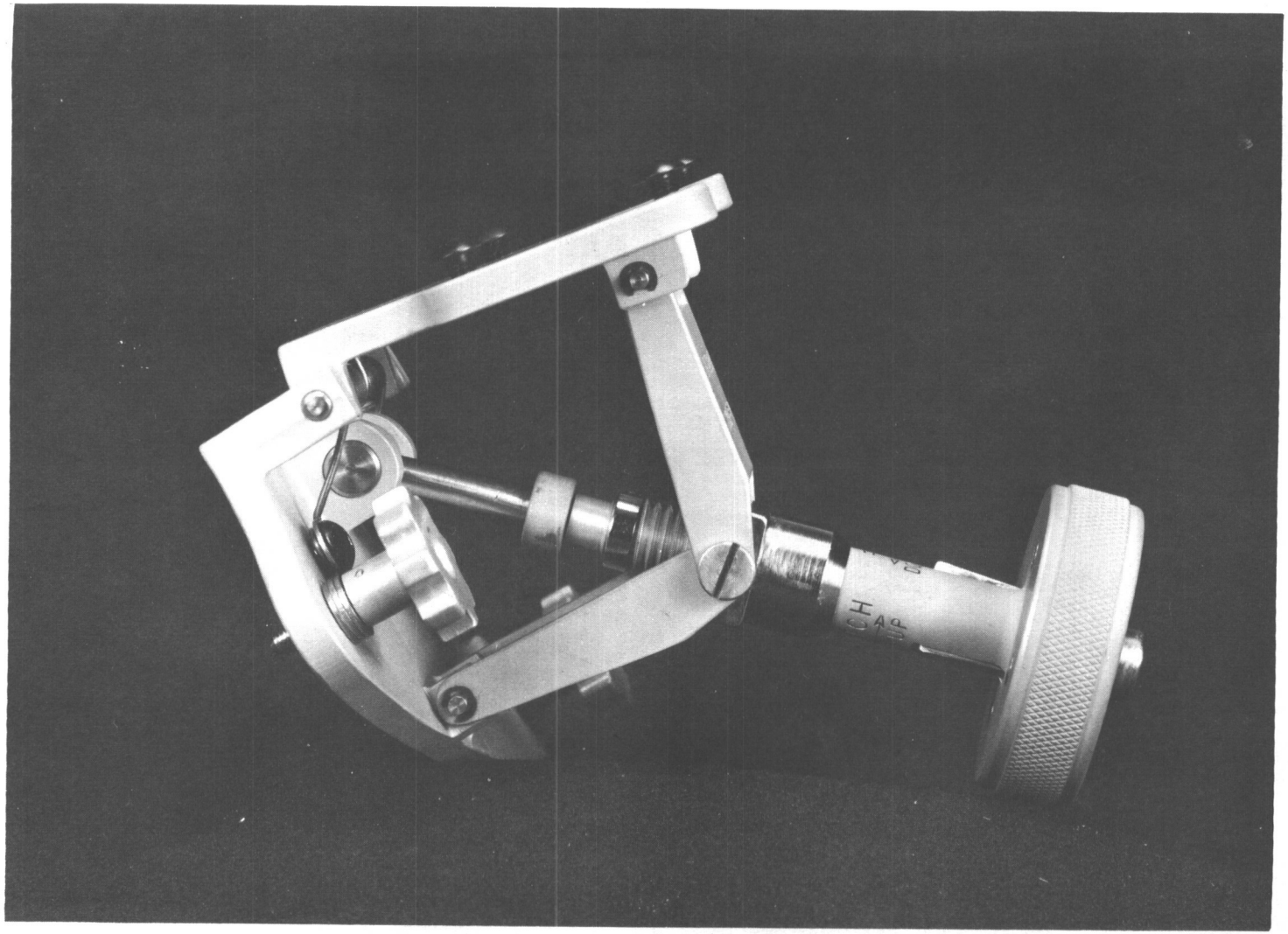

Figure 3.3.- Pitch-adjustable bracket for mounting camera to lower edge of spacecraft right-hand window.

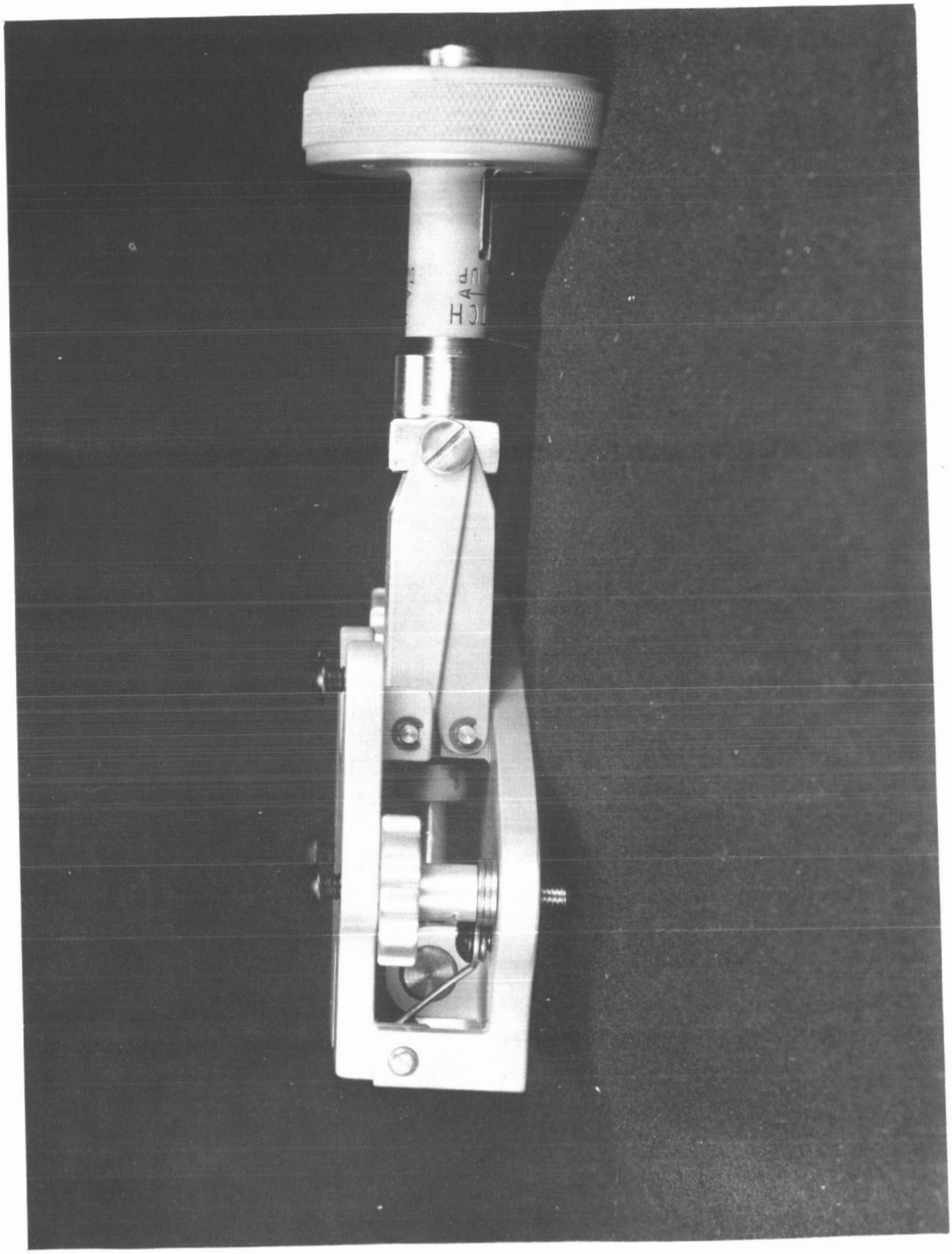

Figure 3.4.- Camera bracket folded for storage.

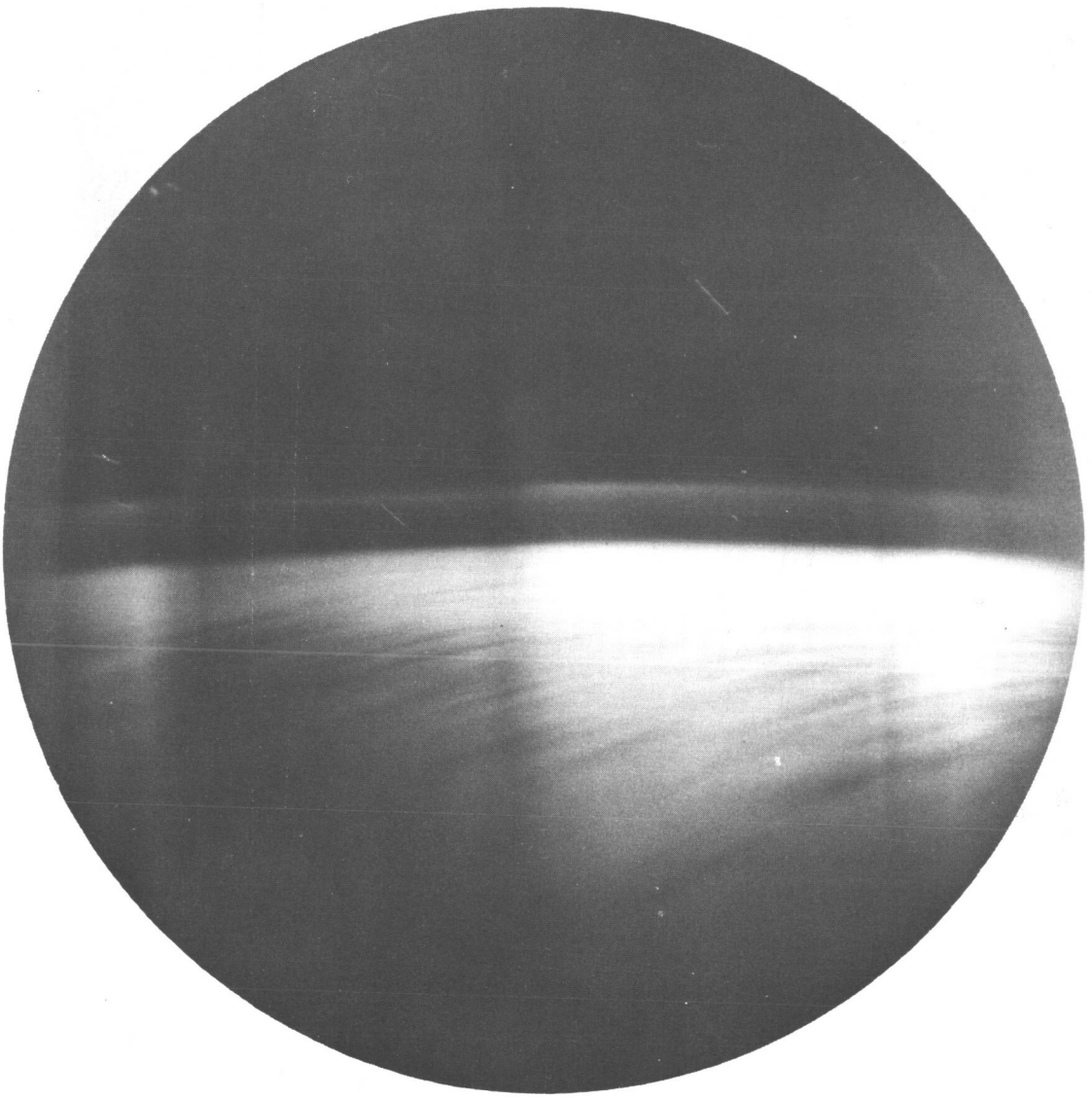

Figure 3-5.- Exposure No. 1, looking east in orbit 19, showing airglow layer and moonlit earth (20-second exposure at f/0.95).

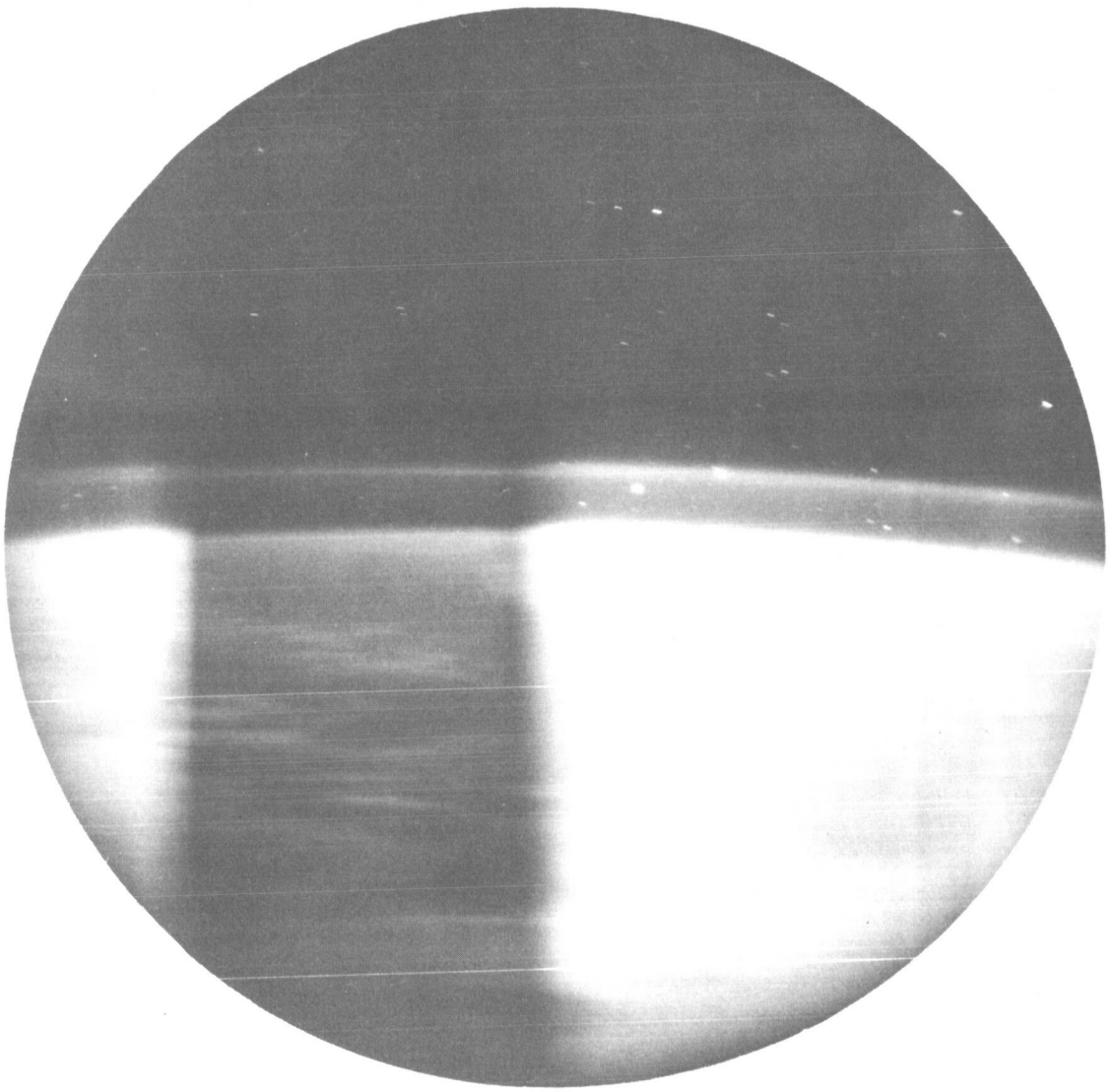

Figure 3-6.- Exposure No. 5, looking north in orbit 19 (5-second exposure at f/0.95).

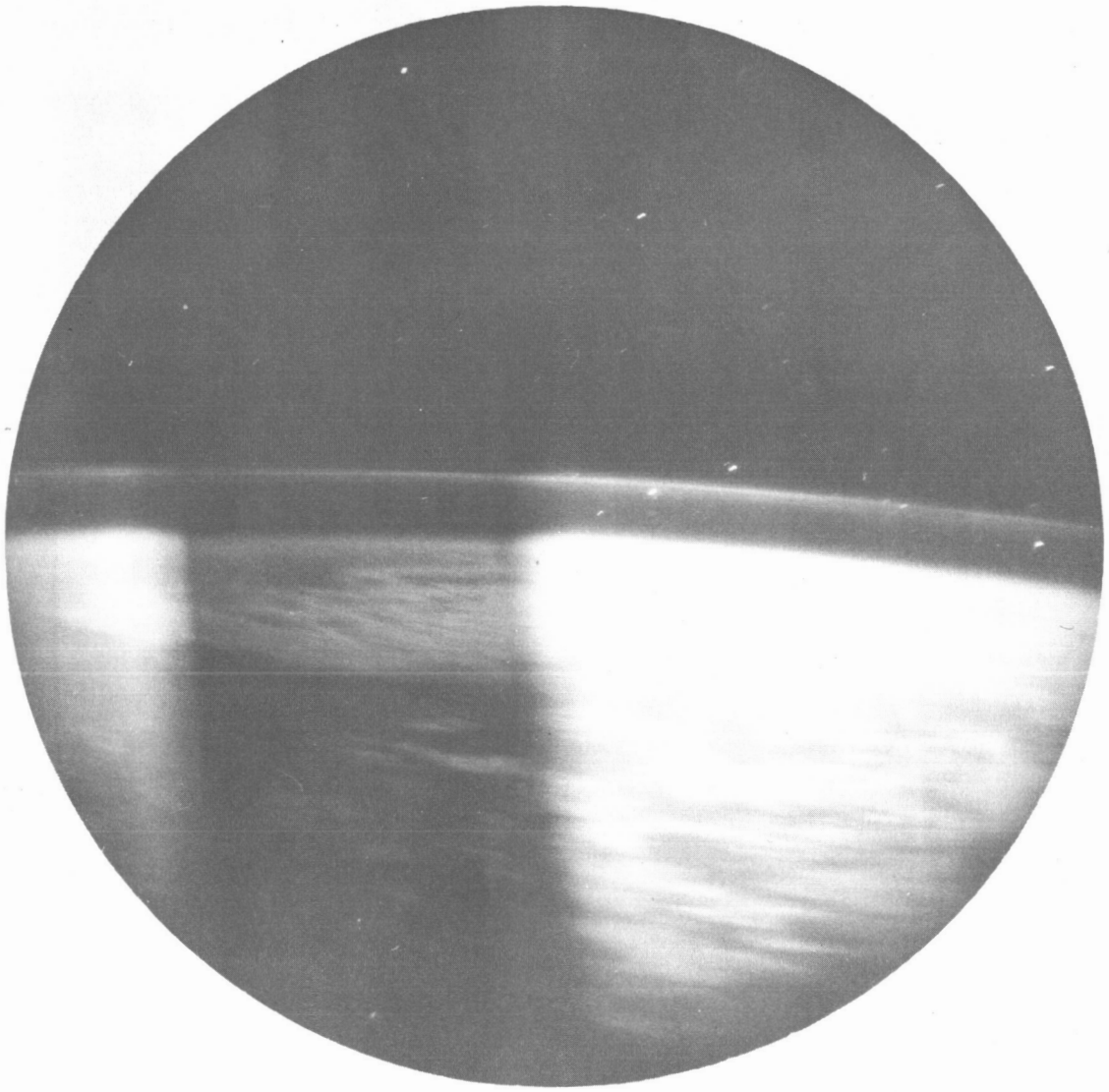

Figure 3-7.- Exposure No. 18, looking north in orbit 20 (2-second exposure).

4. EXPERIMENT S-12, MICROMETEORITE COLLECTION

By Curtis L. Hemenway, Ph. D.
Dudley Observatory

OBJECTIVES

The S-12 experiment was designed to obtain data under carefully controlled conditions for durations of 10 to 20 hours for the following:

(1) The flux of particle material in space, as determined by direct collection, and cratering effects of high velocity impacts

(2) Thin film penetration characteristics of micrometeorites

(3) Lethal effects of the space environment on microbiological specimens

(4) The probability of viable organisms in space either alone or in conjunction with micrometeoritic material.

In addition, through a guest experimenter program, scientists from various institutions were invited to provide samples within the context of the above areas. Guest experimenters for the Gemini IX mission were Robert Skrivanek, Air Force Cambridge Research Laboratory; Uri Shafrir, University of Tel Aviv; Hugo Fetchig, Max Planck Institute; Neil Farlow, NASA Ames Research Center; Michael Carr, U.S. Geological Survey; Paige Burbank, NASA Manned Spacecraft Center; and Otto Berg, NASA Goddard Space Flight Center.

EQUIPMENT

The S-12 micrometeorite collector is shown in figure 4-1. The unit measures 5-1/2 by 11 by 1-1/4 inches and weighs approximately 6-1/2 pounds loaded for flight. Not visible in the figure are the dual internal battery package, the cover drive motor and gear train, the cover limit switches, and the squib-actuated unlatching and locking devices.

Figure 4-2 shows the unit with one cover open and illustrates the 12 sample slides contained in one compartment of the device. The dual cover arrangement was provided to allow for the inclusion of sterile

samples in one area and live micro-organisms in the other. Figure 4-3 shows the sample slides in the second compartment. Figure 4-4 is a diagram showing sample locations and giving a brief description of the nature and source of the sample.

PROCEDURES

Preflight

The final loading procedures were begun approximately 10 days before scheduled launch with a thorough cleaning of the entire S-12 unit. The compartment to be sterilized was loaded in a dust-free hood, and the cover was closed. The entire unit was then placed in a clean stainless steel box, the covers of the S-12 unit were partially opened, and ethylene oxide was introduced for sterilization. After sterilization, the covers were closed and secured. The unit was removed to a dust-free hood and the nonsterile compartment was opened manually for loading the sample slides. After completion of loading and final mechanical adjustments, the unit was wrapped in plastic, placed in a special container, and hand-carried to Kennedy Space Center 3 days before the scheduled launch. Two units were loaded in this way and designated as flight and backup units.

After prelaunch tests, designed to verify operational readiness, the flight unit was installed on the spacecraft retroadapter 17 hours before the scheduled launch. As part of the final countdown, three sterile swabs were used to sample the microbiological environment of three selected areas inside the spacecraft.

After the Atlas failure and the decision to delay the mission, the S-12 unit was removed from the spacecraft, and the internal batteries were charged. Both flight and backup units were then stored in the Biomedical Sciences and Flight Experiments Laboratory, Kennedy Space Center, at a temperature of 50° F until installation on the spacecraft retroadapter on May 31, 1966. The unit remained on board the spacecraft during the 2-day hold necessitated by the computer malfunction.

Inflight

After the successful launch of the Gemini-Titan II vehicle at 8:39:33 eastern standard time on June 3, 1966, the unit was opened by the pilot at 9:29 ground elapsed time (g.e.t.) and closed at 17:10 g.e.t. A second opening was at 35:48 g.e.t. with closing and locking at 44:54 g.e.t. The total exposure time was 16 hours 47 minutes.

The crew was unable to hear the cover drive motor during any of the opening or closing sequences. It is not certain whether the locking mechanism was heard. Postflight examination, however, indicated that the unit did open and close as planned. The experiment hardware was recovered by the pilot and stowed within the spacecraft cabin.

Postflight

The S-12 experiment hardware was removed from the spacecraft after it was brought aboard the recovery vessel. The unit was placed in a special case and was flown to Patrick Air Force Base where a Dudley representative received it and returned it to Dudley Observatory on June 7, 1966. During the recovery procedure, three swabs were again taken from the same areas of the spacecraft cabin as the preflight swabs. These were included in the recovery case and were taken to the observatory. After arrival at Dudley Observatory, the outside of the unit was sterilized by ultraviolet prior to opening. The unit was opened in a dust-free hood, and the samples were removed for analysis.

Two indications were used to assure that the collector did open in space. One was a piece of photographic paper located in a section of the collector. The paper appeared to be almost black even without processing. The second assurance of opening was that portions of the various micro-organisms were killed.

RESULTS

To date, only two of the eight samples have been examined in detail. These samples consisted of thin nitrocellulose films supported by 200-mesh copper screen. One sample was preshadowed with palladium to "tag" any possible contaminants, and the other was preshadowed with aluminum.

On the palladium-shadowed sample, an area of approximately 5 square millimeters has been scanned with an electron microscope at sufficient magnification to detect all structures greater than 0.1 micron. A total of 6 square millimeters of control sample has also been scanned. For the aluminum-shadowed samples, approximately 2 square millimeters of exposed area and an equivalent control area have been scanned. The control samples were located in hollow recesses in the bottom of the sample slides.

The samples were scanned to detect and record any particulate matter on the surface of the film and to observe any damage to the film

caused by high-velocity particles. The particulate material collected generally has an irregular shape. A few "fluffy" particles have been observed, and these are similar to those found on samples exposed on sounding rockets. Further analysis will be required before the origin or origins of these particles can be determined.

The most common effects observed in these thin films are penetration holes. Several types of holes have been noted. The most common case is a single hole often with flapped edges. Figures 4-5 and 4-6 show the ragged holes produced by the fast moving particles. Figure 4-7 shows a relatively large area which has been deformed by a large particle or group of particles. Figure 4-8 shows a cluster of holes all confined to a small area. This may have been a single conglomerate particle which was broken up by the interaction of the particle with a "gaseous atmosphere" in the vicinity of the spacecraft. Figure 4-9 shows a single large penetration plus a few small holes associated with it. Similar hole structures were observed during the control flight of the noctilucent cloud sampling experiment in 1962.

Two hundred holes or groups of holes of the types shown have been found on the palladium-shadowed films. These have all been found to be grossly different from any holes or imperfections on the control surfaces. The aluminum-shadowed samples appear to show fewer hole structures than the palladium-shadowed material. This apparent difference may be due to the smaller number of aluminum-shadowed samples studied to date.

A unique hole structure is shown in figure 4-10. Twenty-five of these structures have been observed on the palladium-shadowed samples. In general, these appear to have a rounded outline, an elliptical intermediate region, and an elongated hole in the center. The whole structure generally rises above the surface a distance equal to approximately one-fifth of its diameter. These structures may be the result of higher velocity impact than the holes previously shown.

The biological experiments have produced some useful and interesting results. The sterile surfaces which were intended to collect organisms have been cultured, but to date they have shown no indication that any viable organisms were collected. The analysis of the swabs, taken before and after the flight, serves as a control for this experiment, and the analysis is still in progress. In three of the five

survival tests of known organisms, definite fractions of the organisms survived. The results are tabulated below:

Organisms	Surviving fraction
T_1-bacteriophage in broth concentrate	2×10^{-6}
T_1-bacteriophage in B-4 lysate	0
Penicillium mold	3×10^{-5}
Tobacco mosaic virus	2×10^{-3}
Bacillus stearothermophilus	0

FUTURE PLANS

The work completed to date represents examination of only a small portion of surfaces which were exposed. The stainless steel and Lucite samples will be studied for small craters. The Stereoscan microscope which is being installed should provide useful data on crater structures.

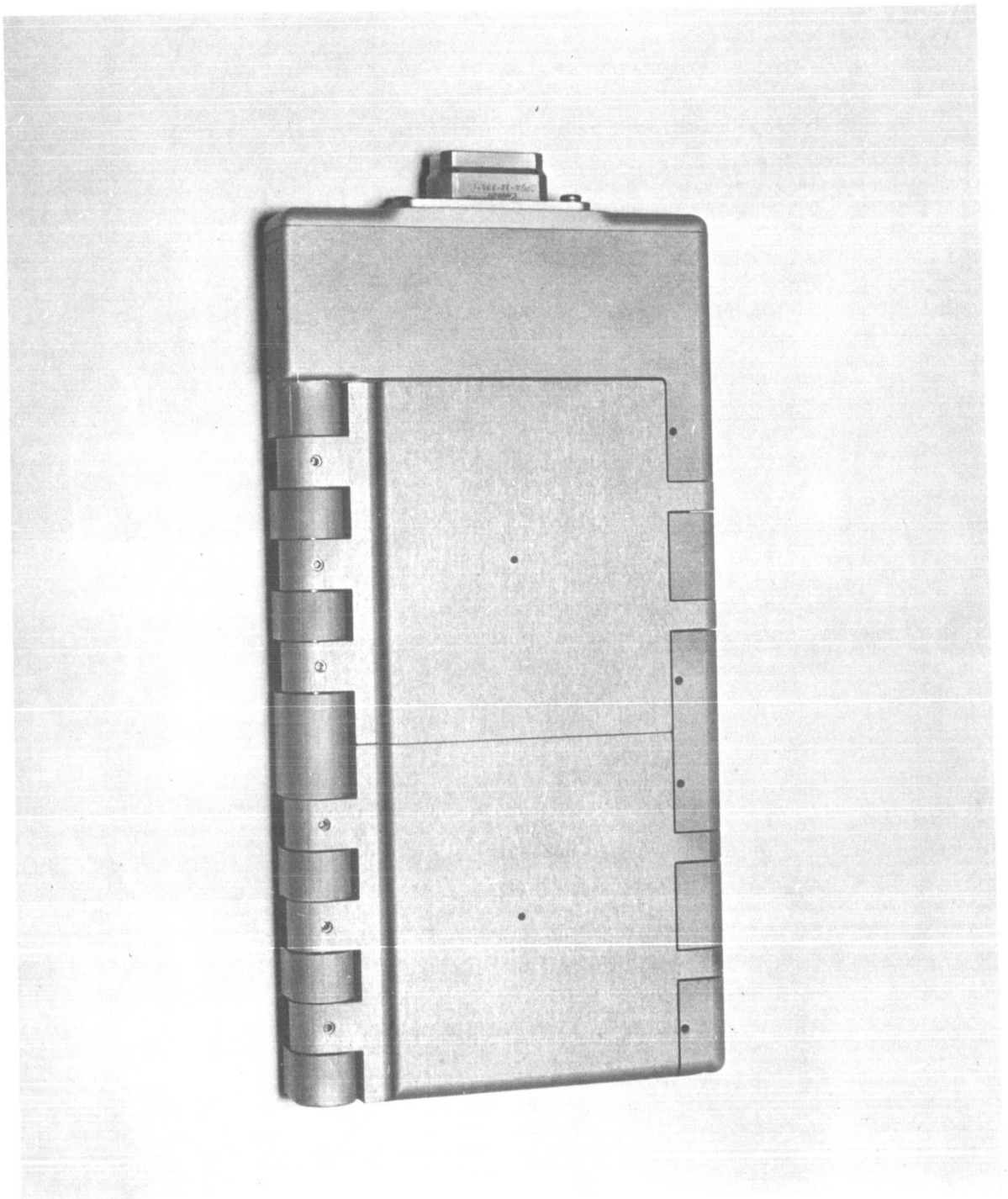

Figure 4-1.- Micrometeorite collector for experiment S-12.

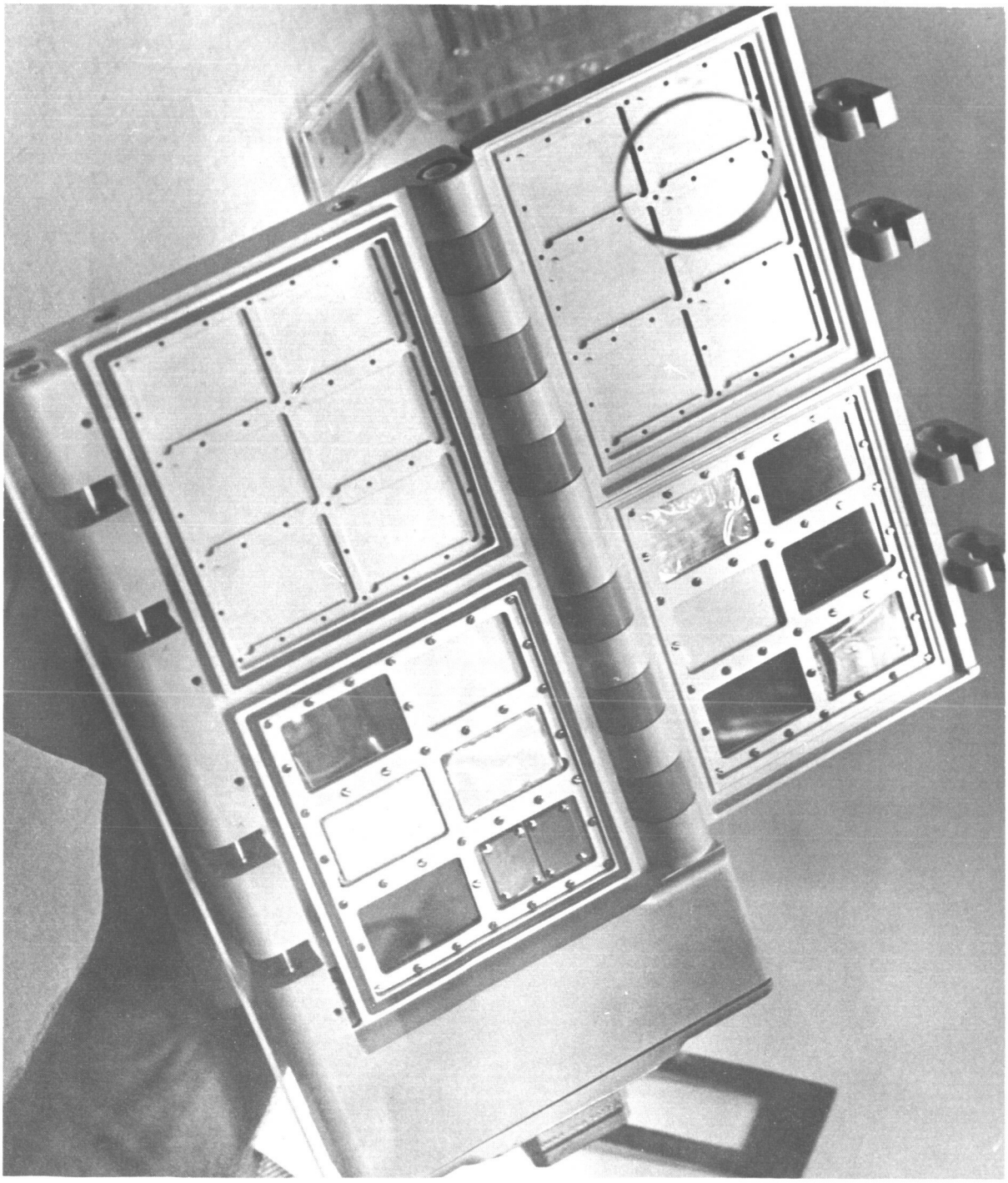

Figure 4-2.- Collector with one cover open.

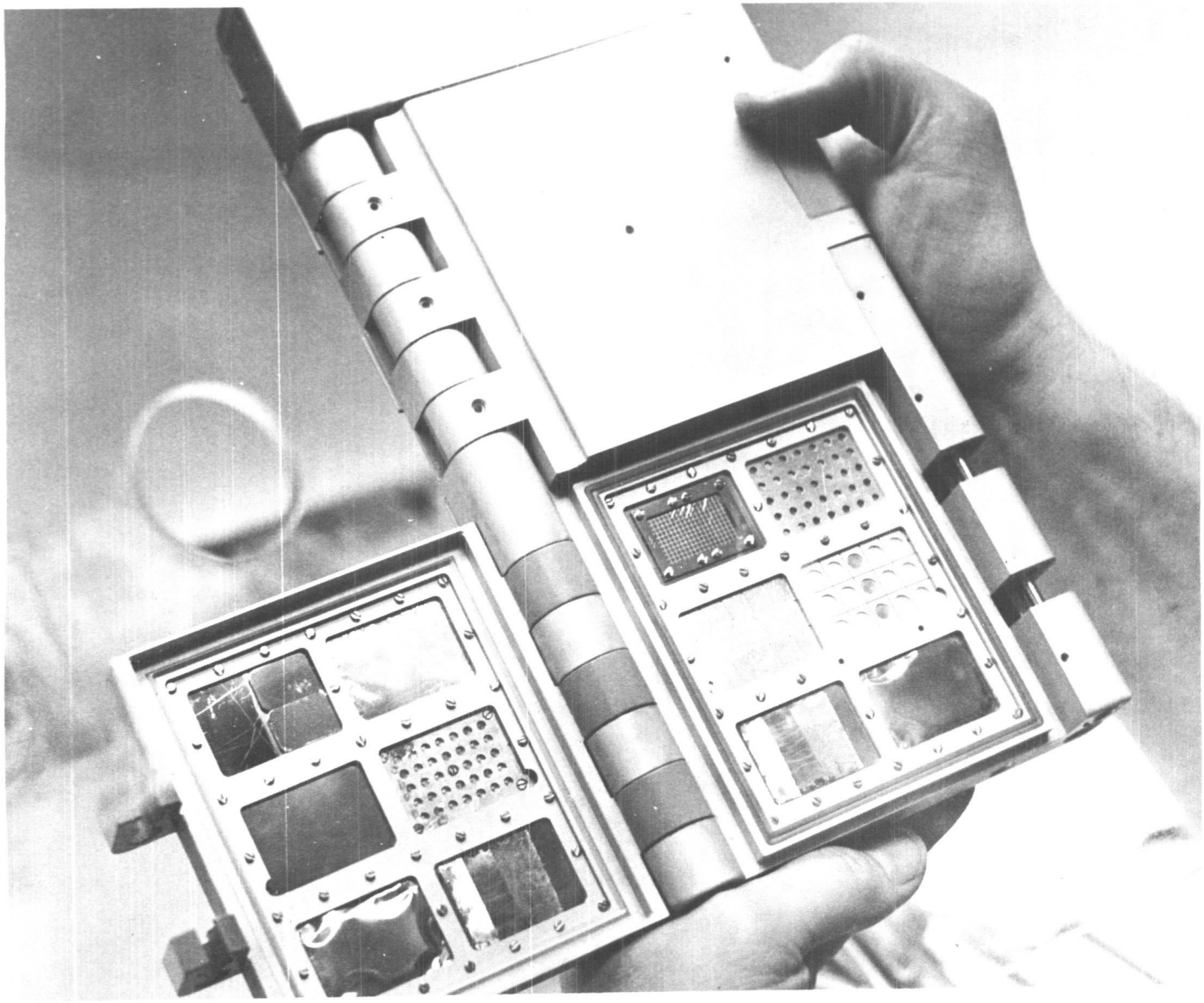

Figure 4-3.- Collector, showing sample slides.

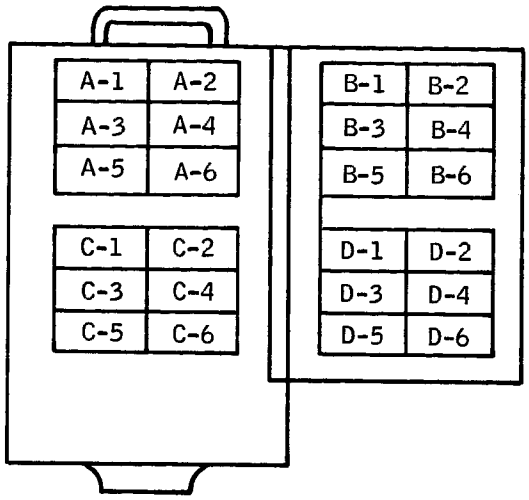

A-1 Dudley Observatory: Nitrocellulose film on copper mesh
A-2 Air Force Cambridge Research Laboratory: Nitrocellulose film on copper mesh
A-3 Dudley Observatory: Biological exposure
A-4 Dudley Observatory: Biological exposure
A-5 Dudley Observatory: Thin film penetration
A-6 Ames Research Center: Copper foil

B-1 Air Force Cambridge Research Laboratory: Nitrocellulose film on copper mesh
B-2 Dudley Observatory: Nitrocellulose film on copper mesh
B-3 Tel Aviv University: Penetration through film
B-4 Dudley Observatory: Stainless steel
B-5 Dudley Observatory: Nitrocellulose film on copper mesh
B-6 Max Planck Institute: Microprobe samples

C-1 Manned Spacecraft Center: Silver coated plastic
C-2 Dudley Observatory: Lucite
C-3 Dudley Observatory: Sterile sample
C-4 Dudley Observatory: Sterile sample
C-5 Goddard Space Flight Center: Titanium coated glass
C-6 Ames Research Center: Copper slide

D-1 Dudley Observatory: Nitrocellulose on copper mesh
D-2 Manned Spacecraft Center: Silver coated plastic
D-3 Goddard Space Flight Center: Titanium coated glass
D-4 U.S. Geological Survey: Beryllium coated slide
D-5 Dudley Observatory: Stainless steel
D-6 U.S. Geological Survey: Nitrocellulose on copper mesh

Figure 4-4.- Loading plan for S-12 micrometeorite collector.

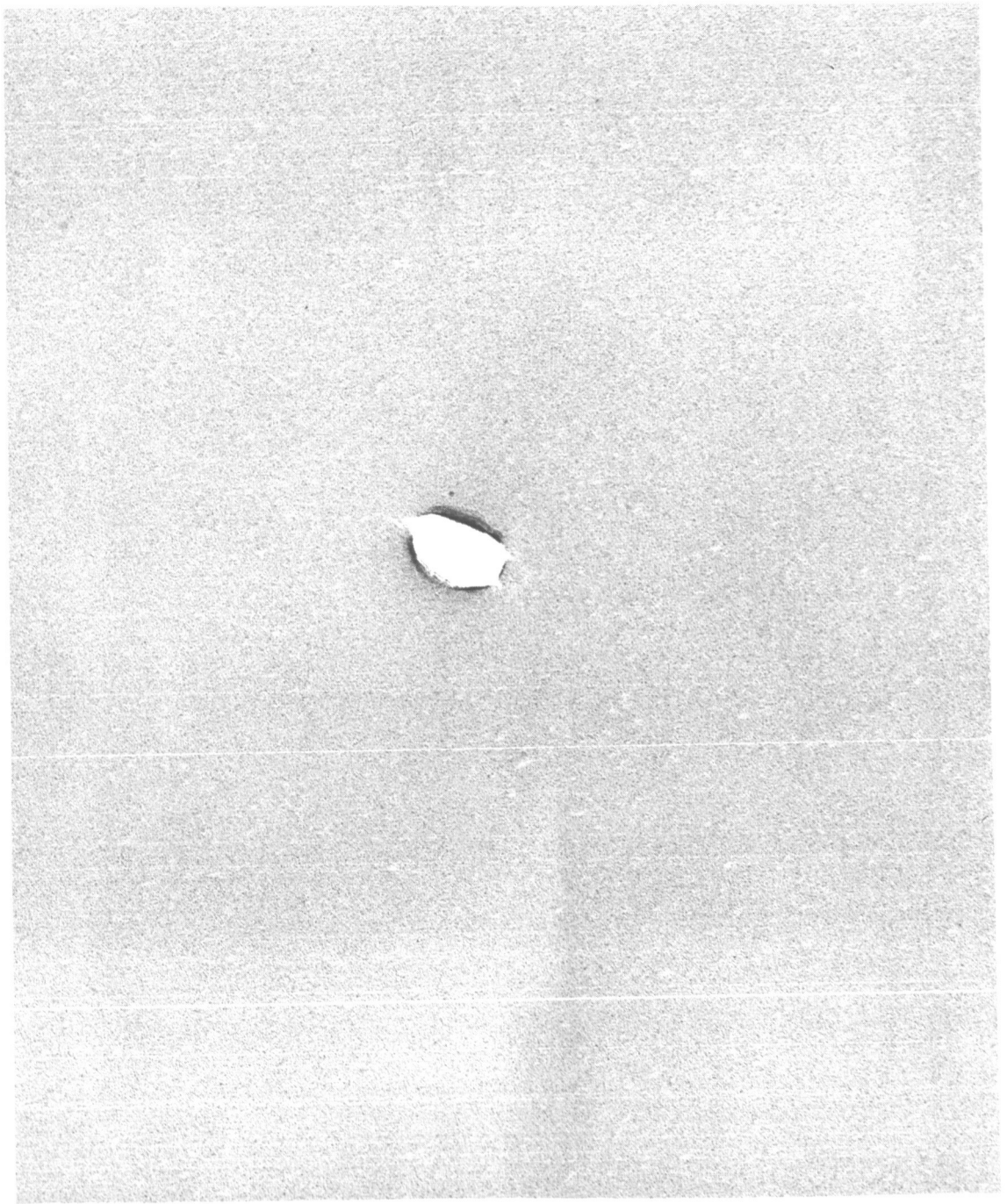

Figure 4-5.- Ragged hole produced by fast-moving particle (40 000 X).

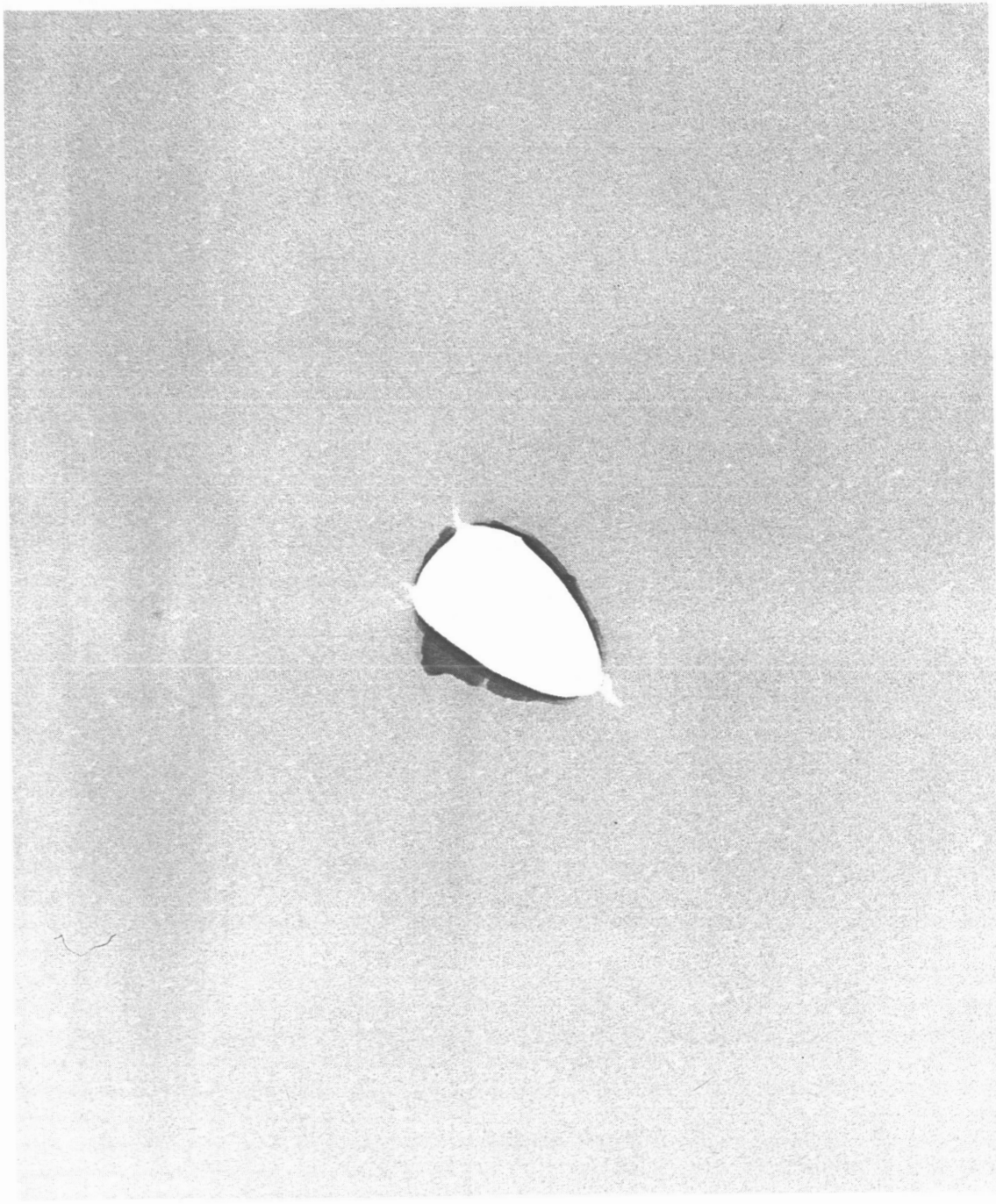

Figure 4-6.- Ragged hole produced by fast-moving particle (40 000 X).

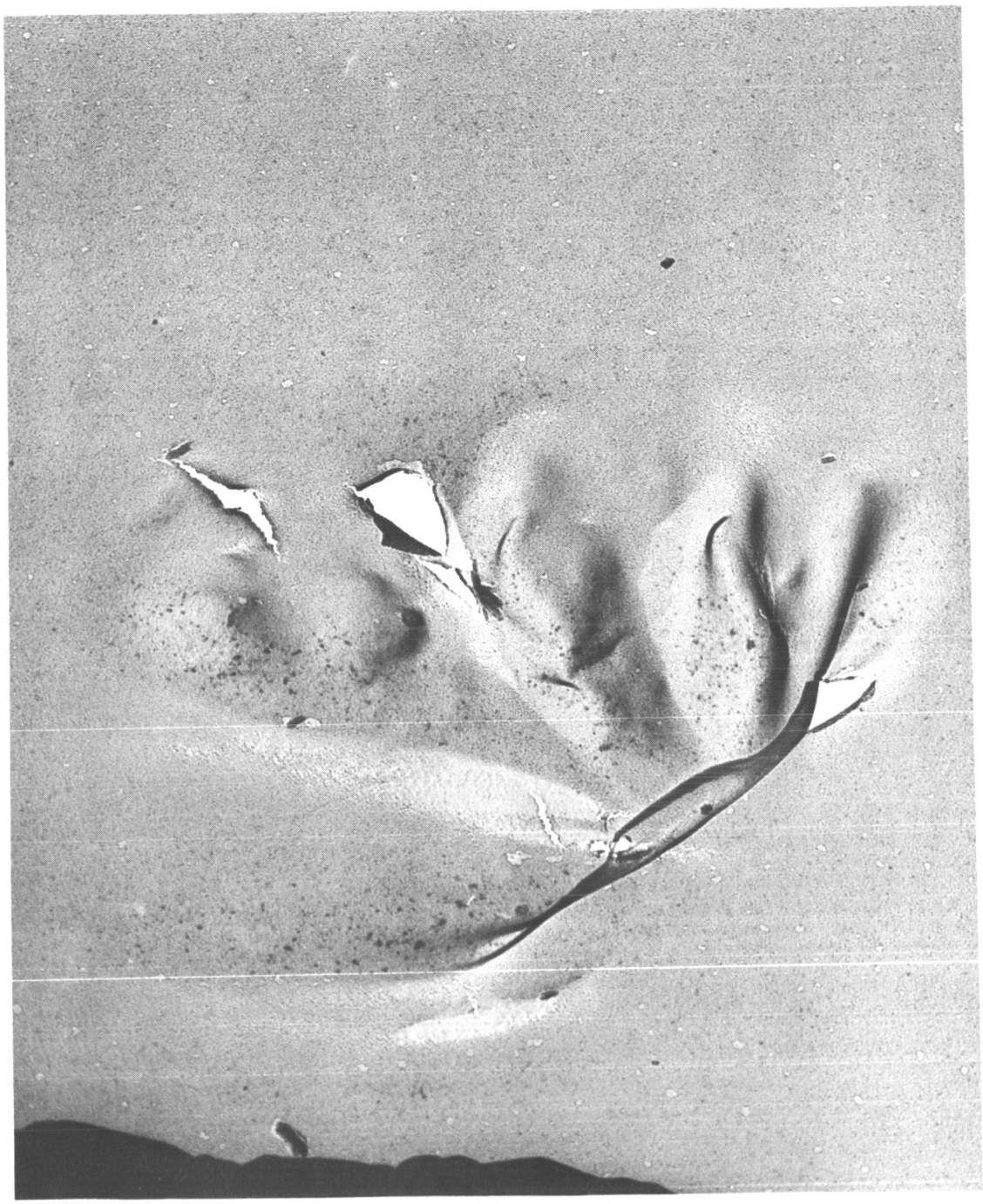

Figure 4-7.- A relatively large area which has been deformed by a large particle or group of particles (20 000 X).

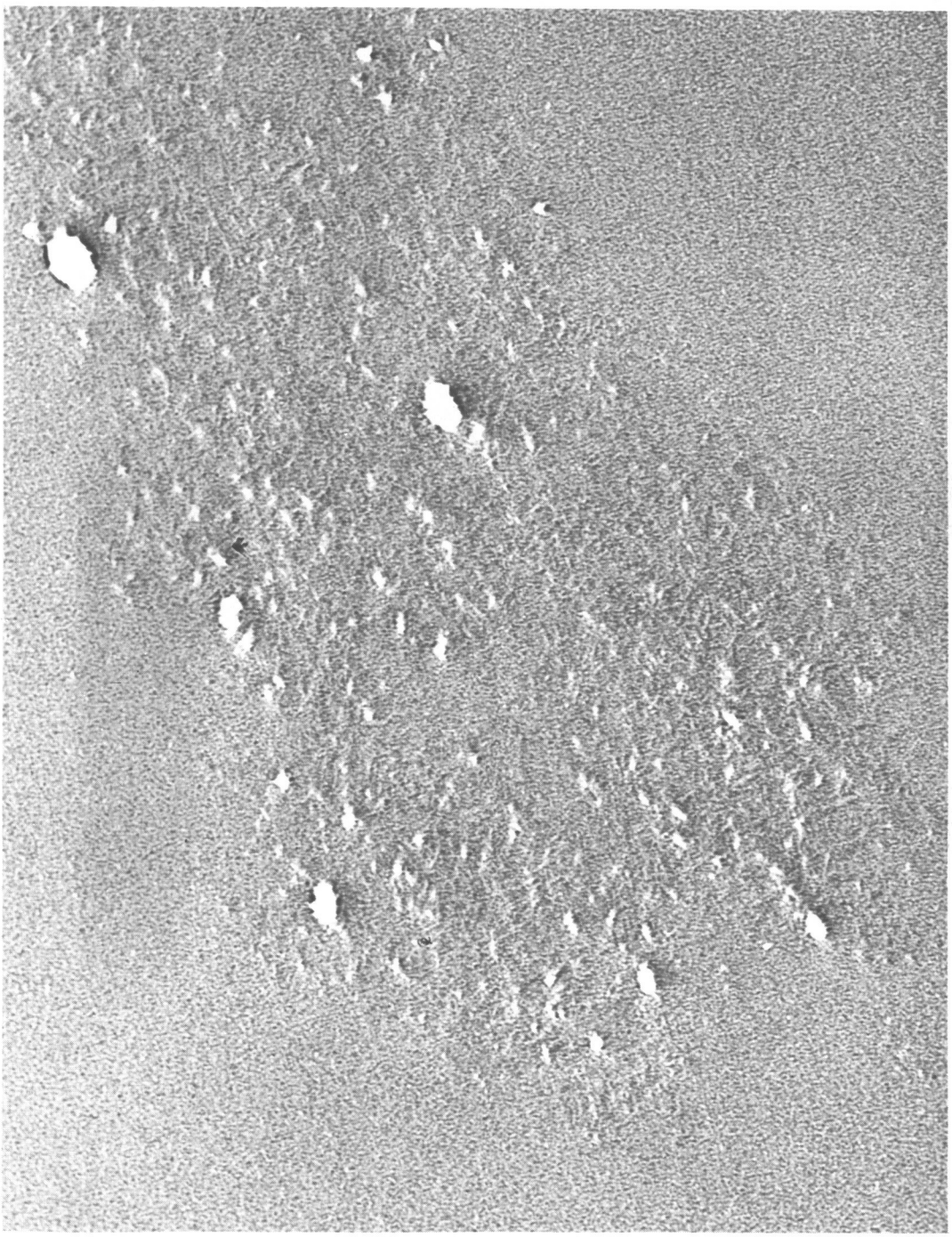

Figure 4-8.- A cluster of holes confined to a small area (40 000 X).

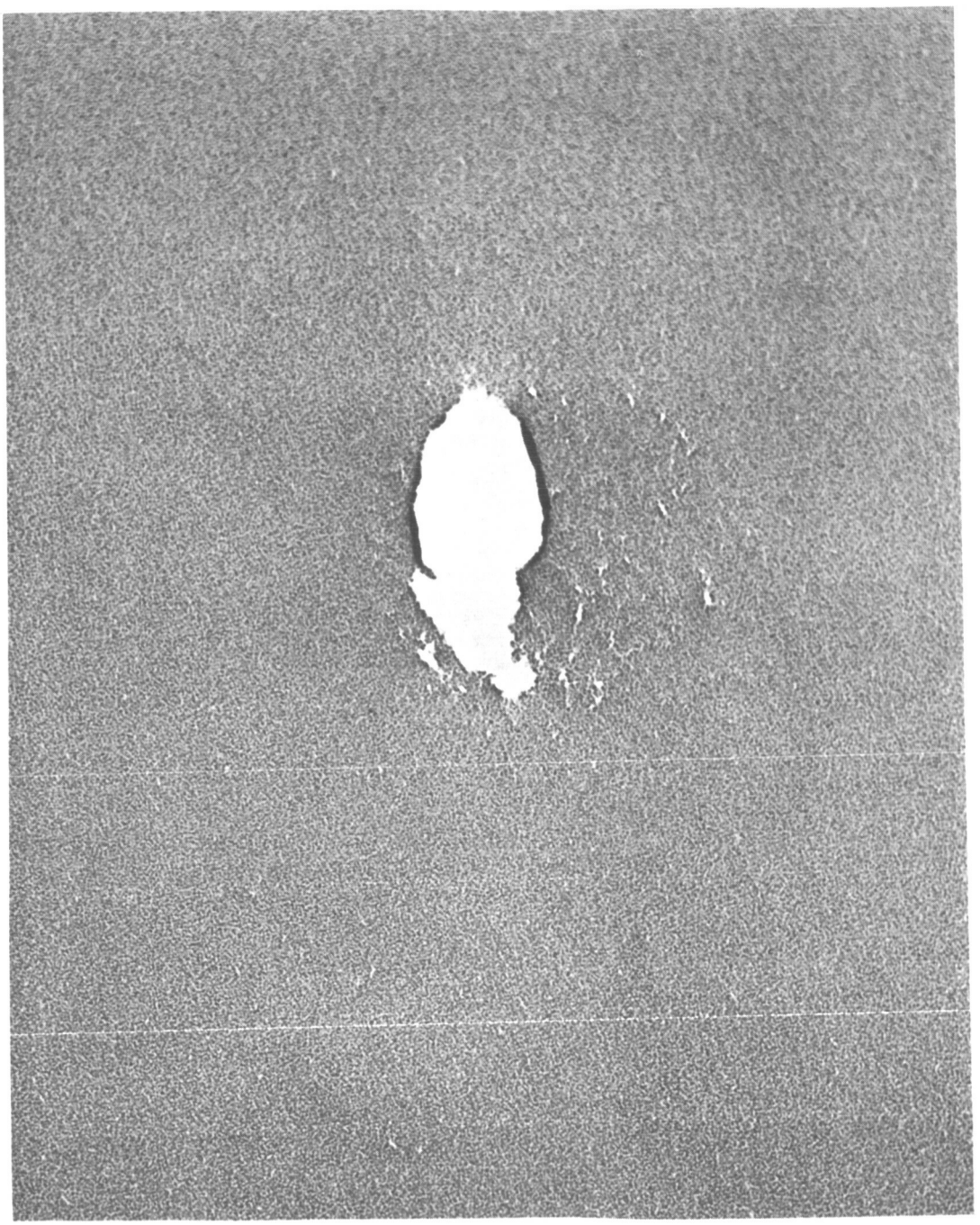

Figure 4-9.- A single large penetration plus a few small holes associated with it (40 000 X).

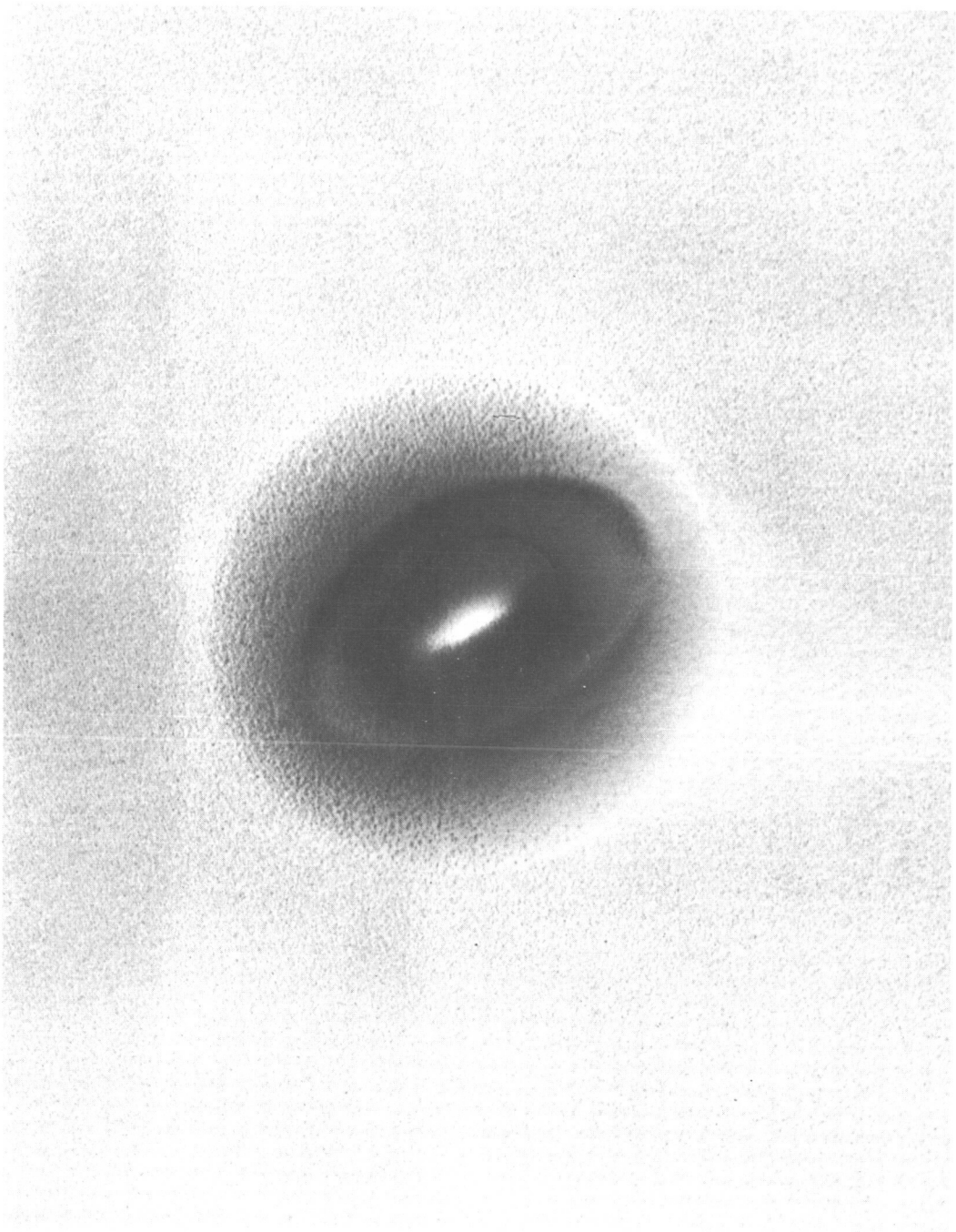

Figure 4-10.- A unique hole structure, perhaps the result of higher velocity impact (40 000 X).

5. EXPERIMENT M-5, BIOASSAYS OF BODY FLUIDS

By Lawrence F. Dietlein, M.D.,
and Elliott S. Harris, Ph. D.
NASA Manned Spacecraft Center

OBJECTIVES

The M-5 experimental measurements were made to determine the metabolic cost of manned space flight by the analysis of biological fluids. Results of the analyses were used as an indication of crewman physiological status. Where changes were found to occur, efforts were made to elucidate the mechanisms producing these changes and to assess their significance relative to space flight.

PROCEDURES

The measurements were divided into three parts. The first part, consisting of the preflight collection of two 48-hour urine samples and two blood samples from each crewman, established the baseline values for the individual crewmember. The second portion of the measurements assessed the physiological status of the crewmen as observed by analysis of the urine samples collected during flight. The final portion of the measurements, utilizing a 48-hour urine sample and the blood samples collected immediately postflight, established the rate of return to baseline preflight values. The biochemical determinations may be grouped into several profiles, each of which provides information concerning the effect of space flight on one or more human physiological systems.

The first profile, water and electrolyte balance, is related to an examination of the weight loss which occurred during flight and the mechanisms involved in this loss. The levels of sodium, potassium, and chloride in the plasma were measured preflight and postflight; and the rates of excretion of these electrolytes in the urine were observed in all three phases of the measurements. Total plasma protein concentrations, measured both preflight and postflight, were used to indicate possible dehydration. Water intake and urine output were measured to determine whether the primary loss of weight was due to sweat and insensible losses or to changes in renal function.

To support the water and electrolyte balance aspects of the measurements and to provide an indication of mechanisms involved, the hormones

vasopressin (antidiuretic hormone) and aldosterone were measured in the urine. The production of antidiuretic hormone is responsive to blood volume changes in the thorax, and it is postulated that, as in recumbency, zero g would produce an increase in the thoracic blood volume. This, in turn, would induce a decrease in the secretion of antidiuretic hormone and a resultant increase in the urinary output.

Aldosterone, a hormone produced by the adrenal cortex, is also posture responsive and controls the renal tubular reabsorption of sodium. Its secretion is decreased in recumbency and increased in an erect position. An increase in its secretion results in decreased urinary sodium, while decreased production results in increased urinary sodium.

The second profile involves the estimation of the physiological cost of maintaining a given level of performance during space flight. This could be considered a measure of the effects of stress during space flight. To this end, two groups of hormones were assayed. The first, 17-hydroxycorticosteroids, provided a measure of long-term stress responses. The second, the catecholamines, provided a measure of short-term, or emergency, responses. The measurement of these parameters will provide an objective long-term evaluation of the cost of space flight. With a sufficiently large sample, individual variations and responses will be eliminated from the evaluation.

The third profile constitutes a continuing evaluation of the effects of space flight on bone demineralization. Calcium, magnesium, phosphate, and hydroxyproline were measured in plasma and urine preflight and postflight, and were measured in urine obtained inflight. Changes in the status of bone mineralization may be accompanied by alterations in the ratio of bound to unbound calcium in the plasma. This ratio can be approximated from an estimate of plasma protein and calcium. It would also be anticipated that there would be an increase in urinary calcium, phosphate, and magnesium with demineralization. In addition, demineralization of bone is accompanied by an increased excretion of hydroxyproline. This amino acid is unique to collagen. It is presumed, therefore, that the increased excretion of hydroxyproline accompanying demineralization results from a dissolution of the bone matrix.

The fourth group, or profile, may be related to protein metabolism and tissue status. Urinary urea is proportional to protein intake and tissue metabolism, while alpha amino nitrogen increases may be related to destructive tissue changes. Creatinine excretion is a function of muscle mass, and, for a given individual, is essentially constant over a 24-hour period irrespective of diet, urine volume, or exercise. Decreases of creatinine excretion, however, are associated with loss of muscle tone and activity.

RESULTS

Two timed-48-hour urine collections were made just prior to the physicals at 10 and 3 days before launch. Blood samples were obtained during these physicals, and the samples were analyzed prior to flight to obtain baseline data. During flight, only the urine was sampled. To accomplish this, and to obtain the total voided volumes, a urine sampling and volume measuring system was used. The system consists of a valve which introduces a fixed quantity of tritiated water into each voiding. A sample of approximately 75 milliliters of each voiding is taken after adding the isotope. Upon recovery, the total volume of each micturition was calculated by measuring the dilution of tritium in the sample. Benzoic acid was used as a preservative.

Postflight plasma samples were taken upon recovery and at 6 and 72 hours postflight. Urine was collected continuously for 48 hours postflight. Each sample was frozen and returned to the Manned Spacecraft Center for analysis. Calculated flight volumes, based upon tritium dilution, presented volumes up to 12 liters per micturition. This wide, and quite evidently unrealistic, variation in urine volumes is indicative of a malfunction; therefore, no further attempt was made to analyze or interpret the inflight urine samples.

As indicated in figure 5-1, there was a marked postflight retention of water. This was accompanied by retention of sodium, potassium, and chloride. Figures 5-2 through 5-4 represent a comparison of 24-hour excretions of these electrolytes during the preflight and postflight periods. Figures 5-5 through 5-7 demonstrate the marked retention of these electrolytes when expressed on a milliequivalent per minute (meq/min) basis for each urine sample.

Urinary calcium, as shown in figure 5-8, was slightly reduced immediately postflight. The excretion of 17-hydroxycorticosteroids showed an increase immediately postflight (figure 5-9). This increase was, in all probability, due to the stress of reentry.

The increase in postflight plasma protein, and the slightly lower postflight plasma electrolytes, are consistent with a water and electrolyte loss during flight, resulting in the postflight retention of water and electrolytes, as shown in figures 5-1 through 5-7. It is still not known whether these losses result from a diuresis during flight or from sweat.

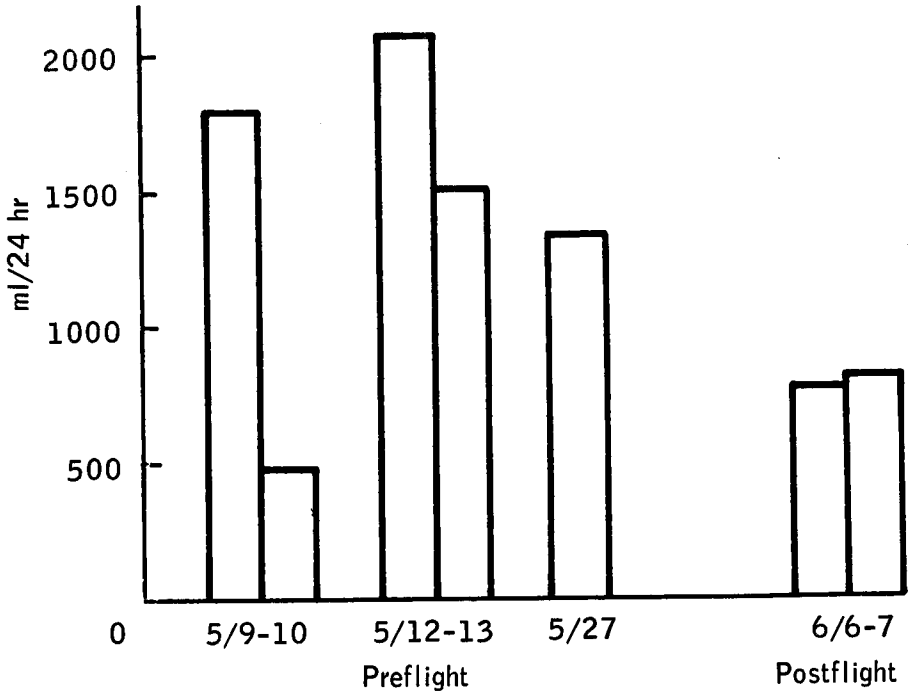

(a) Command pilot.

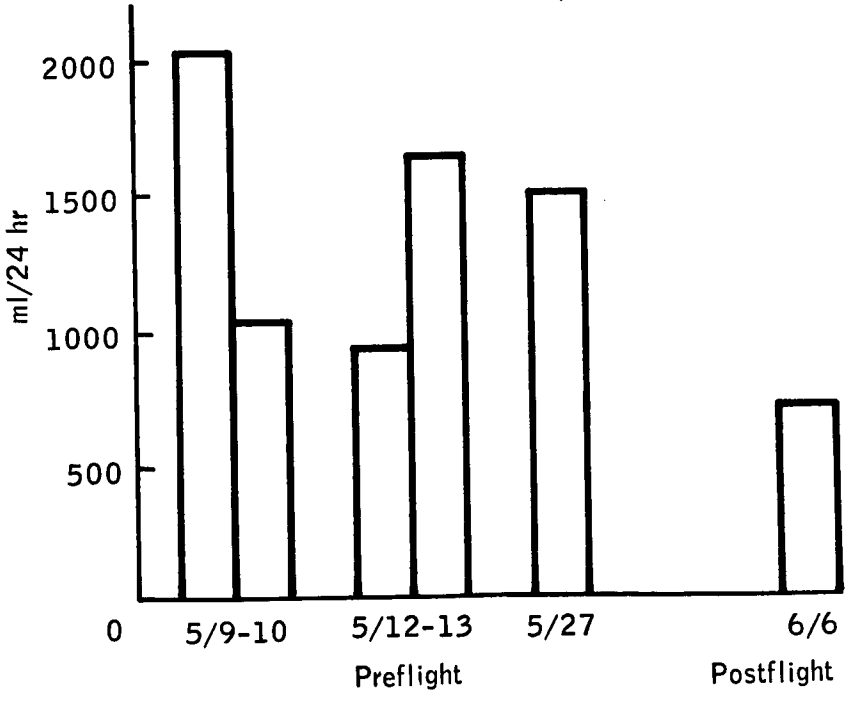

(b) Pilot.

Figure 5-1. - Total urine volumes of Gemini IX-A flight crew.

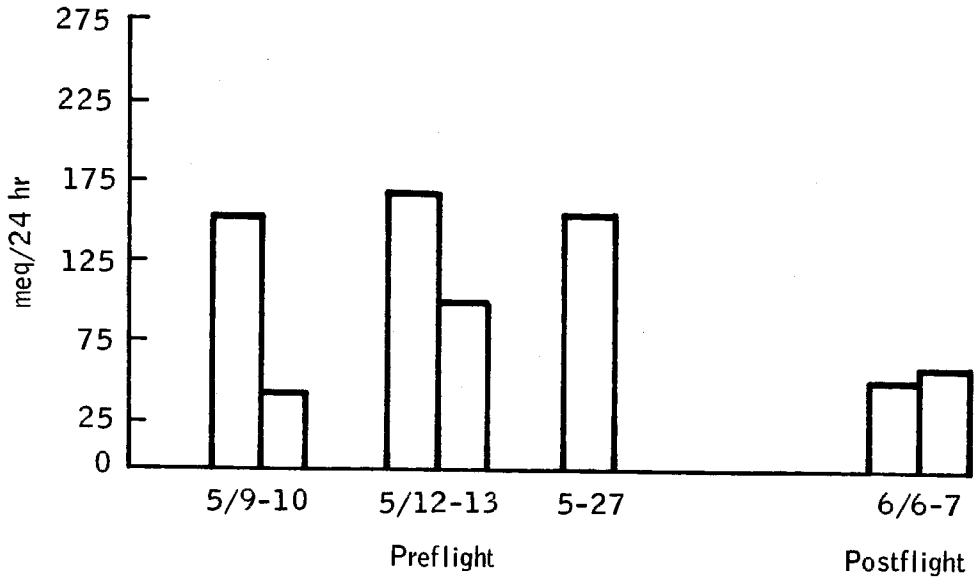

(a) Command pilot.

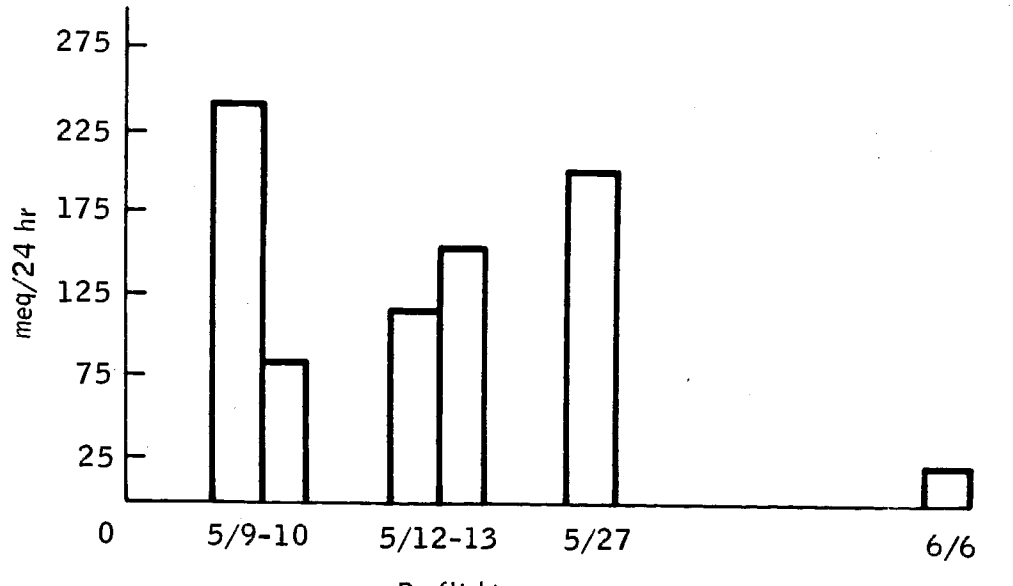

(b) Pilot.

Figure 5-2. - Urinary sodium of Gemini IX-A flight crew.

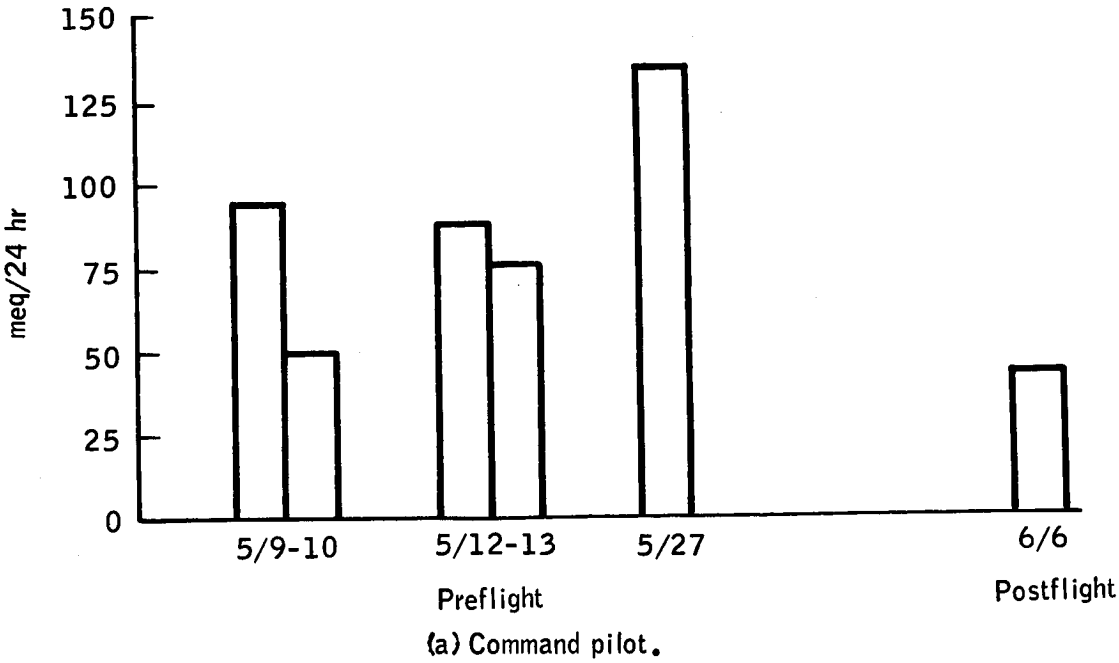

(a) Command pilot.

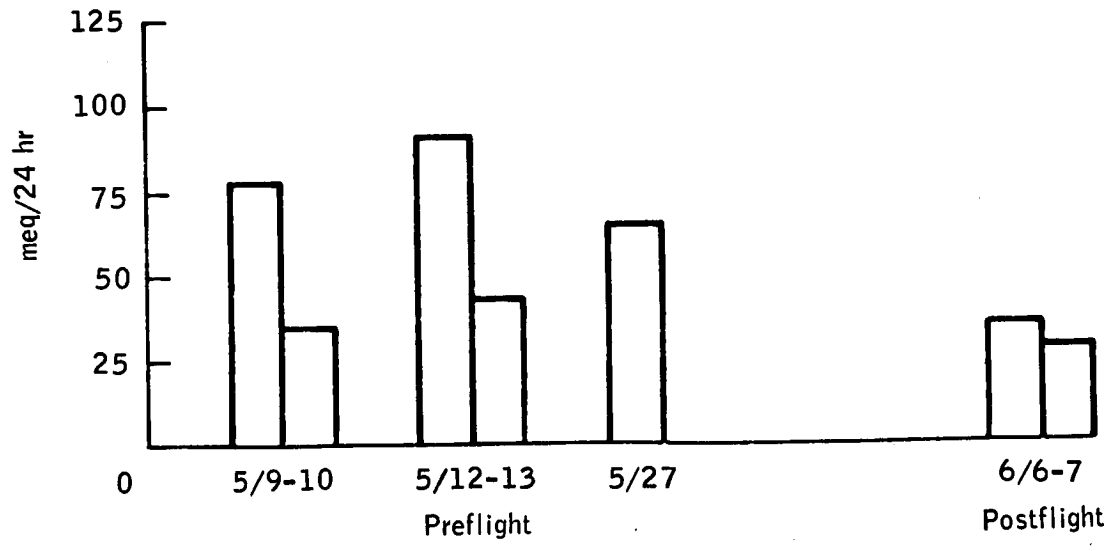

(b) Pilot.

Figure 5-3. - Urinary potassium of Gemini IX-A flight crew.

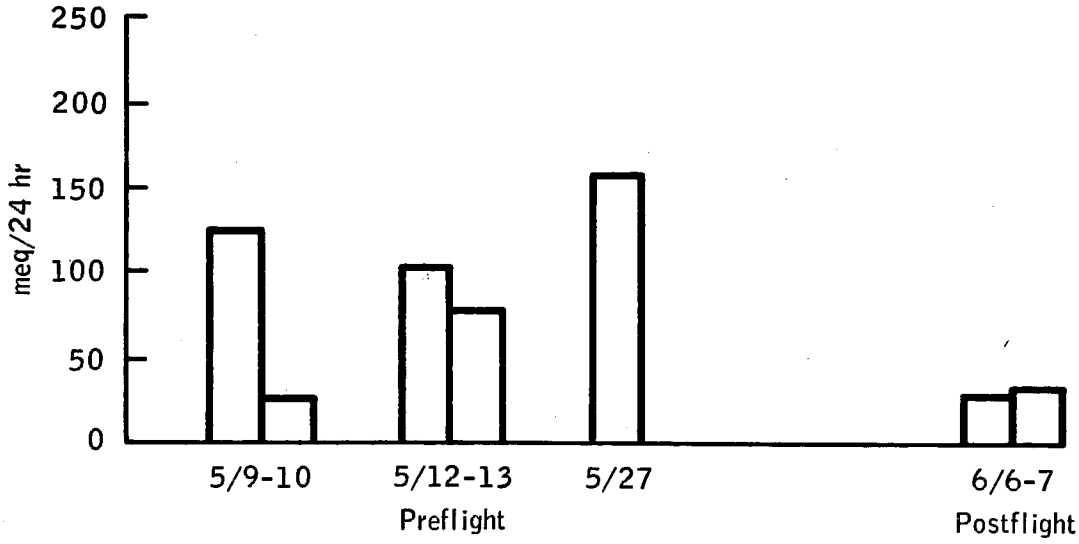

(a) Command pilot.

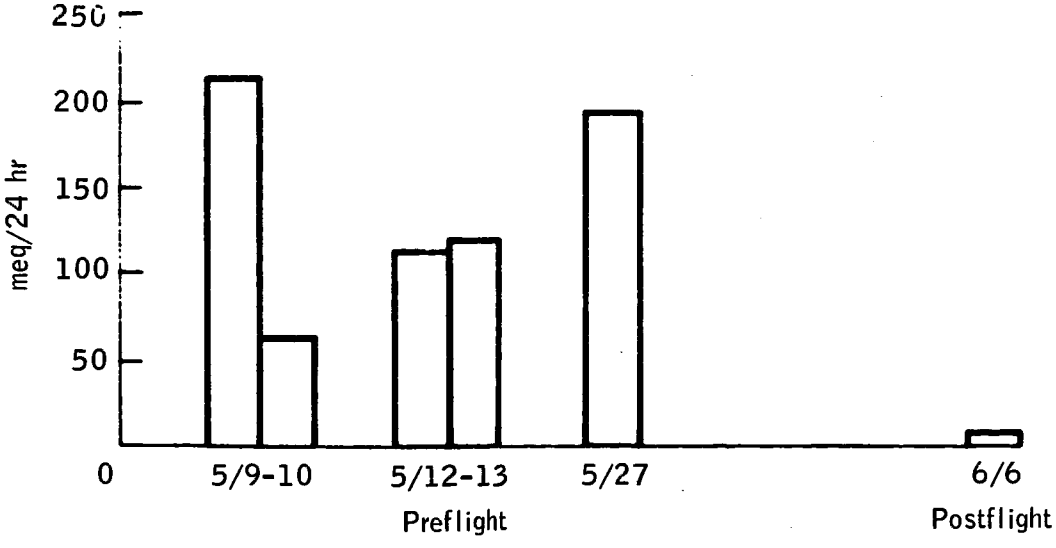

(b) Pilot.

Figure 5-4. - Urinary chloride of Gemini IX-A flight crew.

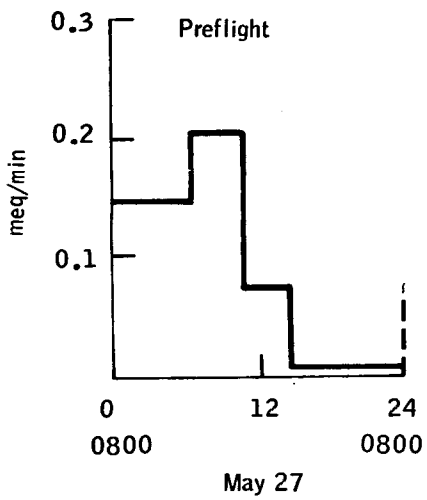

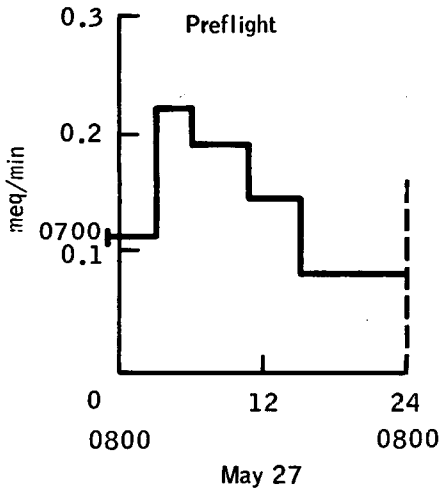

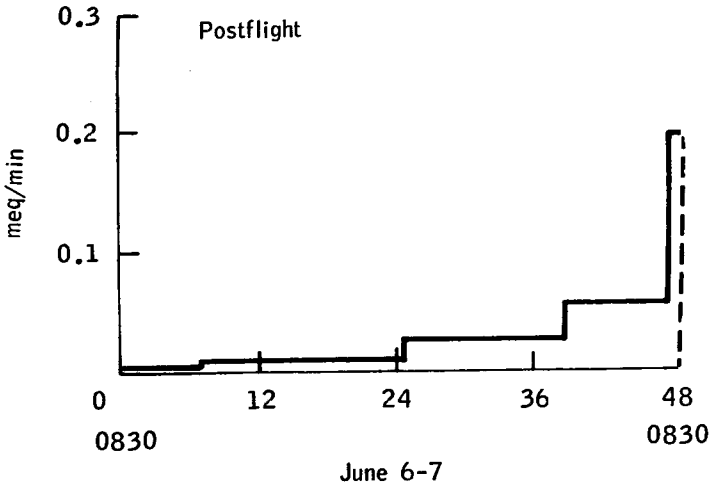

(a) Command pilot.

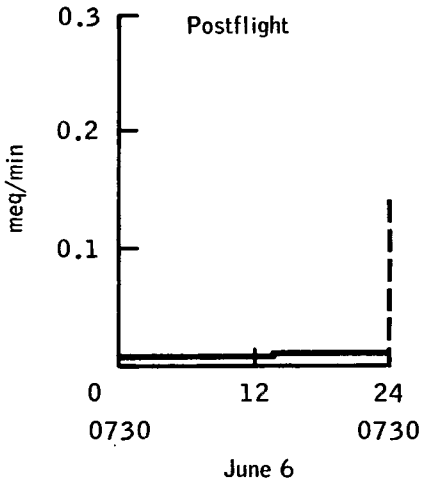

(b) Pilot.

Figure 5-5. - Urinary sodium of Gemini IX-A flight crew, meq/min basis.

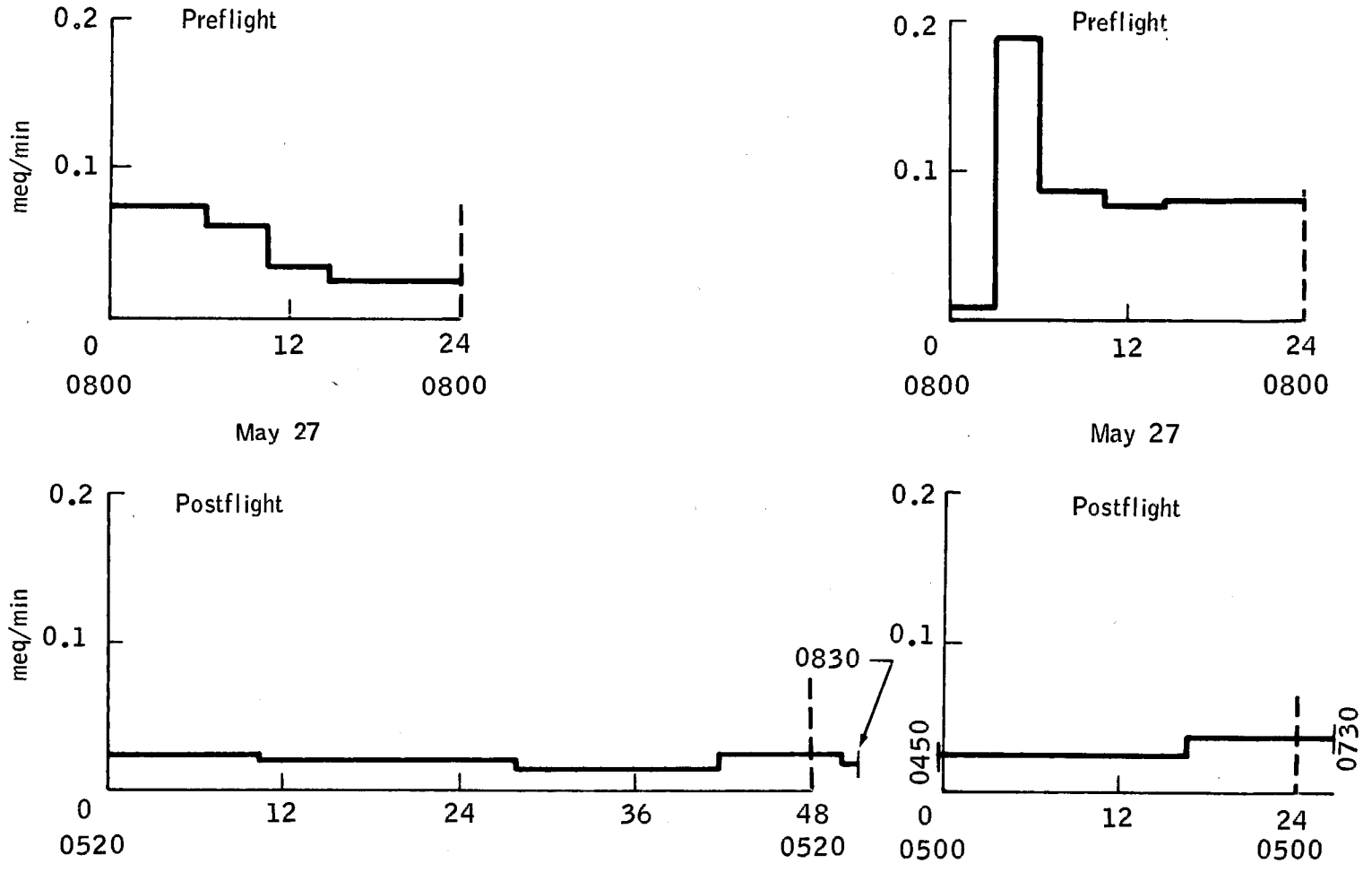

(a) Command pilot.

(b) Pilot.

Figure 5-6. - Urinary potassium of Gemini IX-A flight crew, meq/min basis.

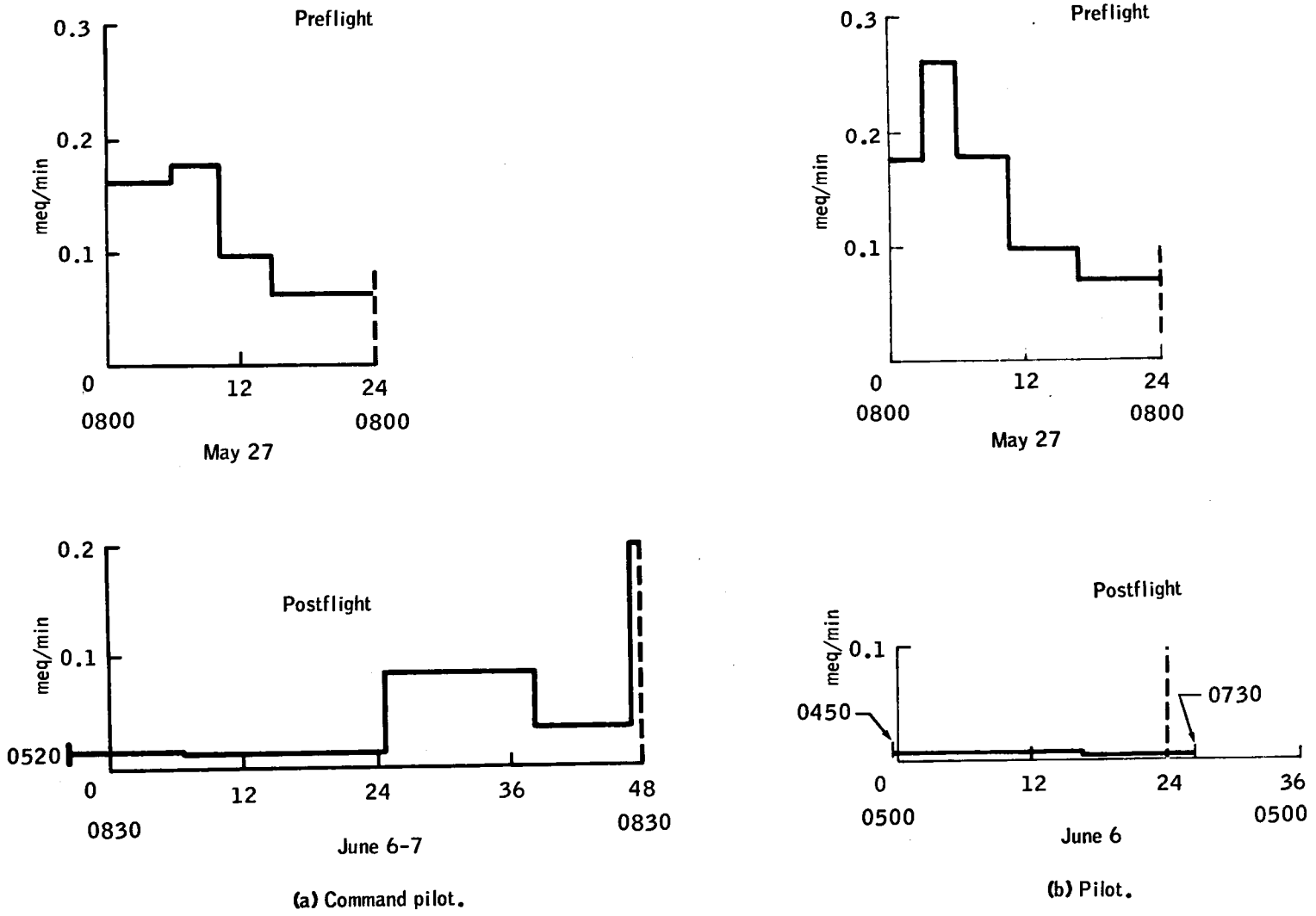

(a) Command pilot.

(b) Pilot.

Figure 5-7. - Urinary chloride of Gemini IX-A flight crew, meq/min basis.

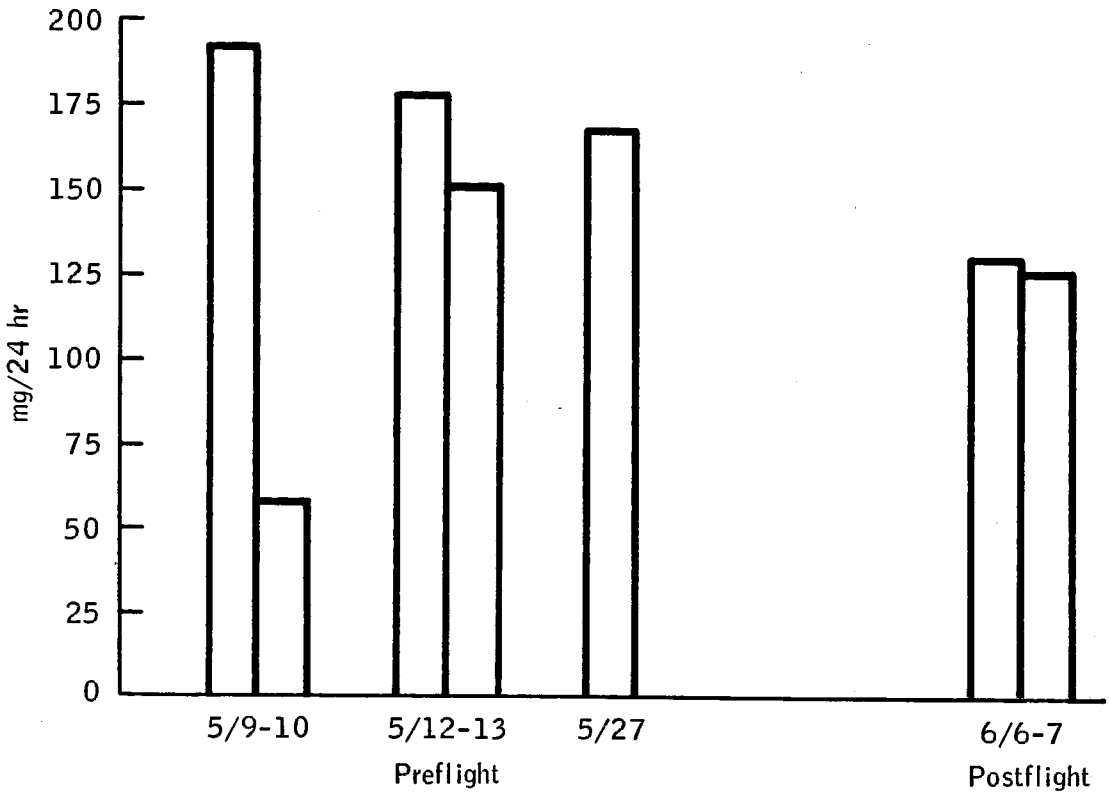

(a) Command pilot.

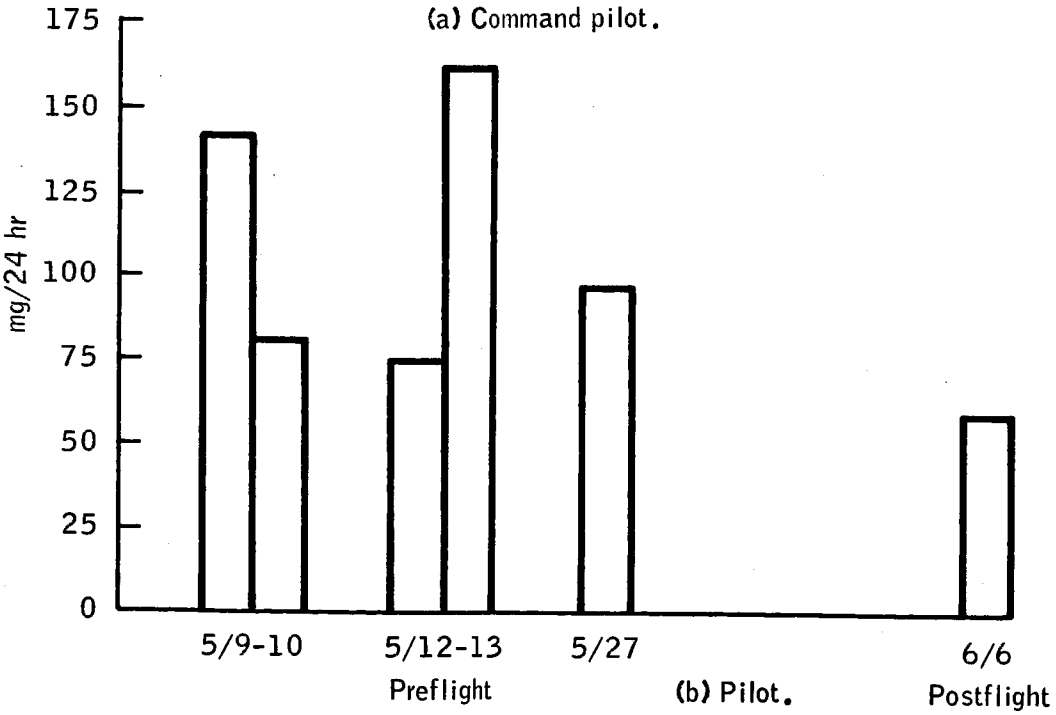

(b) Pilot.

Figure 5-8. - Urinary calcium of Gemini IX-A flight crew.

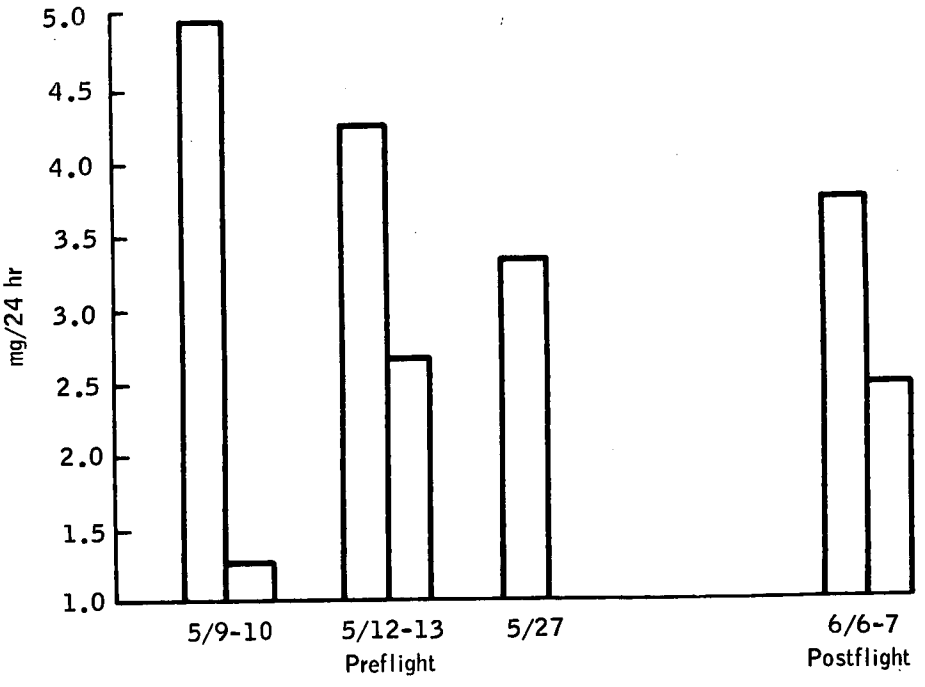

(a) Command pilot.

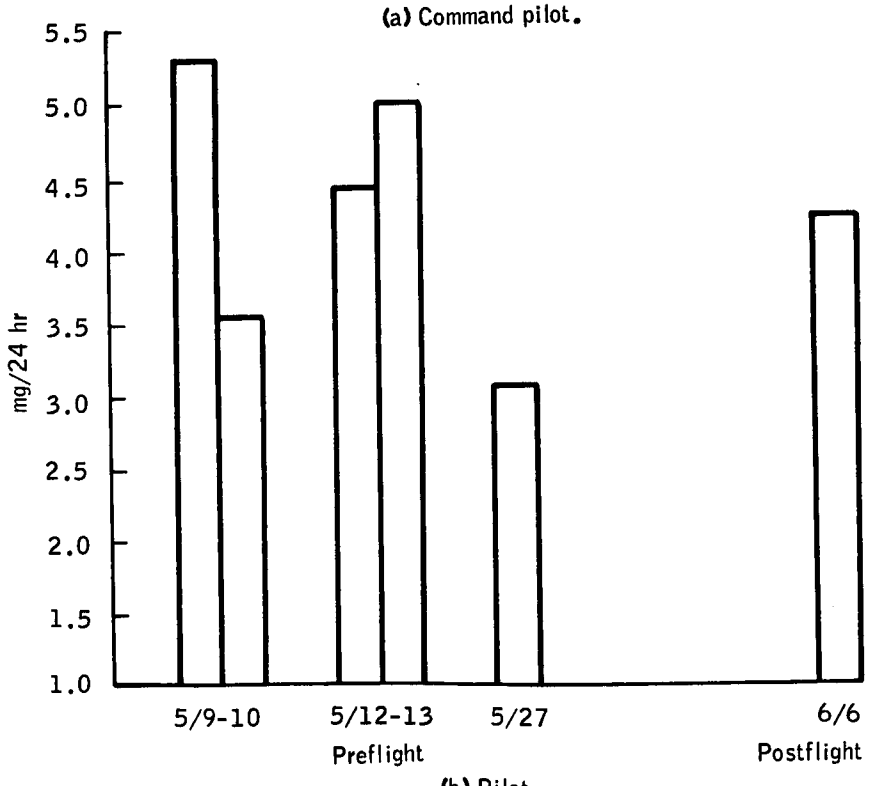

(b) Pilot.

Figure 5-9. - Urinary 17-hydroxycorticosteroids of Gemini IX-A flight crew.

6. EXPERIMENT D-12, ASTRONAUT MANEUVERING UNIT

By Captain John W. Donahue
Air Force Systems Command
NASA Manned Spacecraft Center

INTRODUCTION

Maintenance, repair, resupply, crew transfer, rescue, satellite inspection, and assembly of structures in space are all operations of potential space systems. Many of these operations involve extravehicular activity (EVA) and require man to maneuver in free space for short distances. The astronaut maneuvering unit (AMU) experiment is a fundamental step toward determining the basic hardware and operational criteria for these extravehicular activities. As an experiment, the AMU was designed to provide experience in extravehicular maneuvering operations in the Gemini missions. The experimental results should provide basic information to establish the extent that extravehicular operations will be employed in future space systems operations.

The Gemini spacecraft configuration and environment were major factors in establishing the AMU packaging configuration. The modular concept was mandatory, because stowage volume in the Gemini cabin is not adequate for the entire system, and because the life support system is needed for egress operations. The division of systems into the two basic modules, shown in figure 6-1, was selected to make maximum utilization of the extravehicular life support system (ELSS) chestpack. The chestpack contains the life support systems, emergency oxygen supply, and all of the AMU systems status and malfunction displays. The externally stored module, referred to as the backpack, contains the propulsion, flight control, oxygen supply, malfunction detection, and communications systems. With the Gemini pressure suit, these two modules comprise the AMU, a system that is essentially a miniature manned spacecraft.

The AMU mission on the Gemini IX-A flight was planned to extend over one complete revolution of the earth. The nightside operation was devoted to check-out and donning activities. Maneuvering evaluations were planned for the dayside. The donning phase of the AMU mission consists of inspection, preparation, and the actual donning. The backpack is first inspected after being subjected to the launch environment. In preparing the backpack for donning, valves and switches are positioned to activate the various AMU systems. The AMU 125-foot tether is attached; and umbilicals, harnesses, and controllers are positioned for

easy access when the crewman backs into the unit. The donning consists of changeover from the spacecraft to the backpack life support and electrical systems, checkout of their interfaces with the ELSS and suit, and separation of the AMU from its spacecraft mounting.

The flight plan called for the crewman to leave the adapter and move to the nose of the spacecraft. Limited by 25 feet of AMU tether and the ELSS umbilical, the AMU maneuvering and control capabilities were to be evaluated. If these checks were satisfactory, the full tether length was to be deployed and evaluation maneuvers were to be performed by the EVA pilot, using the augmented target docking adapter (ATDA) and spacecraft for references. Upon completion of these activities, the backpack was to be removed and discarded.

The AMU activities during the Gemini IX-A mission were terminated before the donning was completed. More work effort than anticipated was needed by the EVA pilot to maintain his position in preparing the AMU for flight. Despite this positioning problem, he completed the preparation tasks. After backing into the AMU, he reported that his suit visor was completely fogged. At this point, the AMU mission was terminated. The EVA pilot then returned to the cabin for ingress preparation.

EQUIPMENT DESCRIPTION

The backpack is a highly compact unit consisting of a basic structure and six major systems. These are the propulsion, flight control, oxygen supply, power supply, malfunction detection, and communications systems. The external features of the pack are shown in figure 6-2 and the internal equipment arrangement is shown in figure 6-3.

The structure consists of a backpack shell, two folding sidearm controllers, and folding nozzle extensions. The shell is a box-like structure consisting of three main beams and supporting shelves upon which the components are mounted. The thrusters are in the corners of the structure to provide controlling forces about the center of gravity of the entire AMU. The remainder of the components are located in the available spaces inside the pack. The total volume and shape were somewhat determined by the stowage location in the Gemini spacecraft equipment adapter section. This constraint required the folding features of the nozzle extensions and sidearm flight controllers. The sidearm controllers contain the controller heads by which the pilot commands translation and attitude. This allows the control handles to be accessible for use with the pressure suit. The nozzle extensions aim the exhaust plume from the hydrogen peroxide (H_2O_2) thrusters away from the

helmet and shoulders of the suit. A weight breakdown by system is as follows:

System	Pounds
Structure	34.4
Propulsion	62.6
Reaction control	12.7
Oxygen supply	26.9
Power supply	21.9
Abort alarm	.7
Communications	9.7
Total	168.3

Propulsion System

The propulsion system is a conventional monopropellant system using 90-percent hydrogen peroxide as the propellant and providing a total impulse of 3000 to 3500 pound-seconds. The pressurant gas is nitrogen (N_2). The major components of this system are shown in figure 6-4. Figure 6-5 is a functional schematic of the propulsion system. The nitrogen tank provides high-pressure gaseous nitrogen to a regulator, which, in turn, supplies regulated nitrogen at a nominal pressure of 455 pounds per square inch absolute (psia) to a bladder in the hydrogen peroxide tank. The selection of materials for this bladder represents one of the design problems encountered in the AMU program. Because of the storage requirement (up to 10 days), a material is required which is practically inert in the presence of H_2O_2. In addition, the bladder must be capable of several fill and expulsion cycles. The material selected has proven highly satisfactory for these applications.

The flow of propellant to the thrust chamber assemblies is controlled by the manual valves, which also control the electrical signals to the individual thruster valves. Two manual valves are provided, one for the primary control system and one for the alternate system. There are 12 thrust chambers and 16 control valves. As shown in figure 6-6, the

primary control system utilizes eight thrusters: two forward, two aft, two up, and two down. The fore and aft firing thrusters are used in various combinations to translate fore and aft, and for pitch and yaw control. The up and down firing thrusters are used for vertical movement and roll control. The alternate system uses entirely separate fore and aft firing thrusters, but uses the same thrust chambers for vertical translation and roll control. However, separate control valves are used in the alternate system for the up, down, and roll commands. Relief valves are incorporated in both the N_2 and H_2O_2 lines as a safety feature. These valves vent into thrust-neutralizing overboard vents.

Flight Control System

The flight control system provides automatic three-axis attitude control and stabilization, and provides manual translation in two axes. Translation to the side can be accomplished by a 90° roll or yaw followed by translation in one of the modes available. The major components which make up the flight control system are shown in figure 6-7. A functional block diagram is shown in figure 6-8. It should be noted that completely redundant systems are available. Manual control commands are made through the controller heads on the sidearm controllers.

The left hand controls translation commands in vertical (up and down) and horizontal (fore and aft) directions. The controller knob movement is direction oriented; that is, the knob is rotated forward to translate forward, and up to translate up. Also located on the left-hand controller assembly are the mode selection switch, a voice communication volume control, and a communications selector switch. The mode selection switch is used to select either automatic or manual attitude control and stabilization. The three-position communication selector switch permits the EVA pilot to select the most desirable mode of operation with respect to the voice-operated switches in the AMU transceiver. The right-hand controller provides control in pitch, yaw, and roll. These commands are also direction oriented. To pitch down, the control knob is rotated in the down direction; and, to yaw right, the knob is rotated clockwise. When the knobs are released, they return to the "off" position.

While under automatic stabilization, a fixed rate command (18° per second in pitch and yaw and 26° per second in roll) is entered into the control system when the knob is rotated. Then the system goes into a hold position at the attitude where the knob is released. The automatic mode will permit the pilot to park in space in a stabilized position, with the thrusters firing as required to maintain this position within a dead band of ±2.4°. In the absence of the external torques, the period of limit-cycle operation within the dead band is in excess of 20 seconds about all three axes. In the manual mode, the gyros are out of the loop,

and a direct fly-by-wire system results. While in the manual mode, the thrusters will fire only on a manual command.

Oxygen Supply System

The purpose of the oxygen supply system (OSS) is to supply expendable O_2 to the chestpack ELSS at closely regulated values of temperature and pressure. The components of the OSS are shown in figure 6-9, and a functional schematic is shown in figure 6-10. A total of 7.3 pounds of O_2 is stored in the supply tank at a pressure of 7500 psia. A minimum of 5.1 pounds of O_2 can be delivered to the chestpack at a pressure of 97 ± 10 psia and a temperature of 65° ± 10° F. Peak design flow is 8.4 pounds per hour (lb/hr), with a normal flow of 5.0 ± 0.2 lb/hr. The delivered gas pressure can be maintained at the desired value until the tank pressure drops below 200 psia. A low-level switch illuminates a warning light on the chestpack when the tank pressure reaches 800 ± 160 psia.

Power Supply System

The power supply system supplies electrical power to the AMU systems for the planned mission duration, with a 100-percent reserve capacity. The electrical power is provided by two batteries consisting of silver-zinc cells, which are enclosed in a sealed cylindrical can. The battery can is shown in figure 6-11. Two of the cans are mounted on the backpack to provide the required redundancy. One battery in the can provides power for the reaction control system (RCS). A block diagram of this arrangement is shown in figure 6-12. One set of taps on this battery provides ±16.5 volts for control logic circuitry, and a separate set of taps provides ±15 volts for the rate gyros and valve amplifiers. An entirely separate battery in the can provides 28-volt dc power for the other systems. The 28-volt power supplies in each can feed to a common bus, but are electrically isolated by diodes to prevent a short circuit of one battery from draining the other. This system is shown in a block diagram in figure 6-13. The batteries are installed as one of the last operations prior to mating the spacecraft adapter section to the launch vehicle, because the backpack is subsequently inaccessible. The batteries are isolated from the AMU systems by the main power switch, which the EVA pilot closes as part of the predonning procedure.

The power distribution unit contains mechanical fuses in all power circuits to protect the lightweight wires and cables used in the AMU electrical systems. Dual fuses are used to provide mechanical failure redundancy. That is, two fuses are used in parallel, so that if one of the fuses is blown for some reason other than an overload, the other

fuse will maintain the circuit integrity. The power distribution unit also includes the diodes which electrically separate the two 28-volt systems.

Malfunction Detection System

A malfunction detection system provides both crewmembers with a warning when certain critical out-of-tolerance conditions exist. The critical parameters monitored are low fuel pressure, low oxygen supply, low fuel quantity, and those indicative of certain control system anomalies. A functional schematic of the system is shown in figure 6-14. The warning is given both as an intermittent tone in the headset and as a warning light on the chestpack display panel. Individual warning lights that identify the out-of-tolerance system are located on the upper surface of the chestpack. A manual switch is provided to permit the pilot to silence the audio tone if he so desires, but the warning light will remain on as long as the out-of-tolerance condition exists. However, if a new alarm condition occurs, the tone will come on again, and the appropriate warning light will appear on the chestpack.

Communications System

The communications system consists of a telemetry system and a voice system. The major components of these systems, as well as the power supply and malfunction detection systems, are shown in figure 6-15. The telemetry system monitors certain backpack parameters and biomedical parameters. The information is transmitted over a radio frequency (rf) link to a tape recorder on the Gemini spacecraft. The data are available for postflight analysis only. A functional schematic is shown in figure 6-16. A list of the AMU telemetry parameters is shown in table 6-I. The voice communications transceiver is an ultrahigh-frequency (UHF) transmitter-receiver which is controlled by redundant voice-operated switches. It is designed to be compatible with the basic spacecraft onboard communications system, and utilizes the microphone and earphones in the suit. A three-position switch mounted physically on the translator controller and located electrically in the microphone circuit provides: (1) continuity of the microphone leads for normal voice-operated-switch (VOX) mode of operation, (2) opening of the microphone leads or "listen" mode, and (3) momentary closing of the leads for transmitting. A functional schematic of this system is shown in figure 6-17. The signals from both the telemetry transmitter and the transceiver are diplexed and radiated from a common antenna mounted on top of the backpack. While the AMU is stored in the spacecraft, certain parameters are fed to the spacecraft telemetry system and transmitted to the ground. The pressure and temperature of the H_2O_2 are displayed on a panel in the spacecraft cockpit.

AMU Tether

The AMU tether, shown in figure 6-18, consists of a 125-foot length of 3/8-inch nylon webbing, two hooks (H_3 and H_4), a single ring (R_2), and a bag for stowage. At one end, a hook (H_4) is provided for attachment to the spacecraft/ELSS umbilical tether. This hook permits transversal 125 feet from the umbilical. The second hook (H_3) is located 100 feet from the first. When attached to the umbilical tether, hook H_3 limits the tether length to 25 feet. A ring (R_2) on the opposite end of the tether attaches to a hook (H_2) on the astronaut suit harness.

AMU INTERFACES

Gemini Spacecraft

The AMU backpack is installed in the Gemini equipment adapter before mating the spacecraft to the launch vehicle. Locations of the AMU and the associated spacecraft hardware are shown in figure 6-19. Mechanical mating to the spacecraft is accomplished by mounting a four-legged structure or claw assembly to the backpack and by using a tension bolt to pull the claw down firmly against a sheet metal structure (torque box assembly). The torque box is then hard-mounted to the blast shield door. The bolt is severed by an electrically-detonated pyrotechnically-operated guillotine. The guillotine is actuated from the cockpit after the AMU has been donned during the extravehicular mission. A pull-away electrical connector provides instrumentation and power leads for cabin monitoring and for ground servicing and testing.

Servicing provisions.- To permit servicing of the AMU with hydrogen peroxide after mating the spacecraft to the launch vehicle, a service line is provided from the external surface of the adapter to the AMU H_2O_2 fill port. A second parallel line to the AMU regulated nitrogen port allows reservice of the system in the event an unstable condition in the H_2O_2 is detected, or if the launch is delayed indefinitely. If, for some reason, the H_2O_2 should become unstable and the pressure of the system should rise above 575 psia, the AMU relief valve would open and the H_2O_2 would be vented through a third line to the adapter skin. The fill and reservice lines are severed by the same guillotine which releases the AMU. The vent line is routed through a spring-loaded pull-off housing that is separated when the AMU is released.

Thermal interface.- Because of the temperature limitations of 40° to 100° F for various AMU components, a cover assembly is placed over the AMU to provide passive thermal control. This cover rests against the aerospace-ground-equipment attachment points on the front of the AMU. A line maintains the cover in this position. This line passes through the center of the AMU to a hard-mounting point on the torque box assembly. The line is severed and the cover is jettisoned by operation of the cockpit "EVA BARS EXTENSION" switch.

Donning hardware.- Equipment is provided in the adapter to assist the EVA pilot in donning the AMU. This hardware, shown in figure 6-20, consists of a footrail, two handbars, an umbilical guide, and two floodlights for nightside operation. This equipment is deployed and properly positioned for AMU donning simultaneously with release of the thermal cover.

Instrumentation and communications.- To obtain AMU performance data, a telemetry receiver, capable of accepting the diphase pulse code modulation (PCM) format transmitted from the AMU, is installed on the electronics module in the spacecraft adapter. The receiver demodulates the 433-Mc received signal and provides a 5120-bits-per-second diphase signal to the spacecraft PCM recorder. These data are recorded and stored for postflight analysis.

Two whip antennas are mounted on the adapter surface to receive the AMU telemetry transmissions. Only one antenna is utilized at any time. The proper antenna is selected by coaxial switching from a signal provided by the telemetry receiver. The receiver provides automatic control of the coaxial switch to change antennas when the rf signal on the antenna in use drops below the preset level.

Although propellant status is monitored in the cockpit, the same pressures and temperatures can be monitored through normal spacecraft telemetry to the ground. A 0 to 715 psia transducer and a thermistor in the AMU propellant tank are powered by the spacecraft for spacecraft telemetry channel RA01, H_2O_2 pressure, and channel RA02, H_2O_2 temperture. Readings of H_2O_2 pressure are available until the AMU telemetry switch is placed in the "backpack" position during the donning phase of the extravehicular mission. Temperatures of H_2O_2 can be read until AMU separation from the spacecraft.

During the AMU mission, the spacecraft UHF transceiver is used to maintain communication between the extravehicular pilot and command pilot. This transceiver is voice operated at 296.8 Mc.

Crew station displays.- Spacecraft crew station displays and controls (figure 6-21) are as follows:

(1) The propellant temperature and pressure indicator gage indicates pressure and temperature of the H_2O_2 propellant stowed in the AMU.

(2) The warning light for H_2O_2 pressure is illuminated when pressure reaches 575 ± 20 psia.

(3) The "BUS ARM" switch, located on the Agena control panel, must be in the "EXP" position to energize experiment squib circuits before AMU cover release, footrail extension, telemetry antenna deployment, and AMU release.

(4) The "MMU" switch provides several functions. In the spring-loaded "DEPLOY" position, the AMU is released by guillotine cutting of the hollow retention bolt and servicing lines. In the telemetry switch "on" position, the telemetry receiver and its associated antenna coaxial switch are powered; and the tape recorder is activated.

(5) The "INDEX BARS/EVA BARS EXT" switch, when placed in the "EVA BARS EXT" position, releases the AMU thermal cover and deploys the footbar and handrails to the operational position. In addition, the AMU telemetry antennas are deployed to permit reception.

Extravehicular Life Support System

The ELSS becomes an integral part of the AMU system during the donning phase of the extravehicular mission. It provides electrical, mechanical, and life support connections between the extravehicular pilot and the AMU. Through an umbilical from the AMU oxygen supply system, oxygen is delivered to the ELSS environmental control system at 97 ± 10 psia and 65° ± 10° F. To allow oxygen flow, a quick disconnect on the umbilical is attached to a mating connector on the ELSS. The OSS interface was discussed earlier under the AMU backpack systems. Other AMU/ELSS interfaces are presented in the following paragraphs.

AMU restraint harness interface.- A restraint harness is provided as part of the backpack. The harness holds the backpack to the space suit by pressing on the forward surface of the ELSS.

Malfunction detection system interface.- Four alarm lights, visible to the EVA pilot, are provided on the ELSS to indicate out-of-tolerance conditions in the backpack propulsion (fuel quantity and pressurization), the oxygen supply, and the reaction control subsystem. The lights are

activated by electrical signals from the backpack through the AMU electrical umbilical. The signals are continuous as long as an alarm exists. Light arrangement and function are as follows:

(1) The oxygen warning light illuminates at 800 ± 160 psia tank pressure or when O_2 temperature drops below 5° ± 5° F.

(2) The fuel quantity warning light illuminates when 30 percent of the total fuel remains.

(3) The fuel low-pressure warning light illuminates at an N_2 pressure of 650 ± 100 psia or H_2O_2 pressure of 350 ± 50 psia.

(4) Certain critical functions of the reaction control system are monitored, and the failure of any one of the functions will result in illumination of the warning light.

A switch is installed on the ELSS to test the operation of the alarm lights and portions of the backpack abort alarm subsystem. The test signal to the backpack is provided through the electrical umbilical. The ELSS supplies a 1700-cycles-per-second audio tone signal to the backpack radio receiver-transmitter upon receipt of a signal from the AMU alarm subsystem through the electrical umbilical. The signal to the backpack is continuous until the reset switch, which is located on the top of the ELSS, is actuated. This action generates a signal to backpack, via the electrical umbilical, to reset the alarm trigger in the backpack.

Telemetry interface.- The backpack telemeters the following parameters received from the spacesuit and ELSS through the electrical umbilical:

(1) Electrocardiogram

(2) Respiration rate

(3) Suit pressure

Hydrogen peroxide quantity indication interface.- A meter, visible to the EVA pilot, is provided on the ELSS to indicate quantity of H_2O_2 in the backpack. Signals are supplied to the meter from the backpack through the electrical umbilical.

Gemini Suit

An exhaust-plume heating analysis, conducted early in the program, indicated that the Gemini thermal coverall materials would be heated beyond acceptable limits during an AMU mission. As a result, the decision was made to add extensions to the upper forward thrusters and to modify the leg portion of the basic Gemini coverall. Eleven layers of superinsulation (a woven fabric, a superinsulation spacer material of fiberglass, and an aluminized reflective material) were used. The nozzle extensions were evaluated to determine their effect on performance, systems design, and predonning activities. Performance tests on extension configurations indicated that the extensions could be added without markedly affecting thruster performance. Thermal analysis of the selected design verified this solution of the heating problem associated with the upper forward firing thrusters.

Prior to the Gemini IX mission, the Gemini VIII extravehicular glove was adopted because its mobility and tactility characteristics were superior to the glove which had been developed for the AMU application. The Gemini VIII glove afforded very little thermal protection from the AMU exhaust plume, and protective shields were put on the AMU controllers. Although temperatures on the gloves are significantly lower than those anticipated in the leg areas, the shields utilize the same materials and layup as the modified extravehicular coverall.

AMU/GEMINI IX-A FLIGHT PLAN

The AMU mission on the Gemini IX-A flight was planned to cover one complete revolution around the earth. The nightside was to be devoted to checkout and donning activities, and the dayside was to be devoted to maneuvering evaluation. Electrical power, oxygen, and propellant supplies limit the maneuvering or independent operating capability of the AMU to approximately 1 hour.

At dark, the EVA pilot was to move via handholds along the surface of the retroadapters and equipment adapters to the interior of the equipment adapter to check out and don the backpack. After positioning himself on the footrail, he was to proceed with the predonning checkout of the AMU, which consisted of the following:

(1) Visually checking the O_2 supply-system and N_2 tank pressures to verify adequate supply levels

(2) Manually opening the O_2 and N_2 supply-tank shutoff valves

(3) Turning on the master electrical-power switch

(4) Unstowing the sidearm controllers and arranging the restraint strap, electrical umbilical, and O_2 umbilical in the donning positions.

Assuming satisfactory systems checks, the EVA pilot would back into the AMU using the handholds and footbars for support. Attachment of the single restraint strap across the front of the chestpack would physically unite the chestpack and backpack. The backpack OSS would be connected to the chestpack ELSS through a separate connector, so that external (to the chestpack) O_2 supply would be uninterrupted. To verify satisfactory operation, the command pilot would manually shut off the external supply before the spacecraft O_2 umbilical was disconnected. The spacecraft umbilical electrical connector and the backpack electrical connector both attach to the same chestpack connector. Since voice communications are carried through this chestpack connector, they would be interrupted briefly during the changeover operation.

After the check-out, donning, and changeover operations were complete, the backpack would be released from its adapter mounting by the command pilot by cutting the attachment bolt and propellant servicing lines. The propellant vent line and the electrical cable are equipped with pull-away connections. After release, the EVA pilot would return to the spacecraft cabin area, via the handrails, to detach the spacecraft umbilical and complete attachment of the AMU tether.

The command pilot would keep the EVA pilot in sight while the EVA pilot performed the initial flight check-out on the 25-foot section of the tether. The EVA pilot would make short translations and rotations about all three axes by exercising both primary and alternate propulsion systems while operating in both stabilized and manual control modes. Following these checks and the performance of enough familiarization maneuvers for pilot confidence in the AMU, the 25-foot tether hook would be detached to permit full tether use. Maneuvers would be performed to evaluate control capability, fuel usage in both stabilized and manual control modes, station keeping, and rendezvous.

After the AMU mission, the pilot would return to the spacecraft nose area to retrieve the spacecraft umbilical. The reverse of the donning changeover, release of the backpack into space, and a normal ingress would be performed. If retrieval of the spacecraft umbilical were not practical, the emergency supply of O_2 in the chestpack could be used for ingress.

RESULTS

The AMU was serviced for flight prior to the initially planned launch date of May 17, 1966. Monitoring of the propellant status (H_2O_2) after launch cancellation indicated a stable pressure rise of 0.2 psia per hour due to normal active-oxygen loss, which was well below the allowable of 0.6 psia per hour. The decision was made not to reservice the propellant. At launch on June 3, 1966, the pressure had increased to approximately 87 psia, a nominal condition for launch.

The O_2 and N_2 systems, which were monitored through special ground equipment, showed no leakage. Fresh batteries were installed in the flight unit on May 25, 1966. A subsequent telemetry check of the AMU indicated that all systems were operating normally.

Immediately after launch, the propellant tank pressure increased to a normal 90.7 psia, where it remained until donning check-out. The propellant temperatures were normal at 72° to 77° F.

When the EVA pilot began the AMU experiment, the left adapter handhold and the umbilical guide were not fully extended; and the AMU adapter thermal cover was not completely released. Also, the left adapter EVA light was not operating. When the pilot pulled on the handhold to enter the adapter, the handhold and umbilical guide moved to the fully-deployed position which released the thermal cover. Donning activities and AMU inspection were completed through the point of connecting the AMU electrical umbilical. These activities included attaching portable penlights, opening the N_2 and O_2 shutoff valves, readout of O_2 and N_2 pressures, positioning the sidearm controllers, positioning the umbilicals and the AMU restraint harness, attaching the AMU tether, turning on the AMU electrical power, and changeover to the AMU electrical umbilical. The O_2 pressure was a normal 7500 psia, and N_2 pressure was normal at approximately 3000 psia. The propulsion system pressure after N_2-valve opening was 455 psia (normal for AMU operation). Because of the difficulty in maintaining position in the adapter, donning activities required a much longer time to complete than expected. The pilot tended to drift away from the work area in the adapter. Position could not be maintained, because both hands were required to extend the sidearm controllers and attach the AMU tether. AMU communications to the command pilot were garbled, but were considered acceptable by both pilots.

Because of the loss of visibility due to visor fogging, the command pilot decided that the AMU experiment could not be completed. The EVA pilot then disconnected the AMU umbilical, connected the ELSS

umbilical, and returned to the cockpit for ingress, leaving AMU power on. The AMU remained in the adapter with the systems activated for flight until retrofire.

Termination of the EVA precluded an evaluation of most of the AMU performance capabilities. However, the backpack successfully experienced a Gemini launch and a 2-day exposure to the space environment. Most of the functions of check-out and donning were performed prior to aborting the mission. Although the AMU was transmitting telemetry data following power-up during the predonning activity, failure of the Gemini data recorder precluded a quantitative analysis of AMU performance. Analysis of the AMU systems, therefore, is primarily based on debriefing comments by the flight crew.

Prelaunch

Stored gaseous expendables, O_2 and N_2, were only serviced prior to May 6, 1966. Both tank pressures indicated a full charge when they were checked on May 29, 1966. The AMU was serviced with H_2O_2 on May 15, 1966. Ullage pressure built up from the initial 19.7 psia to 87.9 psia at launch. The final prelaunch pressure could not be determined precisely because of a slow leak in the ground servicing and monitoring equipment. Temperature of H_2O_2 was comparable to that afforded the spacecraft during the prelaunch period.

Both batteries were replaced on May 21, 1966, because they were approaching their demonstrated lifetime. The replaced batteries had been activated on May 5, 1966, and were considered good for rated load until June 13, 1966.

No major problems were encountered in the installation of the AMU in the adapter. Some interference was encountered in installing the AMU thermal cover because of the AMU sidearm controller thermal shields. After evaluation, the interference was judged acceptable for flight.

Readings on the cockpit H_2O_2 pressure gage were approximately equivalent to telemetry readings through the prelaunch period. However, the cockpit temperature gage read 6° F lower than the telemetry readings. The range of the cockpit H_2O_2 pressure gage was 0 to 500 psia, and the range of the cockpit temperature gage was -100° to +200° F. Both gages had small dial faces. These instruments are difficult to read closer than ±10 psia and ±10° F, respectively.

Launch

The only AMU parameters available during launch were H_2O_2 pressure and temperature. No change in either parameter was detected by the crew, who monitored both parameters periodically during the launch. No temperature change was noted on telemetry during launch. An increase of two PCM counts in H_2O_2 pressure (approximately 6 psia) was recorded on telemetry at lift-off. No change in H_2O_2 pressure was noted during the launch.

Orbit

During an approximate 2-day pre-EVA period, H_2O_2 pressure and temperature were monitored. These parameters were monitored by telemetry at least once per orbit. Low activity of both parameters resulted in few cockpit readouts. During the pre-EVA period, the predicted active oxygen loss (AOL) buildup was continuously computed and plotted against the recorded AOL buildup.

Actual AOL pressure buildup was much lower than predicted. (A rise of 8.5 psia had been predicted.) During the 50 hours 37 minutes before the backpack telemetry switch was changed to "backpack" (during AMU donning), the total pressure rise was less than one PCM count (3 psia).

It was predicted that H_2O_2 temperature would decrease. During the pre-EVA period, the temperature varied from 69° to 78° F. Readings on the cockpit gages during this period were 69° F for temperature and 90 psia for pressure.

Detailed Extravehicular Activity

On this mission, ingress to the spacecraft adapter was accomplished at 50:09:00 ground elapsed time (g.e.t.). Dangling lines or lanyards, as seen on the Gemini VII/VI-A flight, were not encountered. The thermal cover and left handhold had not fully deployed. The EVA pilot grasped the handhold while entering the adapter. Both the handhold and the thermal cover deployed normally at this time. Standing on the footbar, the EVA pilot pulled out some of the slack in the umbilical. The umbilical guide only allowed some movement in the cockpit direction, but the pilot reported enough umbilical slack for AMU donning.

The adapter floodlight to the left of the predonning position was not on. The pilot removed the two penlights from the tether bag and

turned them on. One of the lights did not work. The operating penlight was mounted on the side opposite the functioning floodlight. This lighting arrangement was considered marginal for night donning activities. The mirrors were unstowed and positioned. The AMU was found in the prelaunch configuration when examined by the pilot.

At 50:19:00 g.e.t., the black hook on the tether jumper was attached to the ring on the AMU tether. A short piece of tether was secured to the AMU seat, which provided a three-point support (both feet and the tether), and freed one of the EVA pilot's hands to snap the hook over the ring. Next, the tether bag was unstowed from the AMU and the pilot tried to attach the small AMU tether hook (the 125-foot portion) to the ring on the tether jumper. This operation proved very difficult; the EVA pilot was unable to connect the small hook to the ring. The decision was made to either connect the small hook after donning or to operate only on the 125-foot tether. During this time, the EVA pilot changed the setting on the ELSS to high flow because of a hot spot on his back.

At 50:28:00 g.e.t., the EVA pilot unstowed and checked the sidearm flight controllers. Unstowing the attitude controller proved difficult under both one- and two-hand operations. His feet slipped out of the footbar stirrups during this task. This tendency to slip was noted earlier during the tether hookup and was the principal difficulty experienced in the adapter. Unstowing was finally accomplished by using both hands and a quick, hard pull. Fogging on the suit faceplate was also noted at this time.

At 50:31:00 g.e.t., the EVA pilot unstowed the O_2 umbilical, electrical umbilical, and restraint harness without difficulty. The VOX switch was difficult to reach and check with the controller in the down (donning) position.

At approximately 50:33:00 g.e.t., the N_2 and O_2 shutoff valves were opened. The N_2 valves opened easily, but more than one try was needed to open the O_2 valve. The EVA pilot reported that the control was tighter than during any simulation. Finally, the valve opened easily until it hit the stop. The pilot read both pressure gages on the front of the backpack. Readings of 7500 psia on the O_2 gage (which is normal) and approximately 3000 psia on the N_2 gage (normal 2775) were reported. The O_2 gage was fairly easy to read, but the N_2 gage was read with some difficulty. The command pilot reported that the H_2O_2 pressure rose to

450 psia immediately after the N_2 valve was opened and then rose slowly to 455 psia, which is nominal regulated pressure.

At 50:37:00 g.e.t., the EVA pilot deployed the nozzle extensions, switched the H_2O_2 transducer from spacecraft to backpack telemetry, and turned on the main power switch. The upper position lights were illuminated. Fogging of the EVA pilot's visor and of his suit pressure gage was, again, reported.

At 50:39:00 g.e.t., the pilot backed into the AMU. After turning and positioning himself in the AMU with his feet on the footbar, he had no difficulty maintaining position.

At 50:42:00 g.e.t., the pilot changed over to the AMU electrical umbilical. No difficulty was encountered in making the change. The RCS warning light came on and the warning tone was heard by both the EVA pilot and the command pilot. The pilot reset his tone and the light remained on. At this point, the spacecraft onboard voice tape ran out. The pilot and command pilot communicated rf until the AMU mission was terminated. The pilot reported that his reception was clear, but it was slightly low in volume and had background noise. He reported no anomalies in the side tone from his transmissions. The command pilot reported the pilot's transmissions to be abnormal after the first syllables. This anomaly was described as wavering noise superimposed on the transmission. The command pilot considered it marginally acceptable but noted that extensive training in the donning exercise permitted him to construct the pilot's messages from less than complete transmissions. The EVA pilot used both AMU switch positions (normal VOX and listen mode) during the transmissions, and the command pilot used both the VOX and push-to-talk (PTT) mode of the spacecraft voice control center.

The pilot checked out the displays and the warning lights on the ELSS and determined that they were normal. The H_2O_2 quantity reading was reported at 85 percent (normal for a full load of H_2O_2).

The EVA pilot located the restraint harness and assured himself that he could hook it up, but he delayed hookup until he could see well enough to check his connections. Complete visor fogging was noted by the pilot at this point. The crew decided to forego complete donning until the fogging problem was alleviated. While resting and awaiting sunrise, the pilot raised both sidearm controllers and locked them in the flight position. The orientation of the plume shields on the attitude controller did not appear correct, but the control head was extended approximately to the correct length. The controller head could not be turned with one hand to check its position. When the pilot left the donning station later, he twisted the control head and thought he detected a further extension of the arm.

Sunrise occurred at 50:56:00 g.e.t., and the pilot attempted to use the donning mirrors to check his configuration with the AMU. At 51:00:00 g.e.t., his visor was completely fogged and he was unable to use the mirrors.

At 51:03:00 g.e.t., the command pilot declared a no-go condition for the AMU evaluation. In postflight debriefing, the EVA pilot reported that the AMU was acceptable for flight in all respects. The decision to abort was based on the unknown that was associated with the visor fogging problem and the fact that the visor fogging caused a behind-schedule condition. The pilot changed over to the spacecraft electrical umbilical and egressed from the adapter without incident.

Post EVA

There were no established procedures for conditioning a backpack that was to be left in the adapter section subsequent to an abort. After the pilot returned to the cockpit, and the cockpit was repressurized, the backpack condition was as follows:

Portion	Position
Main power switch	On
RCS handles	Off
Telemetry switch	Backpack
N_2 valve	Open
O_2 valve	Open
Attitude controller	Flight position (horizontal)
Translation controller	Down position
Electrical umbilical	Stowed on translation controller
Oxygen umbilical	Probably stowed on translation controller
Restraint straps	Stowed on translation controller

The AMU was left in the adapter because of the unknowns associated with jettisoning it in its postdonning configuration. Tests had shown there was no potentially hazardous condition in the backpack, with the possible exception of the propulsion system. An unsafe condition would occur only if the pressure of the H_2O_2 propellant increased significantly. Adequate instrumentation was available to detect an impending unsafe condition in the H_2O_2 (telemetry, cockpit gages, and cockpit warning light). Previous flight data had shown that the H_2O_2 was extremely stable. The H_2O_2 pressure rise from EVA through retrofire was no greater than expected, and it was not necessary to jettison the backpack.

CONCLUSIONS

All AMU systems exercised during the mission were in an acceptable condition for flight when the AMU evaluation was terminated. Some difficulty was experienced with reception of the AMU voice signal by the command pilot. The AMU transceiver, the spacecraft transceiver, and the conditions in the adapter must be investigated to determine the cause of this problem.

All of the donning provisions appear practicable in the orbital environment; however, the donning activities were more difficult to perform than experienced in the one- and zero-g training exercises. Improvement of the restraint hardware at the donning station is needed. Lighting was marginal due to the failure of one adapter floodlight and one penlight. This condition must be corrected.

The crew reported a tendency for the EVA pilot and any loose equipment to move outward from the earth relative to the spacecraft. This tendency affects activities at a work station and may have some effect on maneuvering in an extravehicular environment. This tendency must be understood in planning future extravehicular missions. Night retrieval of the propulsion device from the adapter is satisfactory, if artificial lighting is adequate.

For future EVA missions the following general guidelines are recommended:

(1) The propulsion device should be retrieved and used as early in the EVA mission as practical. The propulsion unit should be used to maneuver from the adapter. Based on the crew report, the use of handholds and umbilical is not recommended after the propulsion unit has been retrieved.

(2) Positive body restraint should be provided to minimize the work required to maintain position at a work area. The restraint hardware should allow two-handed operations.

(3) Hardware such as hooks, rings, fittings, et cetera, should be made for easier handling in pressure suit gloves.

TABLE 6-I.- TELEMETRY PARAMETERS

System	Parameter	Range	Number of channels	Type of channel
Pilot	Electrocardiogram	--	1	Analog
	Respiration rate	--	1	Analog
	Suit exhaust pressure	0 to 15 psia	1	Analog
Propulsion	N_2 tank pressure	0 to 4000 psia	1	Analog
	H_2O_2 pressure	0 to 715 psia	1	Analog
	H_2O_2 temperature	0° to 160° F	1	Analog
	H_2O_2 fuel remaining	0 to 100 percent	1	Analog
Flight control	Rate gyro	0.01 to 45°/sec	3	Analog
	Control valve	On to off	8	Bilevel (event)
	Control system valve	On to off	2	Bilevel (event)
	Manual switch position	Manual to automatic	1	Bilevel (event)
	Control switch position	On to off	10	Bilevel (event)
Oxygen	O_2 tank pressure	0 to 8000 psia	1	Analog
Power	28 V	0 to 28 Vdc	1	Analog
	Primary, +16 V	0 to +16 Vdc	1	Analog
	Primary, -16 V	0 to -16 Vdc	1	Analog
	Alternate, +16 V	0 to +16 Vdc	1	Analog
	Alternate, -16 V	0 to -16 Vdc	1	Analog
	Transducer excitation	0 to 10 Vdc	1	Analog
	Signal conditioner reference	0 to 5 Vdc	1	Analog
Abort alarm	Alarm signals	On to off	4	Bilevel (event)
Communications	Voice transceiver AGC[a]	0 to 8 Vdc	1	Analog
	Signal conditioner temperature	0° to 160° F	1	Analog

[a]Apollo guidance computer.

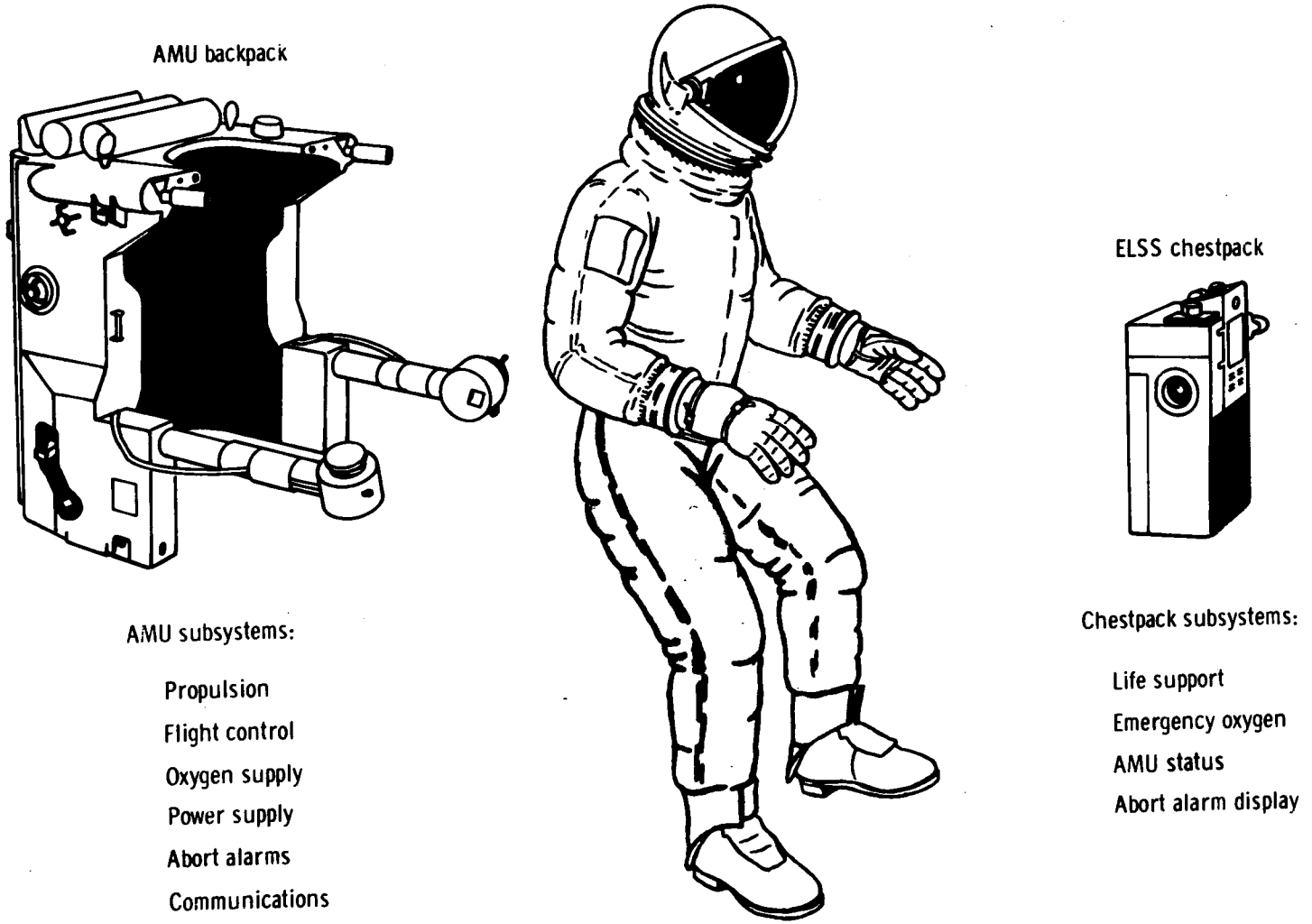

Figure 6-1.- Astronaut maneuvering unit configuration.

NASA-S-66-6958 JUN

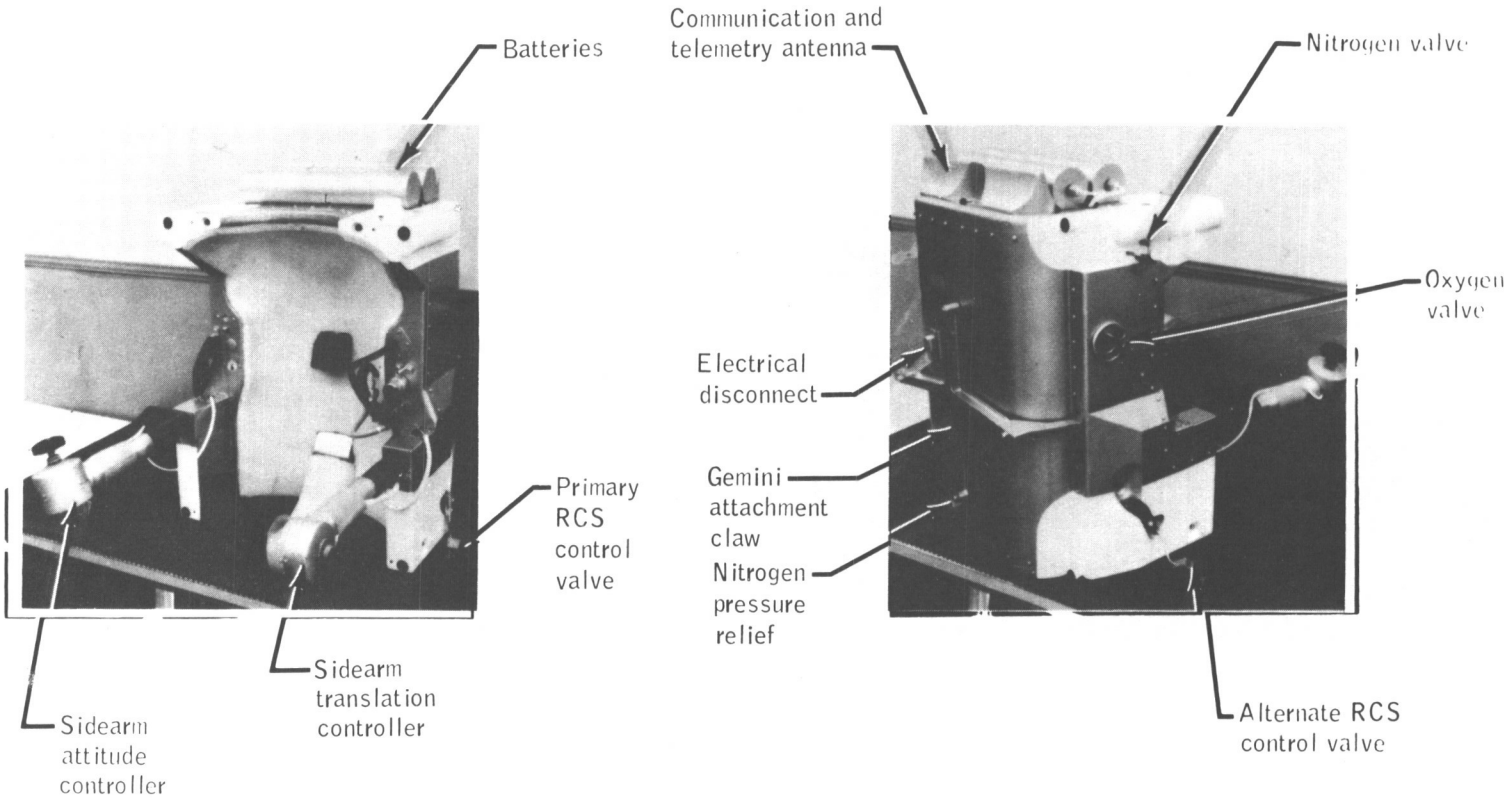

Figure 6-2.- Astronaut maneuvering unit external structure.

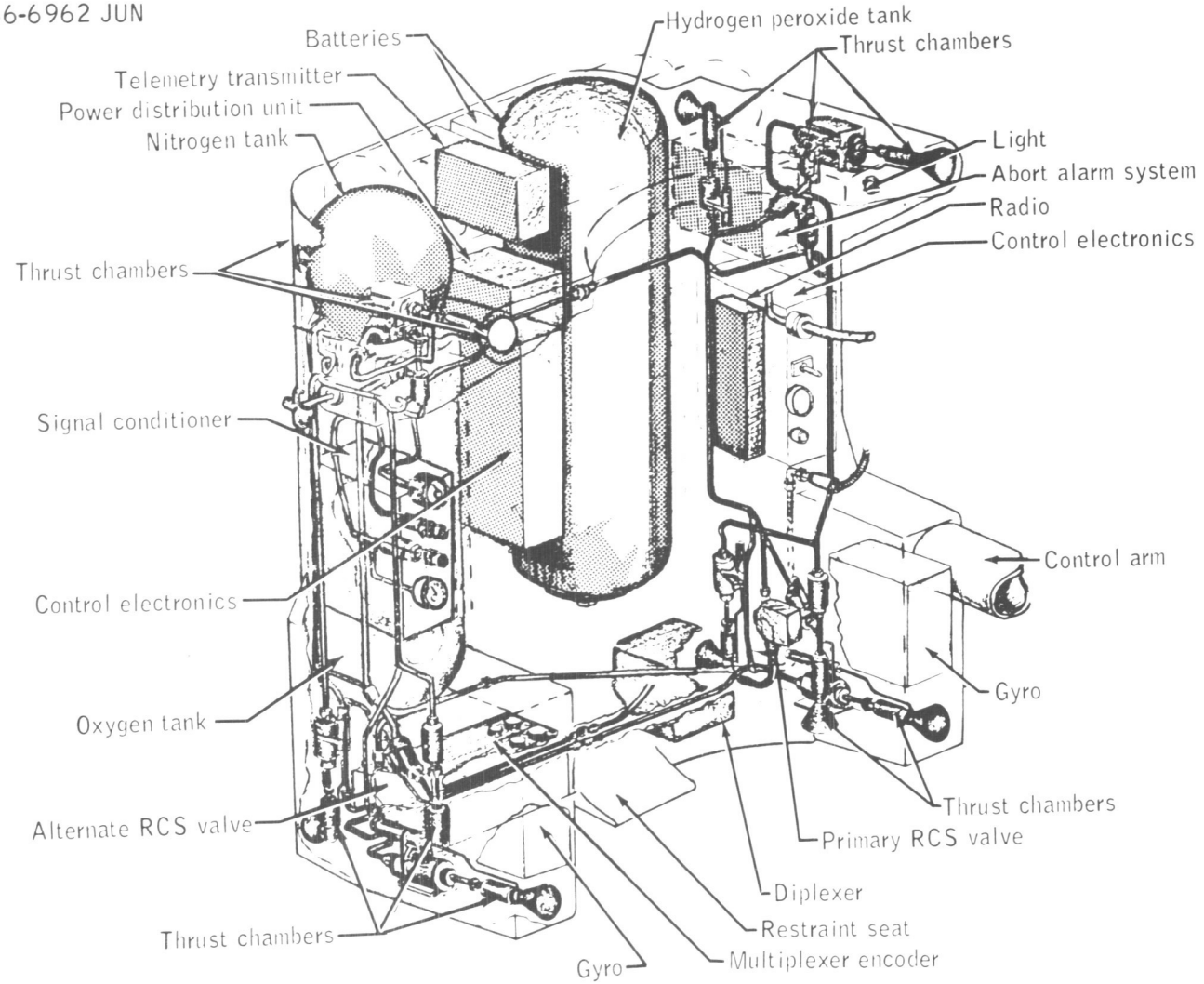

Figure 6-3.- Astronaut maneuvering unit internal arrangement.

NASA-S-66-6961 JUN

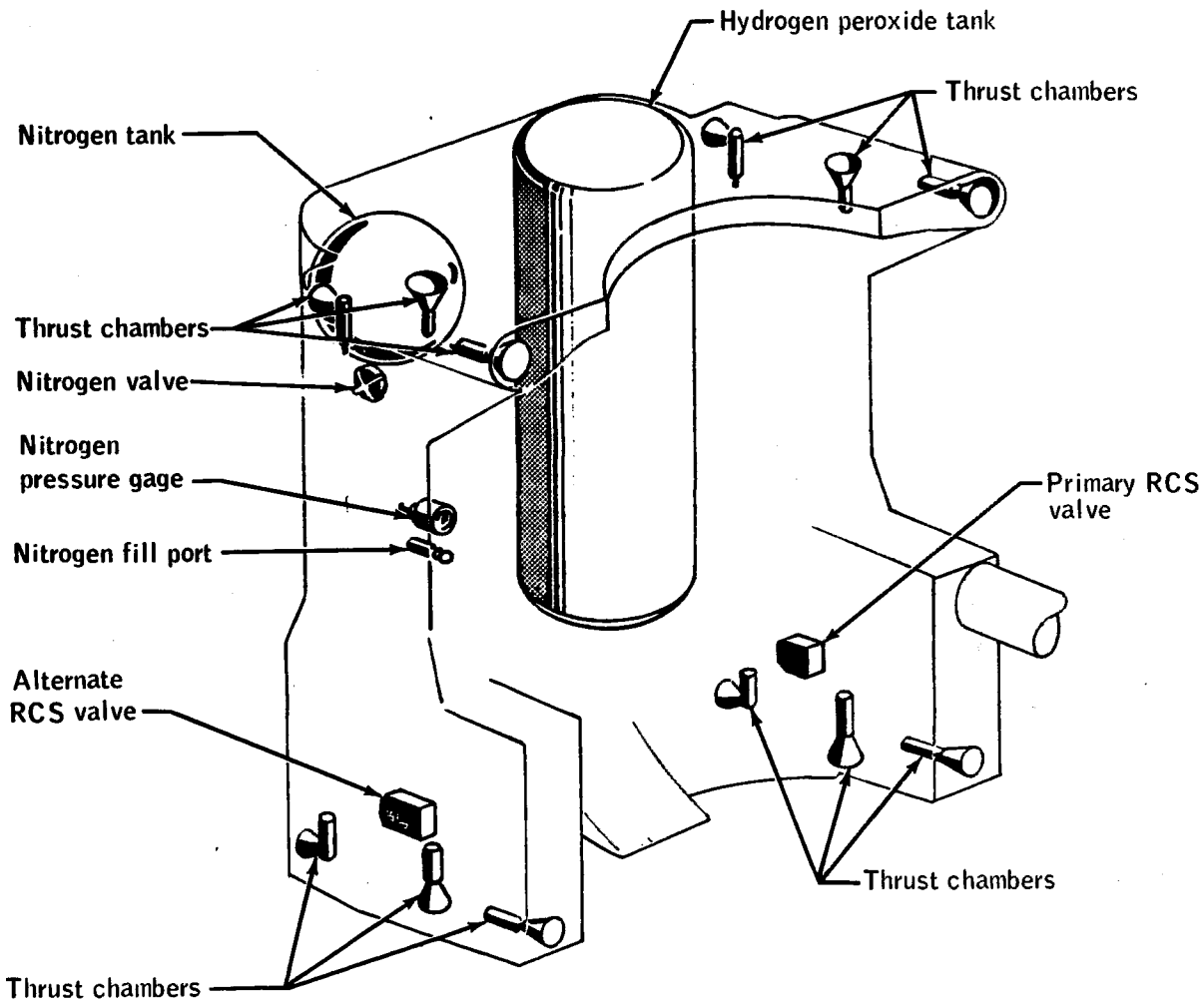

Figure 6-4.- Astronaut maneuvering unit propulsion system.

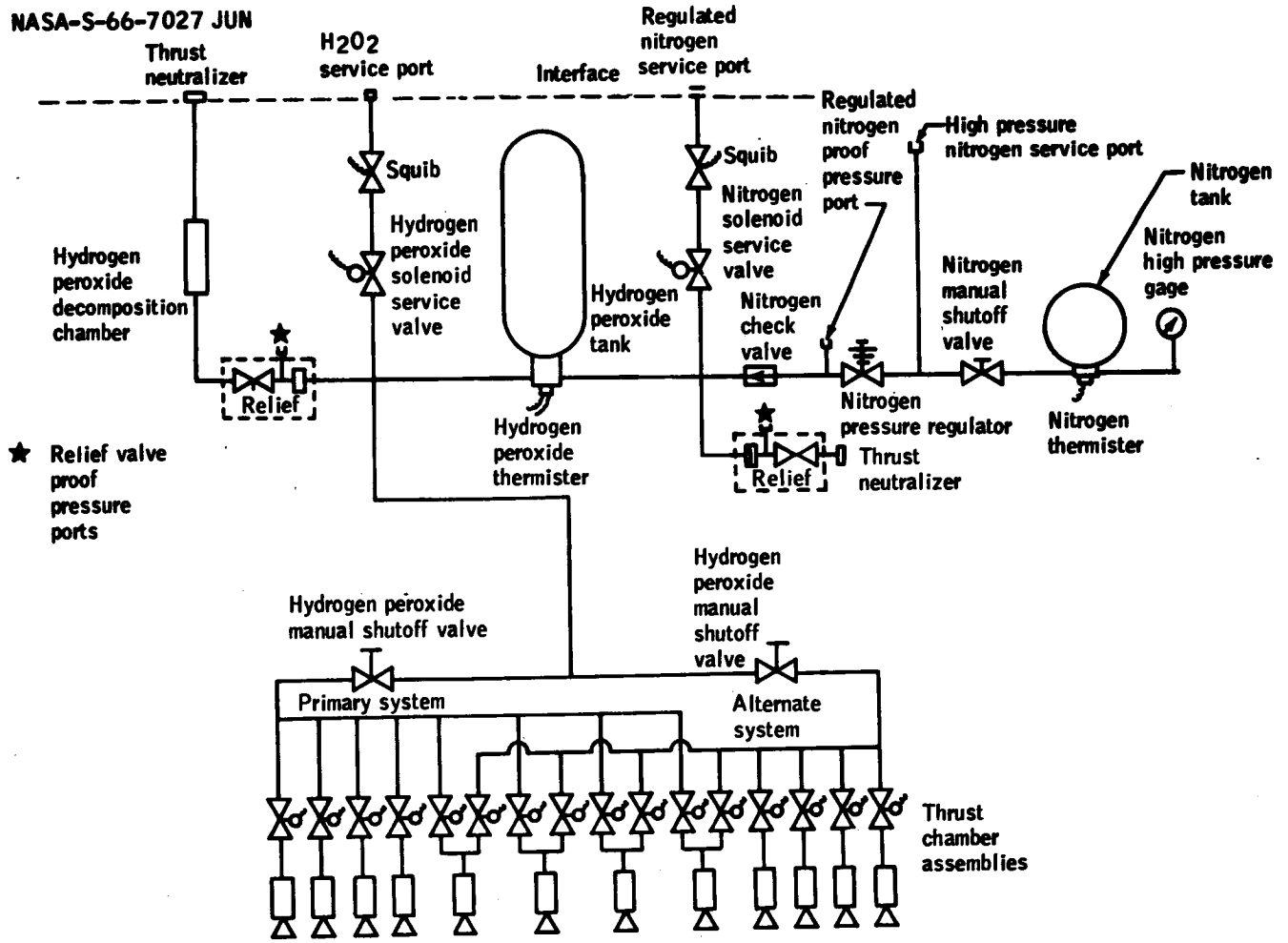

Figure 6-5.- Astronaut maneuvering unit propulsion system schematic.

NASA-S-66-6974 JUN

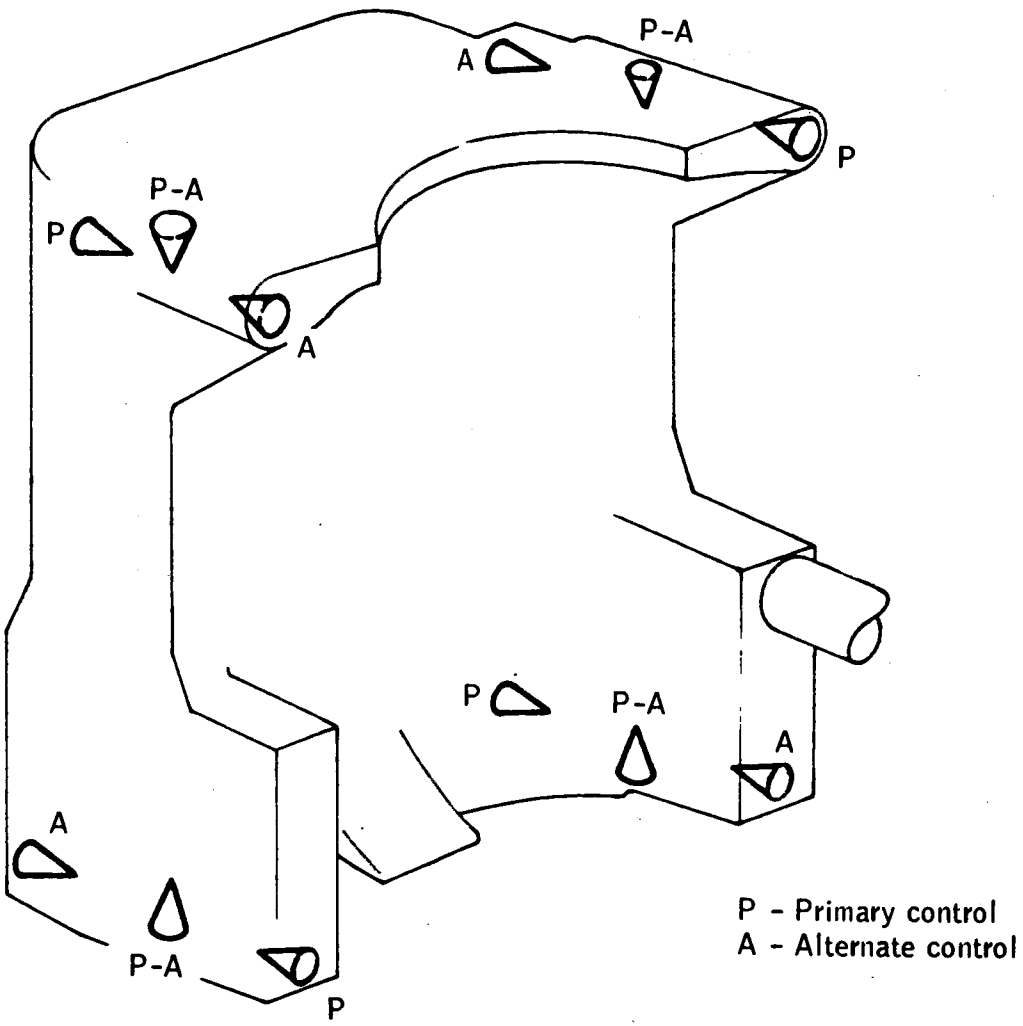

Figure 6-6.- Astronaut maneuvering unit thruster arrangement.

NASA-S-66-6967 JUN

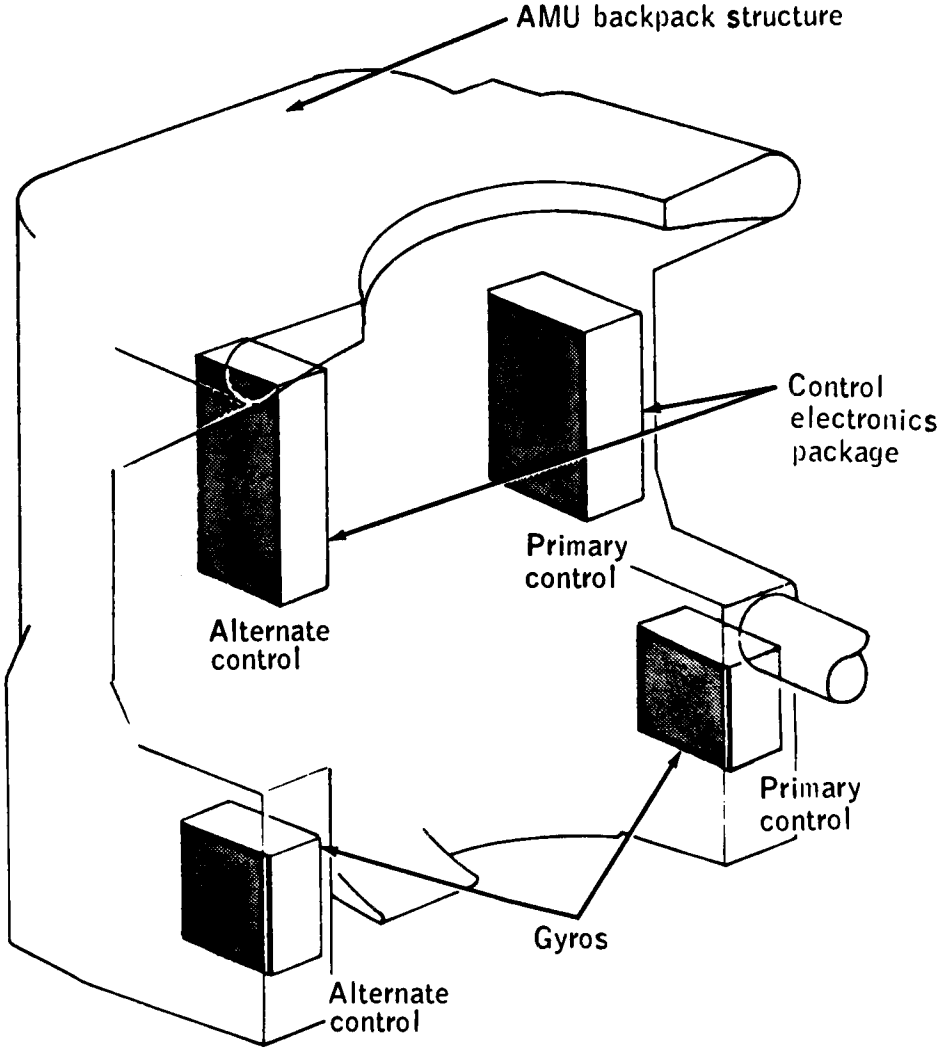

Figure 6-7.- Astronaut maneuvering unit stabilization and control system.

NASA-S-66-6963 JUN

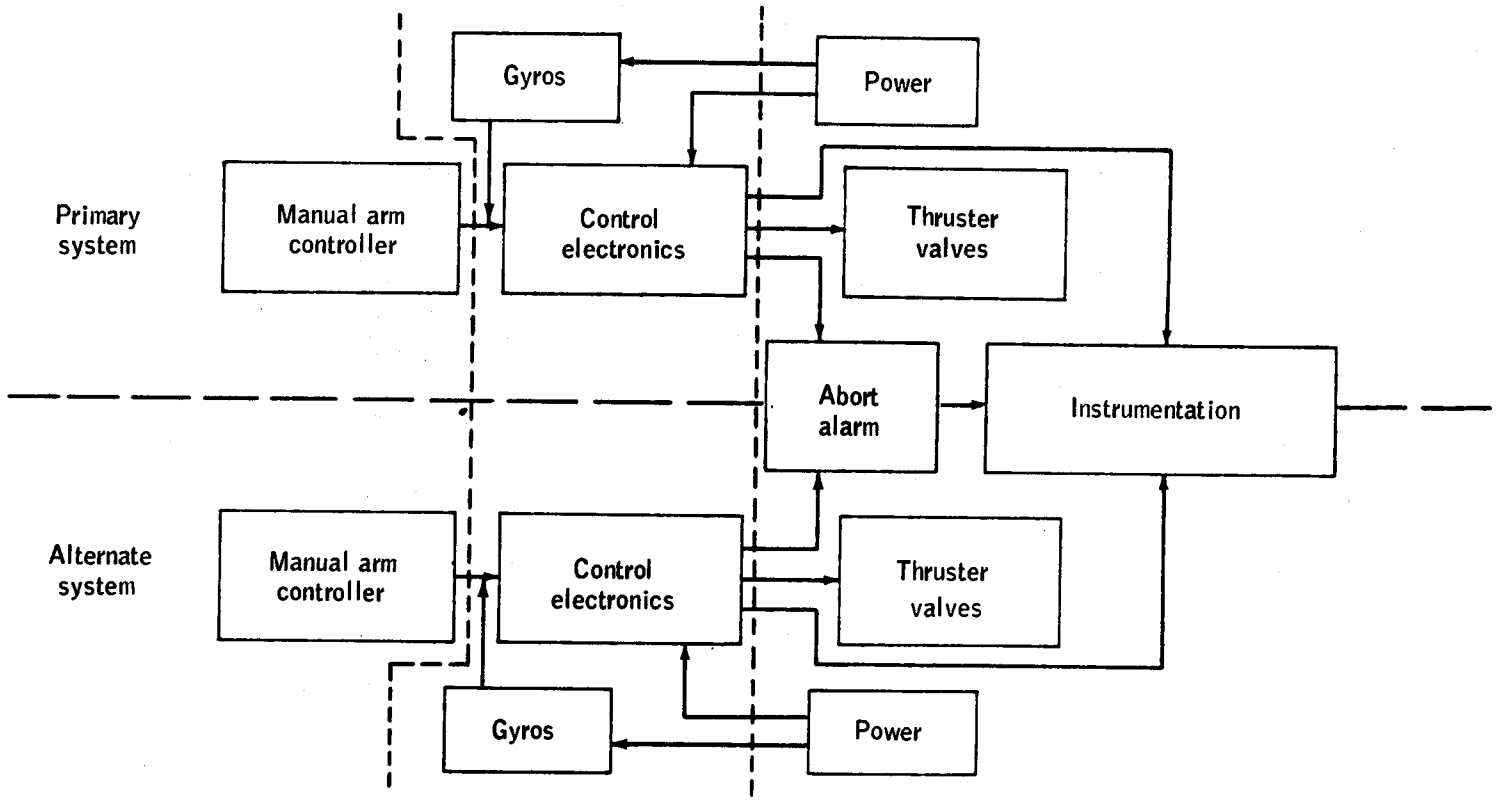

Figure 6-8.- Astronaut maneuvering unit flight control system.

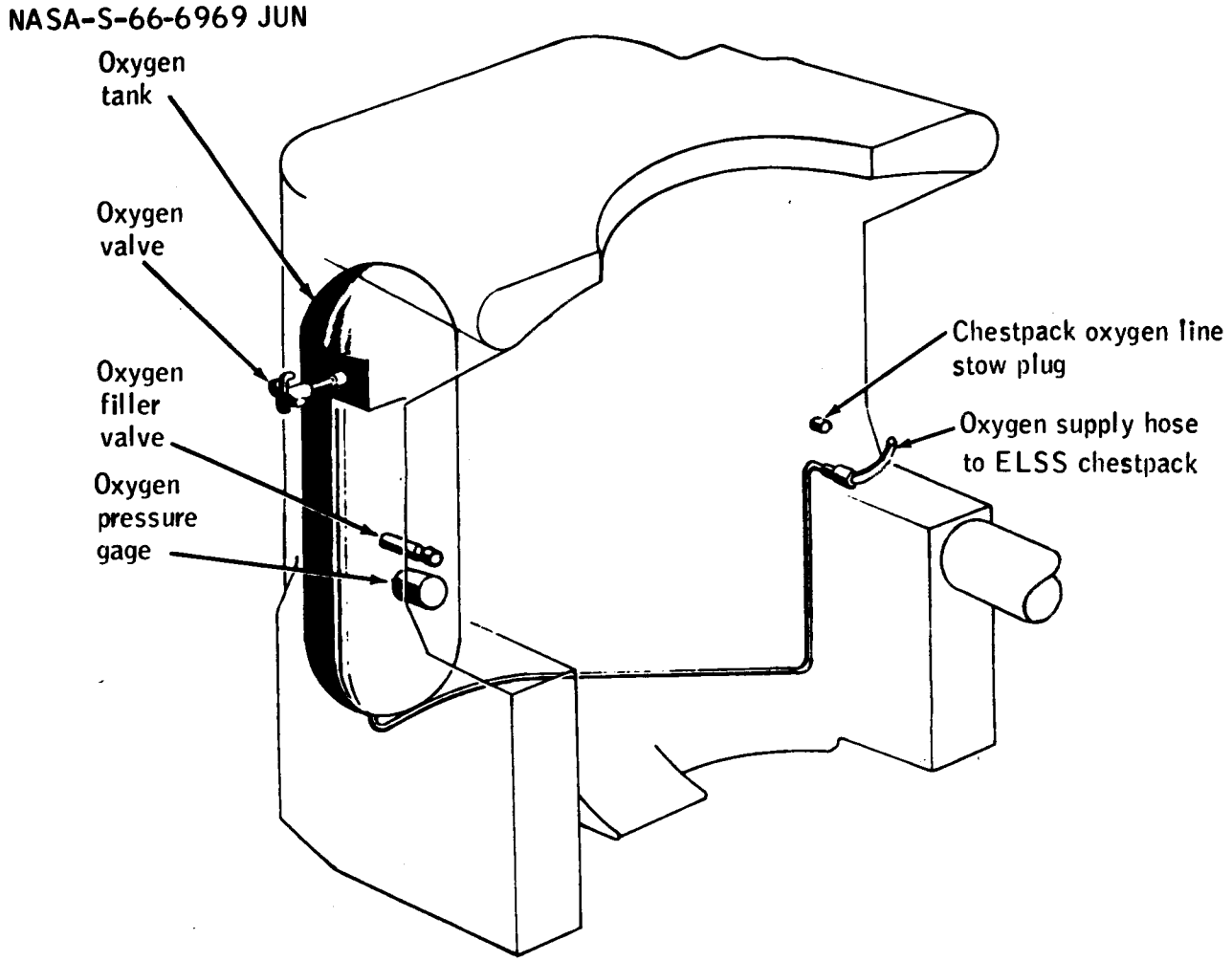

Figure 6-9.- Astronaut maneuvering unit oxygen supply system to ELSS.

NASA-S-66-6966 JUN

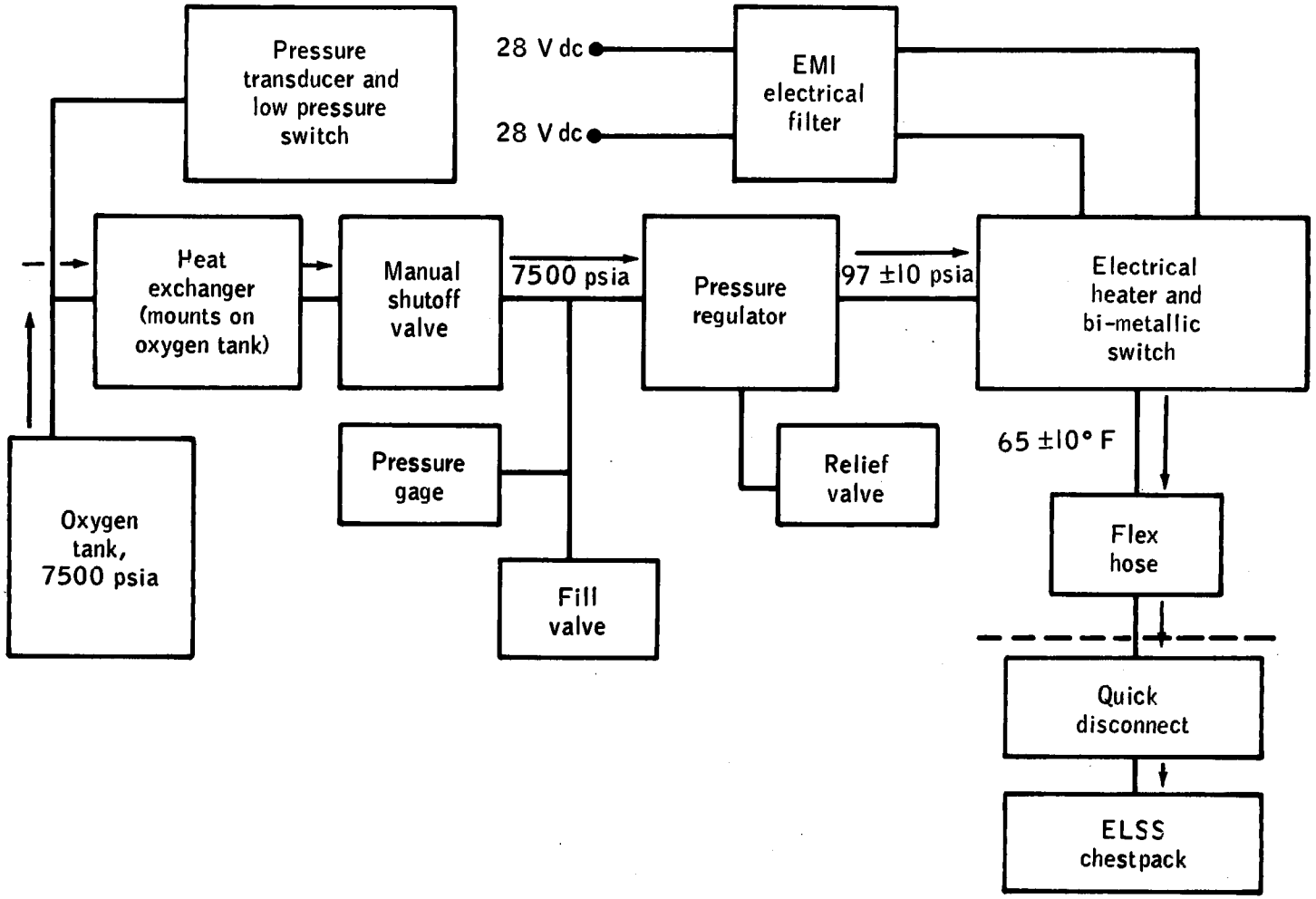

Figure 6-10.- Astronaut maneuvering unit oxygen supply functional diagram.

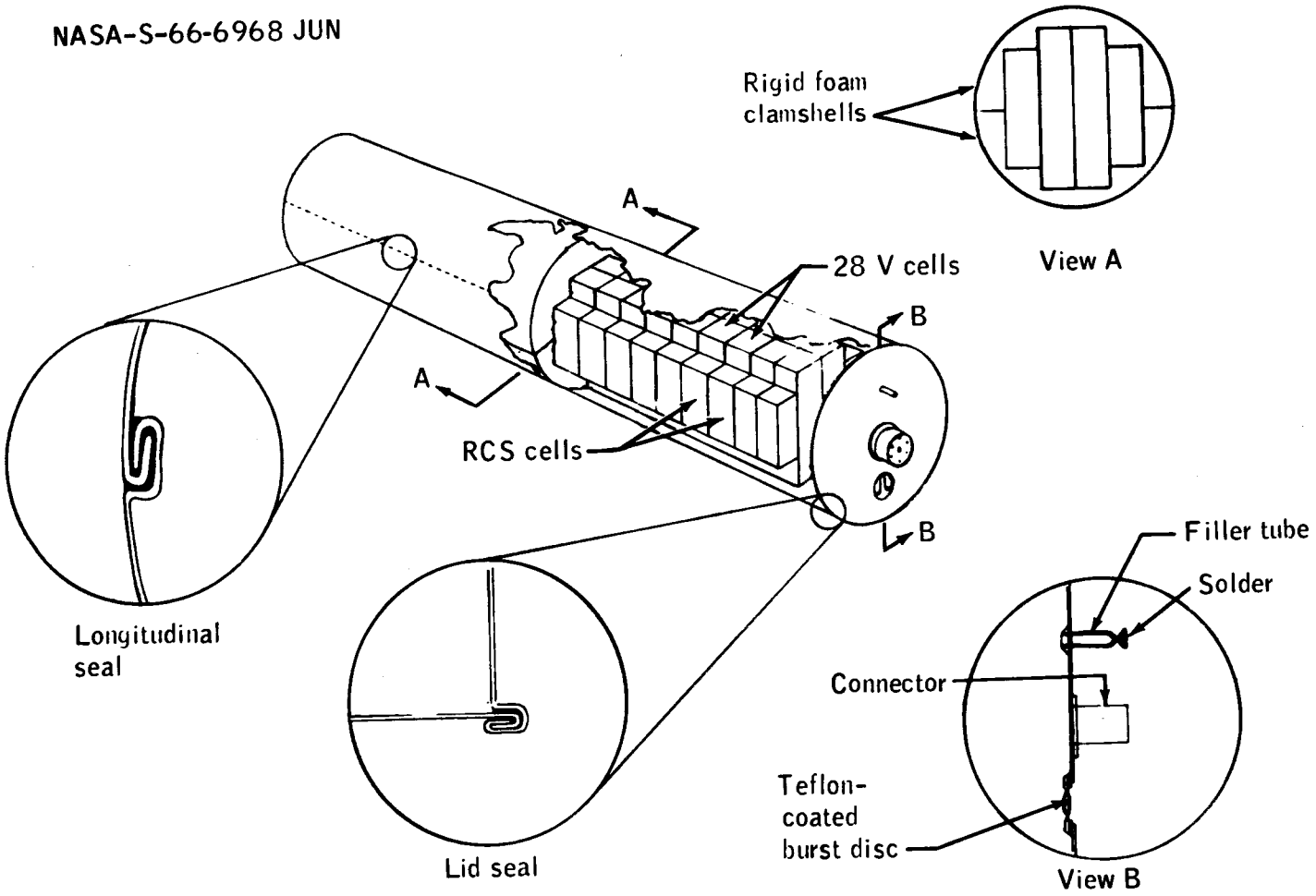

Figure 6-11.- Astronaut maneuvering unit battery pack assembly.

NASA-S-66-6970 JUN

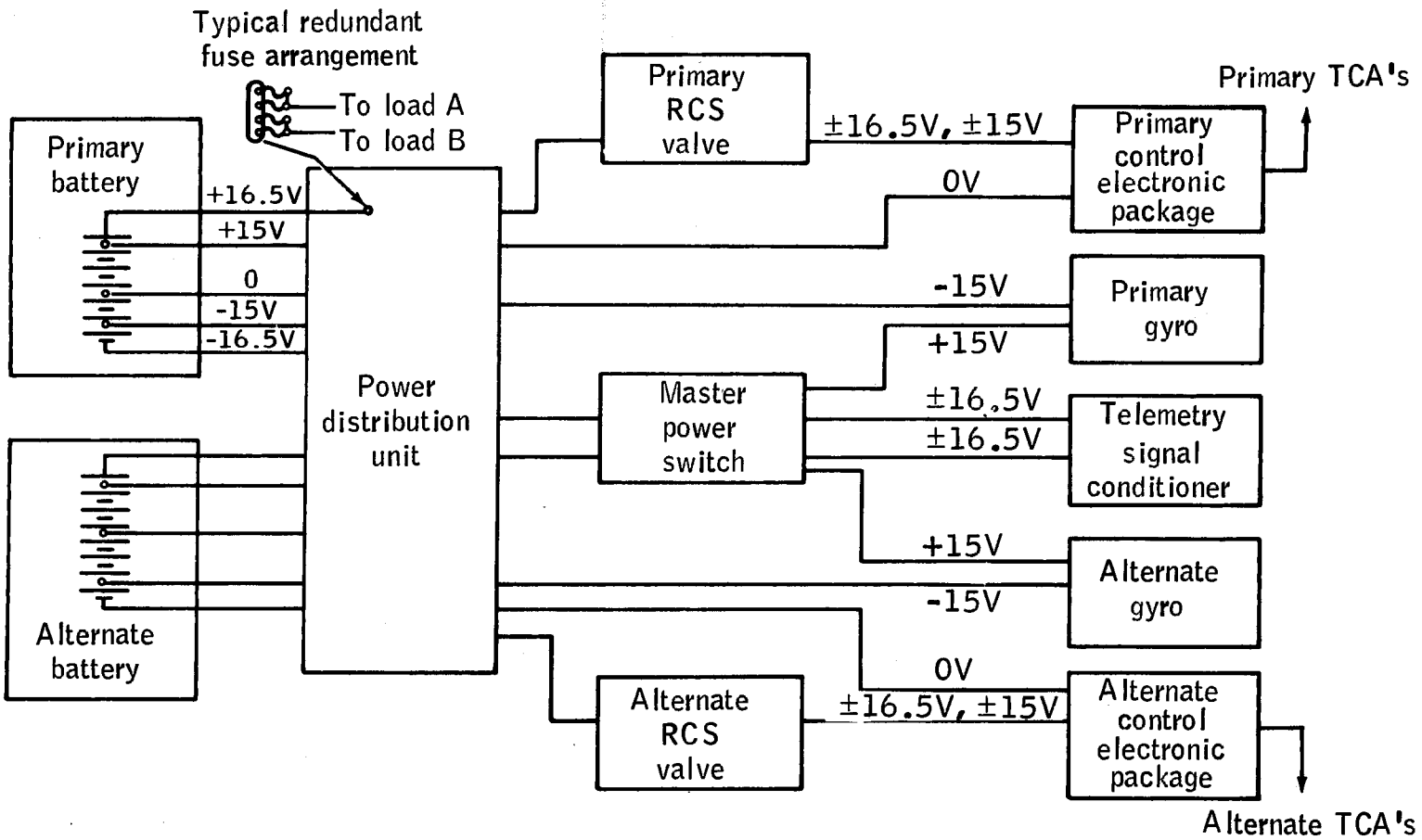

Figure 6-12.- Astronaut maneuvering unit RCS electrical system.

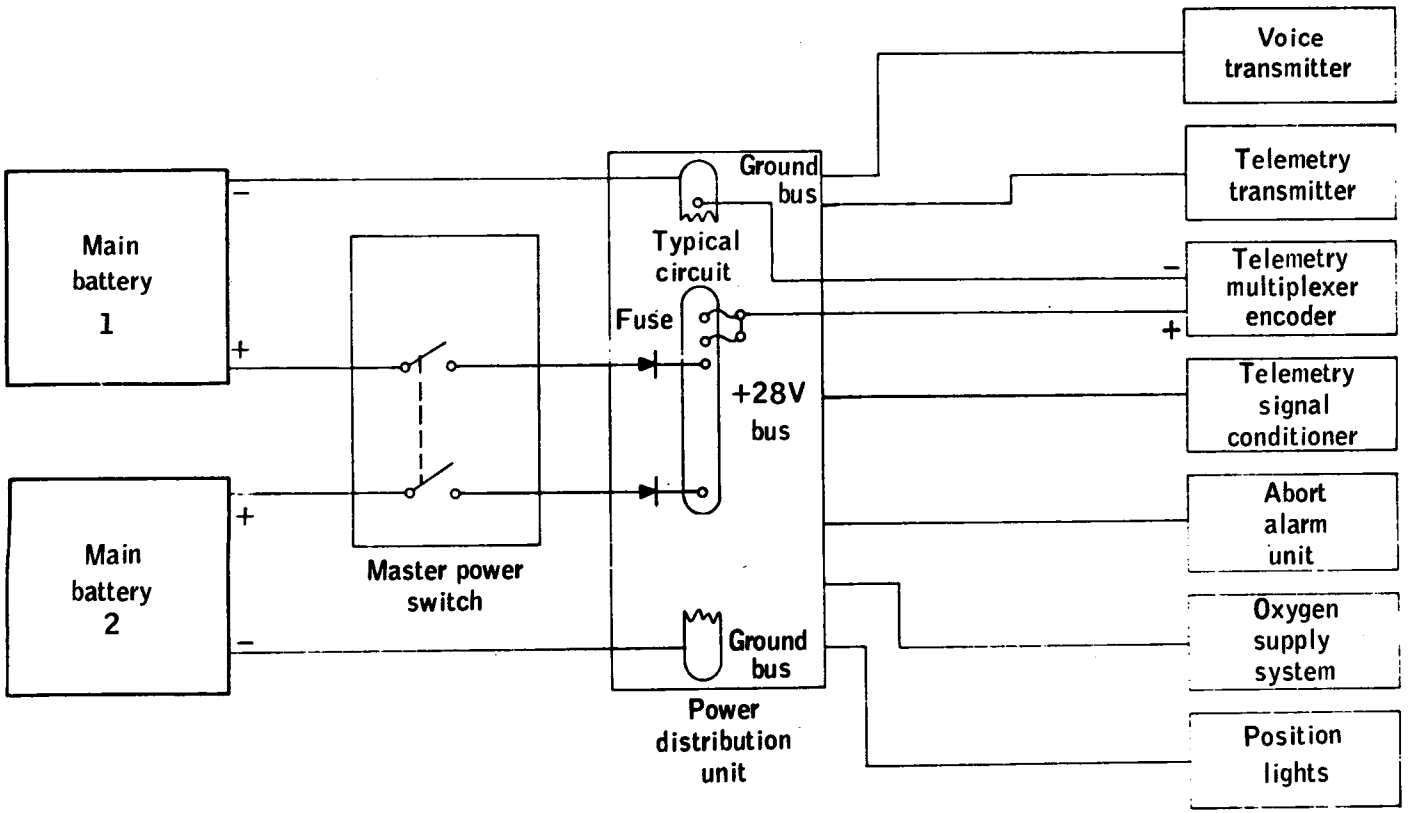

Figure 6-13.- Astronaut maneuvering unit 28-volt dc power supply.

NASA-S-66-6972 JUN

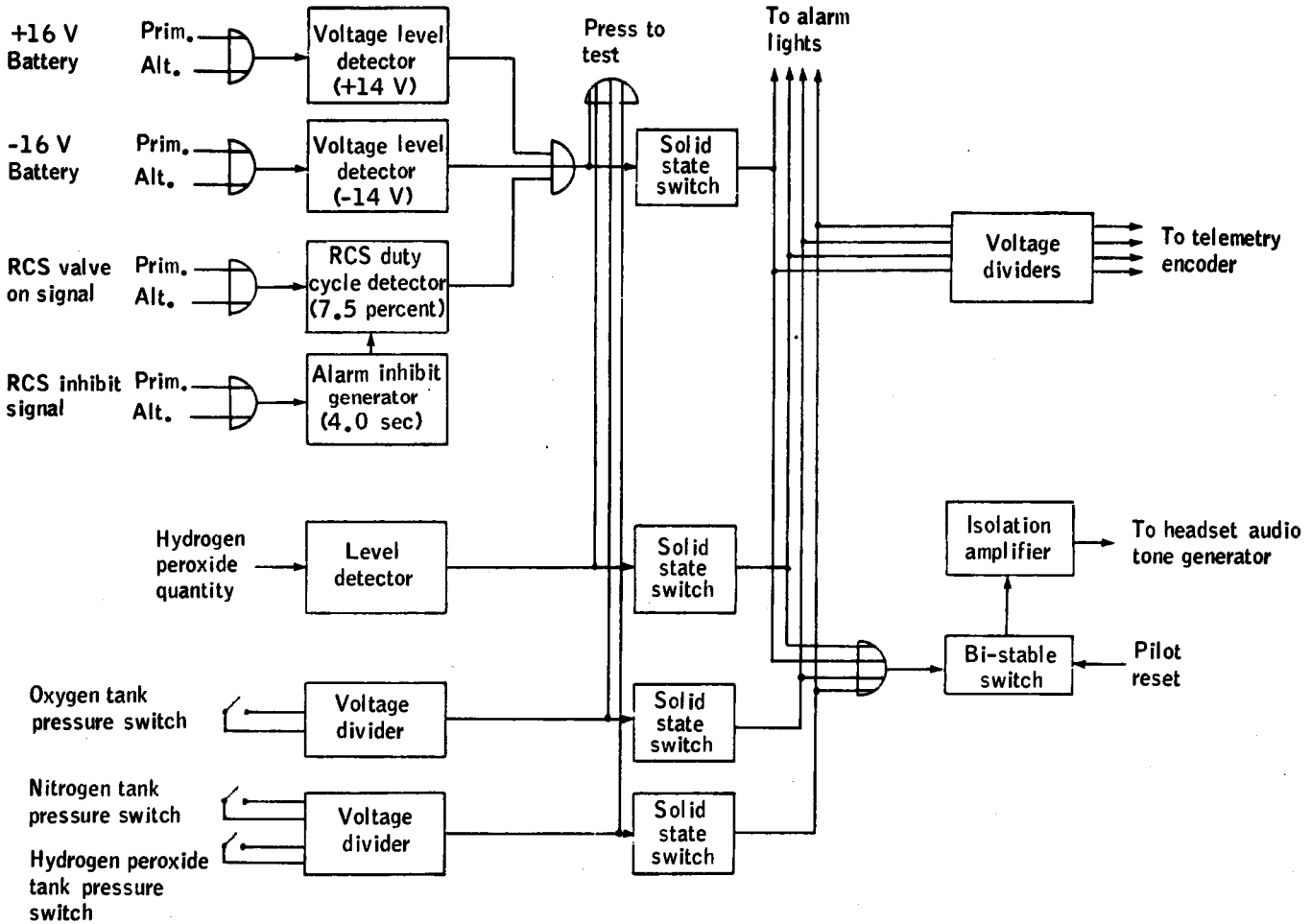

Figure 6-14. - Astronaut maneuvering unit malfunction detection system functional diagram.

NASA -S-66-6964 JUN

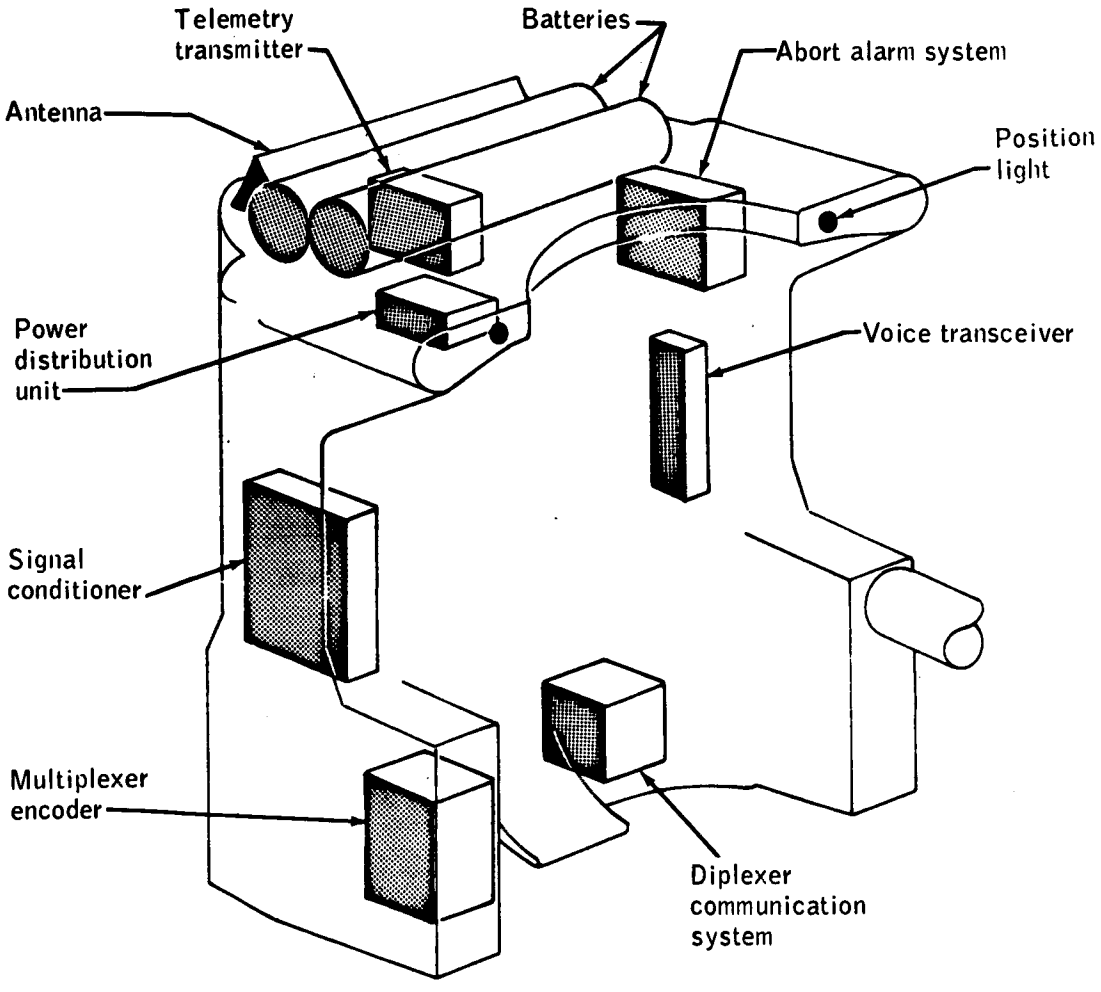

Figure 6-15.- Astronaut maneuvering unit communications, telemetry, and electrical systems arrangement.

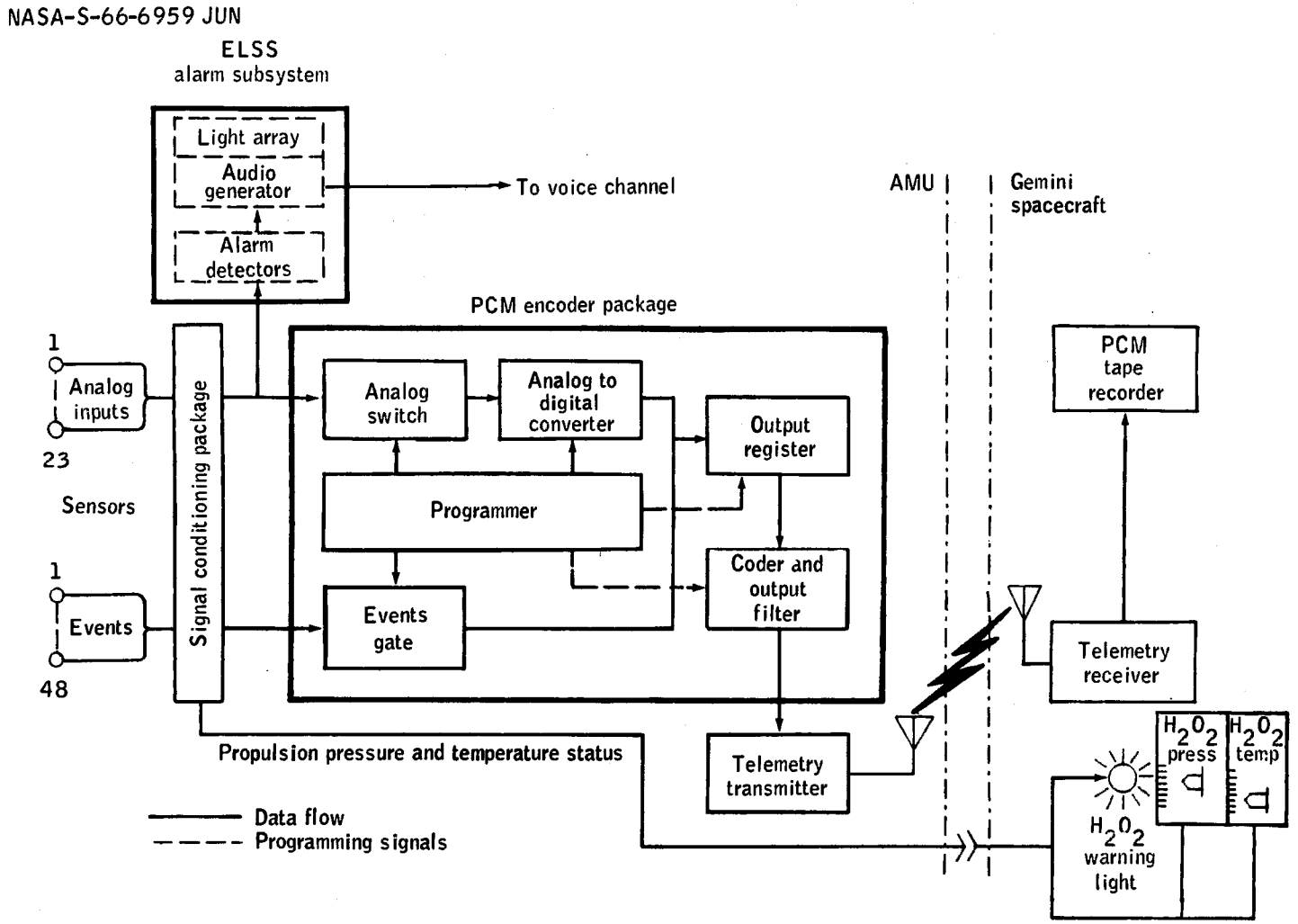

Figure 6-16. - Astronaut maneuvering unit telemetry system functional schematic.

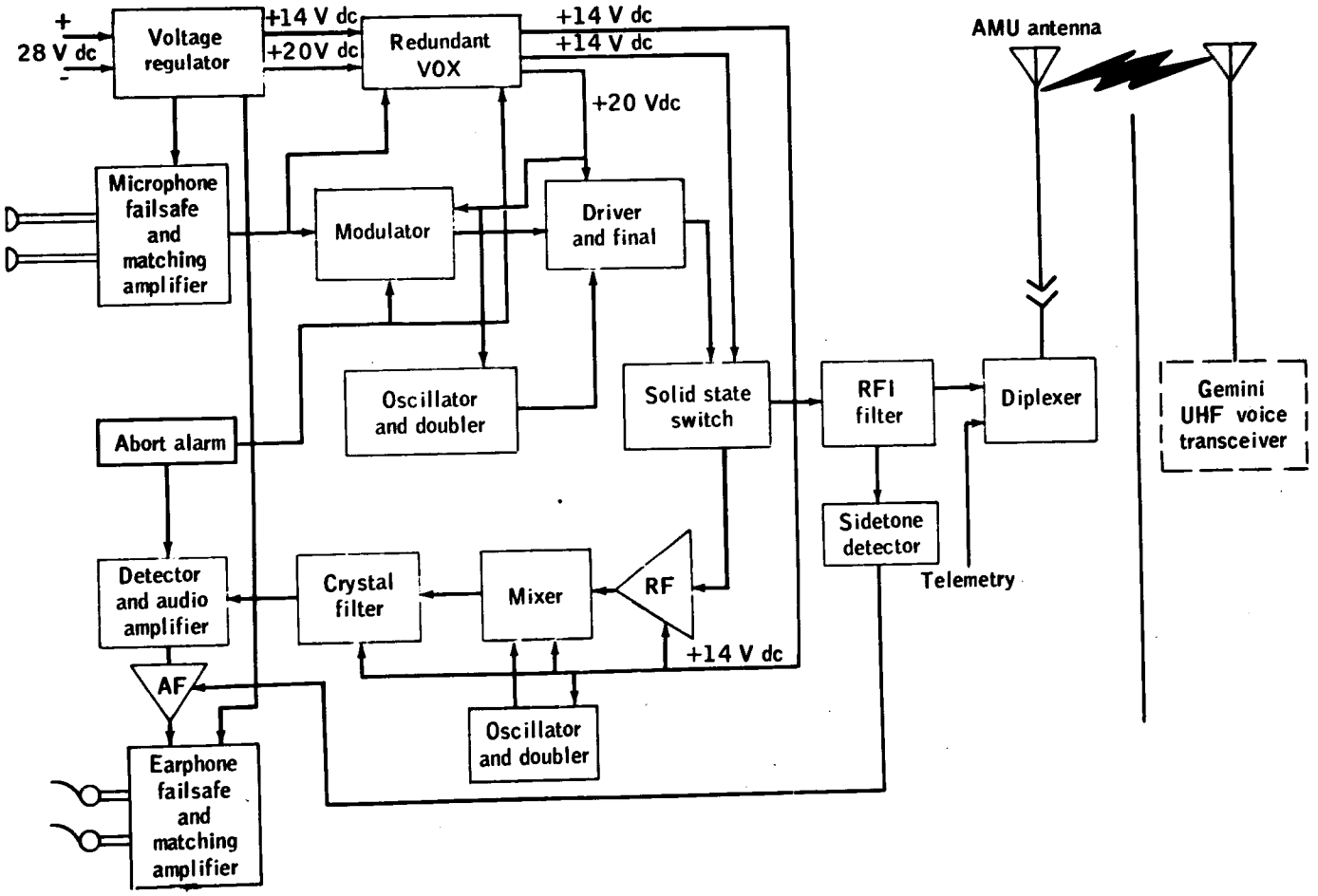

Figure 6-17.- Astronaut maneuvering unit voice communications system functional diagram.

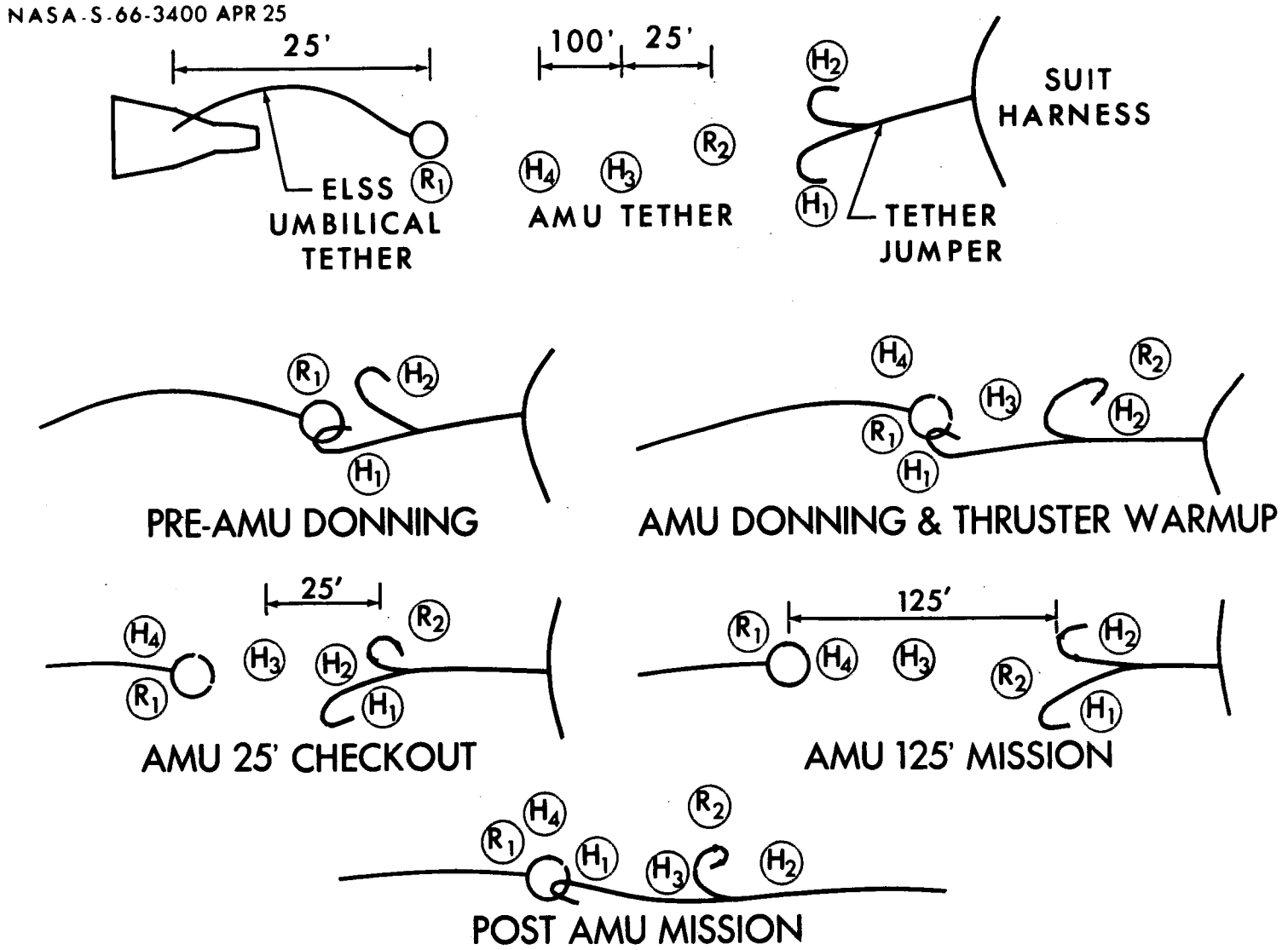

Figure 6-18. - Astronaut maneuvering unit tether operations.

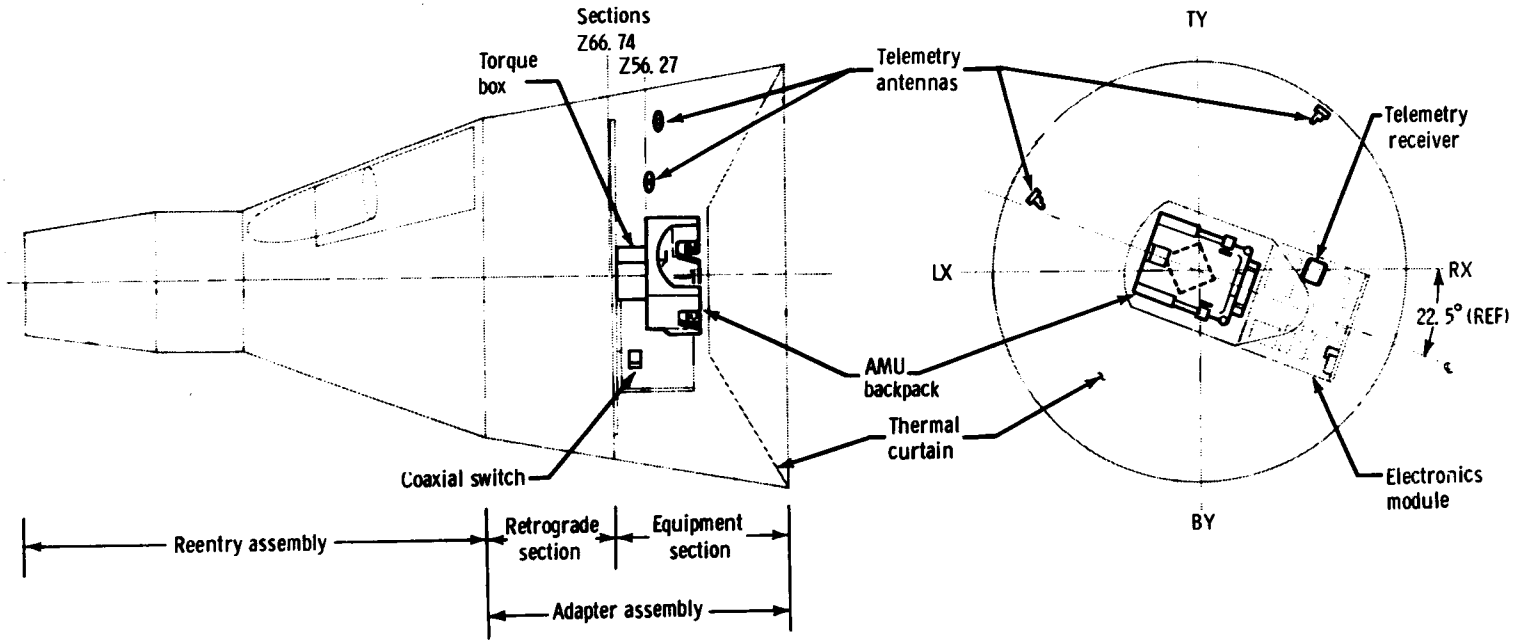

Figure 6-19.- Astronaut maneuvering unit stowage in adapter assembly.

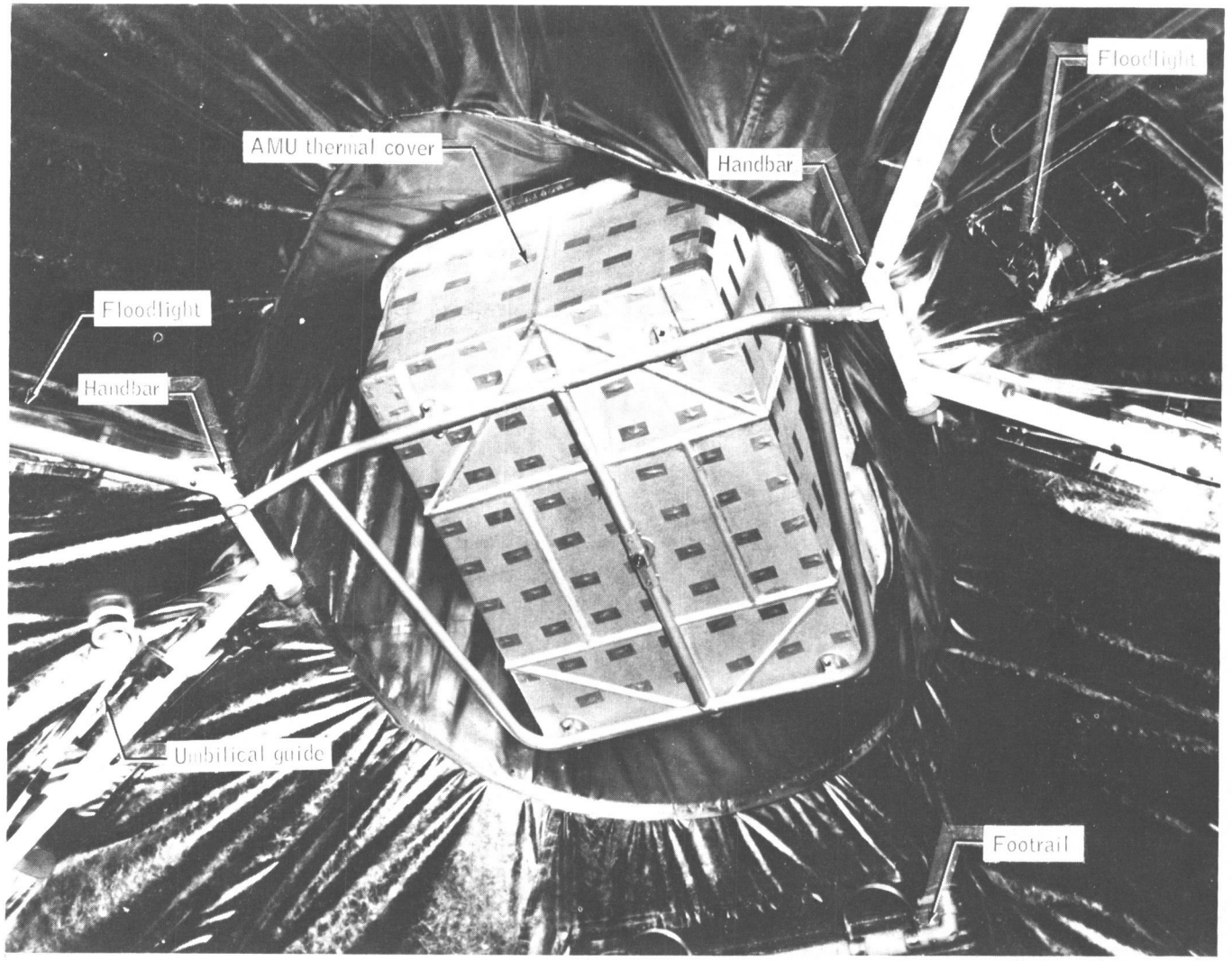

Figure 6-20.- Astronaut maneuvering unit donning hardware.

NASA-S-66-7004 JUN

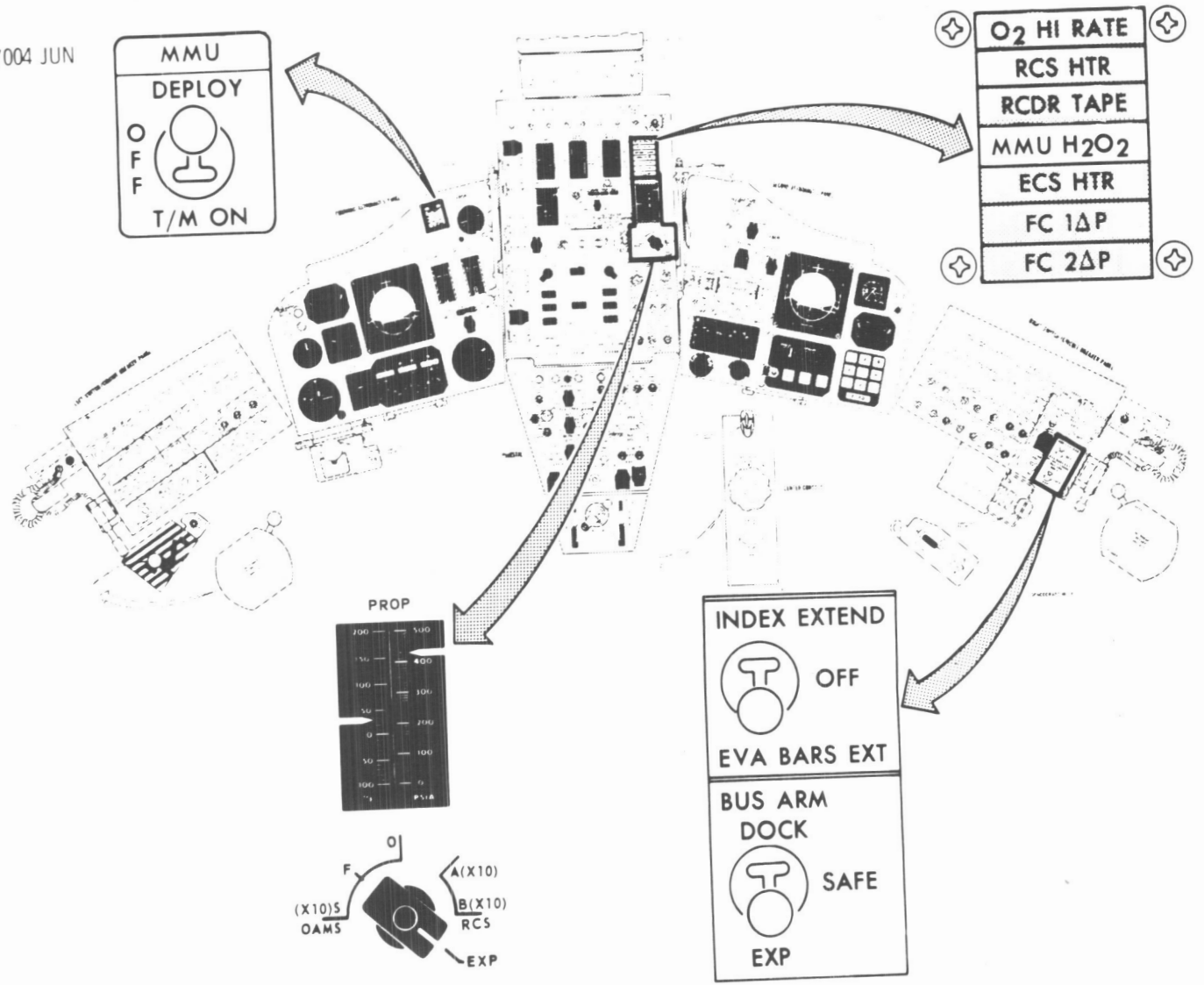

Figure 6-21.- Astronaut maneuvering unit controls and indicators.

7. EXPERIMENT D-14, UHF-VHF POLARIZATION

By Robert E. Ellis
U.S. Naval Research Laboratory

SUMMARY

A VHF-UHF Faraday rotation experiment (D-14) was conducted in conjunction with the Gemini IX spacecraft transits over Kauai, Hawaii, and Antigua, British West Indies. Although the signal-to-noise ratio was lower than anticipated, preliminary analysis indicates that no problem should be encountered in detecting ionospheric inhomogeneities of the order of 1 kilometer in horizontal scale, provided that the excursions exceed 1 percent of the subsatellite electron content. Ambiguity removal has been accomplished by comparing the orientation of the VHF and the UHF polarization ellipses.

Values of the electron content and the effective slab thickness have been determined at the closest point of approach for three of the five Kauai transits. It is apparent that the subsatellite content increases with increasing F2 region electron density; however, the occurrence of slab thickness variations implies that the relationship is not a simple one.

INTRODUCTION

The purpose of the D-14 experiment was to measure the inhomogeneities in the electron content which exists along the orbital path of the spacecraft. Such measurements give increased insight into the structure of the lower ionosphere and its temporal variations.

The experiment was conducted by transmitting two continuous-wave (cw) signals from the spacecraft and receiving them at special receiving stations on the ground. Two separate receiving stations, one located at Kauai, Hawaii, and the other at Antigua, British West Indies, were used to measure the amount of rotation, caused by the Faraday effect, that is introduced to the signals along their transmission path. The rotation angle was recorded as a function of time when the spacecraft passed over each of the two receiving stations. These rotation angles were entered into a computer program to calculate the electron content.

BACKGROUND

Source of Experiment

The concept of this experiment evolved out of the ionospheric measurements being conducted by the Naval Research Laboratory (NRL) employing the 150-foot-diameter dish radar system located at Randall Cliffs, Maryland. These measurements involved radar signal returns from the moon as well as satellite signal transmissions.

Scientific Need for Experiment

The presence of free electrons in the ionosphere results in the fading of radio signals transversing all or part of the ionosphere. There are several types of fading, namely absorption, scattering, and Faraday effect. At frequencies of 40 Mc or lower, radio signals can, under increased solar activity, be completely absorbed, resulting in a complete loss of signal. Scattering by the inhomogeneities in the electron distribution results in scintillation or rapid fluctuation of the signal level. The Faraday effect, which is the rotation of the plane of polarization of a linearly polarized radio wave in the presence of electrons in a magnetic field, may cause either regular or irregular fading, depending upon the state of the ionosphere.

An increased knowledge of the various forms of radio wave perturbation is of fundamental importance to communication engineers and physicists. The size of the inhomogeneities in the electron distribution is of special importance, since inhomogeneities cause irregular fading of radio waves. Also, the altitude dependence of the irregularities in electron distribution is of interest in a study of the origin of perturbations.

Military Need for Experiment

The electron content of the ionosphere will have a direct effect upon any radio signal originating in, received in, or passing through the ionosphere. Therefore, an increased knowledge of the nature and perturbation of the electron content is of military importance, since it will be directly related to the behavior of signals, communications, radar, et cetera used by the military.

Considerable work has been done to measure the irregularities in the electron distribution using several different approaches. One approach involves radio astronomy techniques employing two antennas and a suitable correlation analysis. In this approach, it is not possible

to distinguish between large irregularities with slow motion from small irregularities with rapid motion. Another approach uses signals from radio sources in the cosmos and signals or radar returns from super-ionospheric satellites. In any case, this approach gives an integrated picture of ionospheric irregularities along the line of sight.

Much of the interest, from the military applications point of view, is concerned with the inhomogeneities in the lower regions of the ionosphere. Data from these lower regions are rather sparse. The Gemini spacecraft orbits in the lower ionosphere region and moves rapidly, and hence was an ideal platform to give a rapid cross section of the region of interest.

THEORY

The theory embodied in the Faraday effect method of determining the electron content of the ionosphere is relatively simple and has been used regularly in ionospheric investigations. The Faraday effect is the rotation of the plane of polarization of a linearly polarized radio wave. The rotation of the electric vector of the radio wave is directly proportional to the electron content along the path of propagation and the component of the earth's magnetic field parallel to the path, and the rotation is inversely proportional to the square of the radio frequency.

Under conditions of quasi-longitudinal propagation and at frequencies above 100 Mc, where the plasma frequency and gyro frequency are relatively small, the Faraday rotation is given by the following approximate formula:

$$\Omega = 2.97 \times 10^{-2} f^{-2} \int_0^S (H \cos \theta) N \, ds$$

where Ω is the rotation angle in radians
f is the radio frequency in cycles per second
H is the total magnetic field intensity in ampere turns per meter
θ is the angle between the ray path and the magnetic field vector
N is the electron density in electrons per cubic meter
s is the distance measured along the ray path in meters
S is the distance from the ground antenna to the spacecraft in meters.

At the frequencies below 100 Mc, the above equation becomes invalid because of the high-frequency approximation used in its derivation.

Also, at frequencies below 100 Mc and at low elevation angles, severe refraction and path splitting effects introduce additional complications.

The Faraday rotation may, at the lower frequencies, exceed a complete revolution, resulting in an ambiguity of $M\pi$. One method of removing this ambiguity is to use two frequencies, one at VHF and the other at UHF, with one frequency high enough so that the total rotation angle cannot be ambiguous. For this experiment, using a spacecraft altitude of 160 nautical miles, the rotation angle should always be less than 180° at a frequency of about 400 Mc. By using a second frequency in the 100-Mc range, accurate measurements without ambiguity can be made.

The selection of the exact radio frequencies was influenced by several factors, in addition to frequency spectrum availability. The first factor, the variations in the predicted subsatellite electron content, is a function of sunspot activity, solar zenith angle, and the spacecraft altitude. The second factor, the variations in the effective magnetic field parameter, is a function of the field station location and the spacecraft orbital paths. The third factor, the total angular orientation error, is a function of spacecraft antenna orientation, the purity of polarization of the transmitted signals, and the measurement errors. The first two factors can readily and adequately be estimated, but the third factor is more difficult to assess.

With the selected frequencies of 133.9 and 401.7 Mc and an assumed error of 5° root mean square, it was determined that an error in subsatellite electron content of from 3.5 to 7.0×10^{14} electrons per square meter would be obtained. Since the anticipated subsatellite electron content will be about 1.5×10^{17} electrons per square meter, an error of from about 0.2 to 0.4 percent will be expected. The accuracies will be somewhat less during nighttime measurements, since the total subsatellite electron content of about 5×10^{15} electrons per square meter is anticipated.

EQUIPMENT

Description and Design

Nomenclature and function.- The equipment used for this experiment is divided into two categories: equipment located in the spacecraft

and equipment located on the ground. The equipment located in the spacecraft is as follows:

(1) A dual frequency transmitter generates the two harmonically related coherent cw signals necessary to conduct the experiment.

(2) A diplexer combines the two outputs of the transmitter into a single output so that both frequencies may be transmitted, through a single coax line, to a single antenna without interaction between the two transmitter outputs.

(3) A colinear dipole antenna provides a means of transmitting the two frequencies with linear polarization from the spacecraft to the ground.

(4) An antenna boom assembly provides a means of storing the antenna inside the spacecraft prior to launch and a means of extending the antenna the proper distance outside the spacecraft during orbit for conducting the experiment.

The equipment located on the ground for the receiving system is as follows:

(1) A 28-foot-diameter dish antenna, feed, and pedestal receives the cw signals transmitted from the spacecraft and separates each frequency into its vertical and horizontal polarization components.

(2) A dual channel receiver (Model SR 108) is used to amplify and heterodyne the horizontal and vertical components of the 133.9-Mc signal to a frequency of 120-kc for display. Also, this equipment detects the envelope of the 120-kc signals for display.

(3) A dual channel receiver (Model SR 109) serves the same function as the SR 108 receiver except that it operates at the 401.7-Mc frequency.

(4) An X-Y scope is used to display the Faraday rotation angle of the two signals.

(5) A 35-mm frame-by-frame camera is used to record photographically, at the rate of 2 per second, the Faraday rotation angle displayed on the X-Y scope.

(6) A tape recorder is used to record the 120-kc intermediate frequency (i.f.) signals out of the dual channel receivers.

(7) A Sanborn chart recorder is used to record the envelope of the 120-kc signals out of the receiver.

(8) Camera control units are used to control electronically the frame rate and exposure time of the 35-mm frame-by-frame cameras.

(9) An attenuator control is used to reduce the input signal level into the receivers should this level become too high. This unit also generates tones for recording attenuator setting on the magnetic tape and controls attenuator indicator lights in the recording cameras.

Physical description of equipment.- The dual frequency transmitter is constructed of all solid state circuitry housed in a rugged 6 by 7 by 3.5 inch chassis. This chassis is composed of two units, one of which contains the voltage regulator, filters, and dc-to-dc converter, and the other of which contains the radio-frequency (rf) circuits. These circuits are encapsulated in a foam epoxy so that, after the two units are assembled as the complete transmitter, they are essentially a solid unit. The total weight of the transmitter is 6 pounds. Photographs of the transmitter are shown in figures 7-1, 7-2, and 7-3, and circuit diagrams of the power supply and rf portions of the transmitter are shown in figures 7-4 and 7-5, respectively.

The diplexer used in this experiment is 2.7 by 4.5 by 4.1 inches in size and has a weight of 1.2 pounds.

The colinear dipole antenna consists of two colinear sections. One section serves as a choke to keep the rf radiator off the boom mount and is 2 inches in diameter and 14 inches long, while the other section is 5/16 of an inch in diameter and 31 inches long. The small diameter section is hinged at two points: at the junction to the choke section and at its midpoint. These hinged joints are spring loaded so that the thin-diameter section can be folded to give a total folded length of 15.7 inches for mounting in the spacecraft. During orbit, the antenna is automatically unfolded by the spring loading when it is extended outside the spacecraft. Photographs of the antenna are shown in figures 7-6 and 7-7. The total weight of this antenna is 2 pounds.

The extendible antenna boom can extend the colinear dipole antenna 120 inches from its stowed position. The overall dimension of the boom mechanism is 13.25 by 7 by 5.40 inches. The weight of this unit is 11 pounds. A photograph of the antenna boom assembly with antenna mounted is shown in figure 7-8.

Since the equipment used in the ground receiving station is, for the most part, standard commercial equipment, only the dual channel receivers will be described. The physical characteristics of the SR 108 and SR 109 dual channel receivers are the same. The overall dimensions are 19 by 17 by 5 1/4 inches. The total weight of one unit is 36 pounds.

System description and operation.- This experiment involves a transmitting system, mounted in the spacecraft, and a receiving system and two recording systems located on the ground. A block diagram of the transmitter system mounted in the spacecraft is shown in figure 7-9.

In the spacecraft system, two cw signals, one at 133.9 Mc and the other at 401.7 Mc, are generated from a common crystal-controlled oscillator feeding separate channels of the appropriate multiplying and amplifying stages. These two signals out of the transmitter are fed into a diplexer where they are combined to supply a single common output. The output of the diplexer is connected to the colinear dipole antenna through the coax cable in the extendible antenna boom. The two cw signals are radiated from the antenna with a linear polarization mode.

Before conducting the experiment, the crewmembers must extend the dipole antenna outside the spacecraft. This is accomplished by positioning the antenna control switch to the "extend" position, energizing the boom mechanism, and causing the boom to extend. When the experiment is conducted over either of the two receiving stations, the crewmembers must turn on the transmitter and position the spacecraft to point the antenna toward the center of the earth. This maneuver requires a 158° roll to the right and a 17° nose-down pitch, assuming the spacecraft is in position with the crewmembers sitting up in what might be considered as normal aircraft attitude. The spacecraft yaw must be controlled so that its longitudinal axis is perpendicular to the crbit path, with the nose or small end of the spacecraft away from the ground station. This attitude must be maintained throughout the flight over the ground station from radio horizon to radio horizon. After the spacecraft passes beyond the line of sight of the ground station, the transmitter is turned off and any spacecraft attitude may be maintained or assumed.

A block diagram of the ground receiving stations, which are identical, is shown in figure 7-10, and a composite photograph of the station equipment is shown in figure 7-11. The receiving antenna is a 28-foot parabolic dish with a special cross dipole feed system to separate the signals into their vertical and horizontal components. During any spacecraft flight over a ground receiving station, when the spacecraft is operating for the experiment, this antenna will be slaved from a

nearby tracking radar, so that it points at the spacecraft. As the two cw signals are received from the spacecraft transmission, the antenna feed separates each signal into its vertical and horizontal components. The vertical components of each frequency are fed down a single coax line to a special frequency separating filter. The filter has two outputs, one of which is the vertical component of the 133.9-Mc signal, and the other of which is the vertical component of the 401.7-Mc signal. The horizontal components of the two frequencies are separated in a like manner in an identical filter.

The vertical and horizontal components of the 133.9-Mc signal are fed into the two channels of the 133.9-Mc receiver, and the 401.7-Mc signal components are fed into the 401.7-Mc receiver. In each receiver, common local oscillators are employed to maintain similar phase characteristics between the two channels. After conversion to 120-kc in the 133.9-Mc receiver, the vertical and horizontal signal components are fed into the vertical and horizontal amplifiers of the X-Y scope. In this manner, the Faraday rotation angle is reproduced. For example, if the rotation angle is 45°, both the horizontal and vertical signal components out of the receiver will be equal and a 45°-angle line will be traced on the face of the scope. The 120-kc i.f. signals from the 401.7-Mc receiver are displayed in the same manner on a second X-Y scope. Both scope displays are photographed, at a rate of about 2-1/2 frames per second, along with a clock and the attenuator position indicator lights.

At the same time the 120 kc i.f. signals are displayed on the X-Y scopes, they are also recorded on magnetic tape. In this manner, the tape can be played back later into an X-Y scope and the original display can be examined and re-examined as desired. As with the photographic record, time and rf attenuator settings are simultaneously recorded on the magnetic tape.

The four i.f. signals, two in each receiver, are also detected, and their envelopes are recorded on a four-channel chart recorder. The vertical and horizontal component envelopes of each signal will fluctuate roughly as simultaneous sine and cosine plots. These records can be examined at a later data and information extracted from the short-time fluctuation in the envelopes as to the perturbation in electron content along the spacecraft path. Only time information is recorded directly on the chart recording. The attenuator setting must be entered manually.

Development

Testing.- Both the diplexer and extendible antenna boom were supplied by McDonnell Aircraft Corporation (MAC) and are modifications of equipment used in previous spacecraft. The diplexer is a minor modification of the diplexer used in the Gemini communications system, and the boom mechanism is similar to the high-frequency recovery antenna boom. In view of this, only the dual-frequency transmitter and the colinear dipole antenna will be discussed.

Past experience with solid state circuitry indicates that proper operation over a wide range of temperature environment presents one of the more difficult problems. As a result, all transmitter circuits, power supply regulator, dc-to-dc converter, and rf circuits were subjected to temperature tests at all stages of development. The primary objective was to develop circuits that would give the desired frequency and output power stability with a supply voltage variation of from 20 to 33 volts over a temperature range of -60° F to +160° F without the use of a cold plate. This objective was achieved for the 133.9-Mc output, but could only be achieved over a temperature range of -40° F to +160° F for the 401.7-Mc output.

The major problem in the development of the colinear dipole antenna was to operate at both frequencies with a minimum amount of cross-polarized signal at either frequency. Considerable difficulty was encountered in devising a pattern measurement range that would give a true indication of the direct and cross-polarized signals. In this effort, one-fifth- and one-tenth-scale models were used, and both indoor and outdoor pattern ranges were used. The pattern measurement range, that was finally devised and used for the final measurements, was outdoors, and employed a one-tenth-scale model of the spacecraft and antenna.

The qualification models of both the transmitter and the antenna were subjected to environmental tests by the contractor on temperature, pressure, humidity, acceleration, random vibration, acoustic noise, and radio interference. No problems were encountered during these environmental tests and both the transmitter and antenna were qualified for space operation.

Before the final models of the transmitter were delivered to the contractor, each was subjected to a random vibration test. Each transmitter was also subjected to a modified temperature test, in which a scale time of only 8 hours was used at each of the temperature extremes of -60° F and +160° F, instead of a 24-hour scale period. All transmitter units functioned properly during these predelivery acceptance (PDA) tests.

The antennas were subjected to the modified random vibration tests as described for the transmitters. These tests were made prior to the application of the white radiator paint. Since this paint surface is relatively easy to damage, only a voltage-standing-wave-ratio (VSWR) test was made on the antennas just prior to shipment. No problems were encountered in these PDA tests.

During the preinstallation acceptance tests (PIA), it was observed that the power output from all three transmitters was less than was measured at NRL prior to shipment. It was determined that this power reduction was caused by a difference in the terminating impedance of the 133.9-Mc coax line out of the transmitter during the two measurements. At NRL, the line was fed into a bandpass filter and then into the 50-ohm attenuator for power measurements. The line was terminated in the diplexer and then into the 50-ohm attenuators. In one case, the bandpass filter appeared to be a resistive load, whereas the diplexer appeared to be a reactive load. This was resolved by adjusting the transmitter output networks after the transmitter had been mounted in the spacecraft. After the transmitters were adjusted under these conditions, the proper power outputs were obtained at the proper frequencies.

During the PIA tests of the antenna, it was discovered that the coax cable in the prototype antenna boom had a bad VSWR. As a result, the tests had to be conducted with the antenna mounted on a ground plane instead of on a boom above a ground plane. Similar measurements had been made at NRL, so that the slight changes in VSWR that result from this measurement setup were predicted. As a result, the VSWR measurements were acceptable and no further problems were encountered during PIA.

Technical problems.- Only minor difficulties were encountered with the 133.9-Mc channel of the transmitter during the development program. Very little work was required to get this channel to work over the temperature range of -60° F to +160° F without the use of a cold plate.

In the development program, only one serious problem was encountered in the 401.7-Mc channel. This problem was concerned with the 200- to 400-Mc doubling circuit, which would not operate properly at temperatures below -20° F. Changes in transistor type and circuit configuration gave some improvement, but did not give satisfactory operation. After a cold soak at -60° F, this channel required 3 or 4 minutes of warmup before the proper power output and stable frequency

conditions were obtained. The decision was made to replace the transistor doubler stage with a varactor diode doubler. This modification proved to be the solution to the problem, and satisfactory performance was obtained after the proper alinement technique was evolved. Basically, this technique consisted of a readjustment of capacitive reactance of the circuits to match the varactor impedance to that of the final amplifier, after the unit had stabilized at a -35° F temperature.

The entire development of the colinear dipole antenna presented a problem. Spacecraft space limitations more or less dictated a single antenna for both frequencies and limited the size of the single antenna. These two factors presented considerable difficulties in obtaining: (1) good direct illumination patterns at both frequencies with low cross-polarization patterns and (2) simultaneously obtaining a good 50-ohm match at both frequencies. In general, the solution to the antenna problem was an empirical one. In other words, a unit was designed for both the dipole element length and the impedance matching transformer. This unit was constructed and tested. The design was then modified on the basis of the results obtained from the first model, until a satisfactory unit was obtained.

Measurement of the antenna cross-polarized signal, a measurement not ordinarily of interest, presented difficulties throughout the development program. Variations in these measurements indicated that much of the cross-polarized patterns was contributed from surrounding objects rather than from the antenna. An outdoor measurement range, in which both the spacecraft model with scale antenna and the pattern range antenna were mounted high above the building roof, was found to be satisfactory. In this arrangement, the pattern measurement antenna was mounted as close to the model antenna as possible, yet remaining in the far field.

Quality assurance.- Before the NASA document requiring government-source inspection of all component parts was published or made known to NRL, all component parts had been purchased for the transmitters and antennas. It was considered too costly, and the time schedule was too short, to scrap all these component parts and reorder. However, all parts were of the highest quality and were the type that had been used in other projects requiring space-type environmental operation. In addition, all parts were carefully inspected and tested before being used in any of the equipment. During the construction of the transmitters, regular inspections were made for proper wiring, soldering, and cleaning. At the completion of wiring, as well as just prior to final encapsulation and assembly, the units were again inspected. The antenna was also carefully inspected for mechanical assembly and structure.

Integration

Schedule.- As far as integration of the equipment into the spacecraft is concerned, this experiment is relatively simple; only three pieces, the transmitter, the diplexer, and the antenna, are involved. The transmitter and diplexer only had to be mounted to a cold plate and a bracket, respectively, in the equipment module and the necessary supply and signal cables provided.

The antenna, with its boom assembly, required more care in integration into the spacecraft. The boom assembly had to be alined to provide accurate positioning of the antenna in the extended position. Also, guide blocks were needed to support and guide the upper portion of the antenna when it was folded and retracted into the spacecraft. Some difficulty was encountered in obtaining the proper fit and alinement of the guide blocks. In the process of adjusting these blocks, several upper elements of the antenna were damaged. It was found that, even after proper adjustment of the guide blocks, it was necessary to hand-guide the folded element into the lower set of guide blocks to prevent damage to the antenna. The integration problems encountered in this experiment were simple enough that the spacecraft schedule did not place any constraints on the equipment integration schedule.

Testing.- After the equipment was installed in the spacecraft at the contractor's plant in St. Louis, no further tests were made on the antenna. Just prior to shipment of the spacecraft to Cape Kennedy, half of the work stand was removed, and the antenna boom was extended to its full length. The transmitter power output and frequency were measured prior to shipment of the spacecraft.

During the "Plan X" test on the timber tower at Cape Kennedy, the antenna was extended and signals from the transmitter were radiated. These radiated signals were monitored at the communications hangar, and the frequency and relative signal strength were measured. The spectrum of the transmitter signals was also examined for spurious radiation.

During the Service Engineering Department Reports (SEDR) H460-8 tests on the launch pad, the antenna boom was momentarily energized to extend the antenna a few inches. The boom was then energized to retract the antenna to its fully retracted position. The cable from the diplexer was disconnected, and a power meter was connected to the output of the diplexer, after which the total output power of the transmitter was measured. After the power measurement was completed, an antenna mounted externally to the launch pad "white room" was connected to the output of the diplexer. When the transmitter was turned on, the radiated signals were monitored at the communications hangar; and the frequency, spectrum, and relative signal levels were measured. After the

completion of this test, all cables were reconnected and no further tests were made on the equipment.

Technical problems.- The major problem encountered during integration was the mechanical fit of the antenna in its housing for launch. Guiding the antenna into the housing during retracting was difficult without damaging the small diameter portion of the antenna. This problem was solved by careful adjustment of the guide block.

During "Plan X," some spurious radiation was observed on either side of the cw carrier frequencies. These responses were eliminated by slight readjustment of the circuits in the transmitter.

FLIGHT TEST

Mission as Planned

The procedure necessary to operate the equipment in the spacecraft for this experiment was quite simple and required a minimum of effort on the part of the crewmembers. The operation of the equipment itself involved only the activating of two switches, the "antenna extend" switch and the "transmitter on" switch. The primary effort on the part of the crewmembers was maintaining the attitude of the spacecraft to point the antenna toward the center of the earth. A detail of the operational procedure has been given previously.

The integration of the operational procedures into the flight plan was concerned primarily with the method of controlling the spacecraft attitude. Three modes of spacecraft control were detailed and written into the procedures. The first mode involved the use of the stable platform and the computer; hence, it was the most accurate mode and the one that would be preferred, even though it required the highest power consumption. The next most desirable mode also involved the use of the platform, but not the computer. Pitch and yaw were to be maintained by reference to the 8-ball. The least desirable mode of operation did not involve the use of either the platform or the computer. Attitude would be maintained by use of a reticle mounted on the window and referenced to the horizon.

One other problem in integrating the operational procedure into the flight plan involved the antenna. Since the small diameter end of the antenna is folded and is spring loaded to deploy the first time it is extended, the antenna cannot be fully retracted. When the antenna boom is retracted, after being extended the first time, about 26 inches of the small-diameter portion of the antenna will remain beyond the

surface of the spacecraft. In addition to presenting a possible extravehicular-activity (EVA) hazard under such conditions, the antenna is also subject to being bent during EVA. A bent antenna would destroy the necessary linear polarization, hence negate the experiment. As a result, it was decided not to deploy the antenna until after the EVA was completed.

The only problem encountered in integrating the experiment into the mission plan concerned the number of times the experiment was to be conducted. Since the experiment was statistical in nature, hence, the more data the better, and since no data were obtained from the Gemini VIII mission, a minimum of 10 experiment operations over each of the two ground stations was requested. Because of other mission operations, only four operations over each of the ground stations were scheduled in the final flight plan. This plan called for conducting the experiment during orbits 26, 27, 30, and 42 over the Antigua station and during orbits 30, 32, 33, and 34 over the Kauai station.

Astronaut Training

The crewmembers were given a formal briefing covering the objectives of the experiment and the anticipated procedures and problems. Since the operational procedures for this experiment were quite simple, it was concluded that no special training would be required. Crewmembers were of the opinion that any training to maintain spacecraft attitude would be more than adequately covered by the normal flight simulator training.

Mission as Flown

There were no deviations from the planned operational procedure for the experiment insofar as the operation of the experimental equipment was concerned. However, the experiment operation did not follow the planned mission, because the entire mission was modified following the first rendezvous operation.

Because of the change in mission plan, this experiment was conducted prior to the EVA operation. Six operations of the experiment were made, one over Antigua during orbit 18 and five over Kauai during orbits 17, 18, 19, 20, and 21. Three more operations had been scheduled over the Kauai station during orbits 34, 35, and 36, but the experiment antenna was damaged during EVA.

Flight Equipment Performance

During each of the operations over both ground sites, the received signals were about 30 decibels lower in level than had been planned. Tests indicated that both ground stations were operating about normal. Therefore, it must be concluded that some of the equipment in the spacecraft was not operating normally. Since there was no telemetry and all equipment was mounted in adapter sections which were not recovered, there is no way to establish where the malfunction occurred.

Although the signals were about 30 decibels below expected levels, the experiment was designed to produce signals about 50 decibels above noise, so that usable results were obtained. The main effect of the lower signals was to reduce the accuracy of the end results.

During the EVA operation, the pilot drifted into the antenna, and it broke off instead of bending. The reason for the breakage of the 1/4-inch diameter aluminum tube is not understood. This member of the antenna was constructed of 6061T6 aluminum alloy which is one of the most ductile aluminum alloys and should have bent and not fractured.

Results

Because the spacecraft azimuth, elevation, and altitude, as viewed from Antigua and Kauai for those transits in which the D-14 experiment was conducted, have not been received as of this writing, a fine-scale analysis could not be initiated. However, the ambiguity removal and lower ionospheric slab thickness determinations for five of the Kauai transits has been accomplished through use of five-point plots of local azimuth and elevation, which were made available prior to each transit. The Antigua five-point plot (for revolution number 18) was not available. Consequently, only the Kauai transits corresponding to revolutions 17, 18, 19, 20, and 21 of the Gemini IX spacecraft are discussed in this report.

The first step was to determine if the direction and magnitude of the observed Faraday fading were compatible with that which would be predicted on the basis of the simple theory. Assuming that the subsatellite electron content is an invariant, the magnetic field parameter functions are in direct proportion to their respective Faraday rotation functions. Since without exception, the VHF records indicate that $\bar{\Psi}$ is roughly proportional to Ω_{VHF}, it was concluded that Ω_{VHF} is indeed controlled by changes in $\bar{\Psi}$ rather than changes in electron content C.

The subsatellite electron content may be written as

$$C = 1.24 \times 10^{13} foF2^{2} t \qquad (1)$$

where foF2 is the F2 peak plasma frequency in megacycles per second (Mc/sec) and t is the effective subsatellite slab thickness in kilometers. The largest plausible value for the amount of UHF rotation may be estimated by means of equation (1) and the relation

$$\Omega_{UHF} = 2.97 \times 10^{-2} f_{UHF}^{-2} \bar{\Psi} C \qquad (2)$$

and upper limits for the parameters t, $\bar{\Psi}$, and foF2. Table 7-I is a listing of foF2 and M(3000)F2 for June 4, 1966, over Maui, Hawaii. By inspection, the maximum value for foF2 is 14 Mc/sec. Since the Gemini IX satellite orbits at the nominal altitude of the F2 maximum (based upon Shimazaki's approximation, hF2 = [1490/M(3000)F2] - 176), it may be shown that it is certainly less than 200 kilometers for a subsatellite Chapman profile of electron density. Taking $\bar{\Psi}$ = 25 ampere turns per meter, it follows that the estimated upper limit for Ω_{UHF} is less than 180° for those points at which $\bar{\Psi}$ is less than or equal to 25 ampere turns per meter. In fact, four of the transits of Gemini IX, which occurred on June 4 over Kauai, passed through the quasi-transverse region where $\bar{\Psi}$ is similar to 0 and the remaining transit was such that the minimum value of $\bar{\Psi}$ was, at most, 15 ampere turns per meter. Clearly Ω_{UHF} was resolvable. As a consequence, estimates of the VHF Faraday rotation were conveniently obtained from the equation

$$\Omega_{VHF} = 9\Omega_{UHF} \qquad (3)$$

which follows from the fact that the amount of Faraday rotation is inversely proportional to the square of the radio frequency. This relation is strictly applicable for only the quasi-longitudinal mode of propagation and when the VHF and UHF radiowaves traverse identical paths. However, for the purpose of ambiguity removal, the simple relationship expressed by equation (3) is roughly true. For all spacecraft transits

over Kauai, values of $9\Omega_{UHF}$ were computed and compared with the measured values of Ω_{VHF}. Aside from an expected UHF data point scatter, the agreement was sufficient. The scatter of points corresponding to the UHF data arises from the fact that the naturally larger reading errors associated with the UHF polarization have been magnified nine times.

For the purpose of determining the mean subsatellite ionospheric slab thickness, values of Ω_{VHF} and $\bar{\Psi}$ at the closest point of approach were determined and are listed in table 7-II.

Values of the subsatellite electron content and the effective slab thickness for those transits in which the closest point of approach did not coincide with the region of quasi-transverse propagation were computed by means of the following equations:

$$C = 1.04 \times 10^{16}\left(\frac{\Omega^{\circ}_{VHF}}{\bar{\Psi}}\right) \tag{4}$$

$$t = \frac{C}{1.24 \times 10^{13} foF2^2} \tag{5}$$

where C is in electrons per square meter column and t is in kilometers. The values of content and slab thickness for transits 18, 19, and 21 are listed in table 7-III. Although the content is increasing with time, it is apparent that the content is not strictly proportional to the square of foF2, since the slab thickness decreases at 1300 H.s.t.

CONCLUSIONS

Since the tracking information was not available, the primary objective of the experiment could not be reached. There is, however, no fundamental problem in reaching the objective once the pertinent data are received.

The use of the UHF radio transmission was the primary factor in the successful removal of VHF Faraday rotation ambiguity but, as expected, was not very useful for the purpose of fine-scale polarization studies.

A Faraday rotation study utilizing a frequency in the neighborhood of 133 Mc/sec is not sufficiently accurate within about 10° of the transverse propagation mode, since the total amount of rotation in that region is small and the relative error is inversely proportional to the total rotation. Four of the analyzed transits exhibit a quasi-transverse condition, but it is not persistent for any transit.

Ionosonde data from nearby Maui, Hawaii, were useful in computing the slab thickness at the closest point of approach of the spacecraft. At 0814 H.s.t., the slab thickness was 67 kilometers and the content was $3.12 \times 10^{16} m^{-2}$. At 1301 H.s.t., the slab thickness had decreased to 49 kilometers and the total content had increased to $7.87 \times 10^{16} m^{-2}$.

SYMBOLS

C	electron content per square meter
F2	region in which the maximum electron density in the ionosphere is typically observed, having nominal altitude of 300 km
f	radio frequency, cycles/sec
foF2	critical frequency corresponding to maximum F2, Mc/sec
H	total magnetic field intensity, ampere turns per minute
h	altitude, meters
M	an unknown number of revolutions
M(3000)F2	parameter which represents ratio of the critical frequency for a skip distance of 3000 km to the critical frequency for zero skip distance (foF2)
N	electron density, electrons per cubic meter
S	distance from ground antenna to spacecraft, meters
s	distance along ray path, meters
t	effective subsatellite slab thickness, km
θ	angle between ray path and magnetic field vector
$\overline{\Psi}$	average ampere turns per minute
Ω	rotation angle, radians
$\Omega_{VHF}{}^{\circ}$	rotation angle of VHF signal, degrees

TABLE 7-I.- IONOSPHERIC SOUNDING DATA OVER MAUI, HAWAII, JUNE 4, 1966[a]

Hour	foF2	M(3000)F2	Hour	foF2	M(3000)F2
0	7.5	2.90	12	10.5	2.70
1	7.8	3.20	13	11.4	2.80
2	7.0	3.20	14	11.9	2.85
3	6.2	3.30	15	12.2	2.90
4	4.5	3.70	16	12.9	2.90
5	3.2	3.00	17	12.7	3.05
6	4.3	3.40	18	14.0	3.25
7	5.6	3.15	19	13.7	3.35
8	6.1	2.45	20	10.0	3.20
9	7.6	2.50	21	8.4	3.10
10	8.9	2.60	22	7.1	2.95
11	9.8	2.70	23	7.8	2.80

[a]Courtesy of Institute for Telecommunication Sciences and Aeronomy, Environmental Science Services Administration.

TABLE 7-II.- VALUES OF Ω_{VHF} and $\bar{\Psi}$ AT CPA[a]

Transit	Ω_{VHF}, deg	$\bar{\Psi}$[b], Ampere turns/meter	Closest value of foF2, Mc/sec	Time of CPA, hr:min:sec H.s.t.
17	+5	-4	5.6	06:38:44
18	-60	-20	6.1	08:14:26
19	-175	-25	8.9	09:50:19
20	-30	-3	9.8	11:26:07
21	+341	+45	11.4	13:01:38

[a]Closest point of approach.

[b]Approximate value of $\bar{\Psi}$ based upon an ionospheric mean of 250 km.

TABLE 7-III.- CONTENT AND SLAB THICKNESS FOR TRANSITS 18, 19, AND 21

Transit	c/m^2	t, km
18	3.12×10^{16}	67
19	7.28	74
21	7.87	49

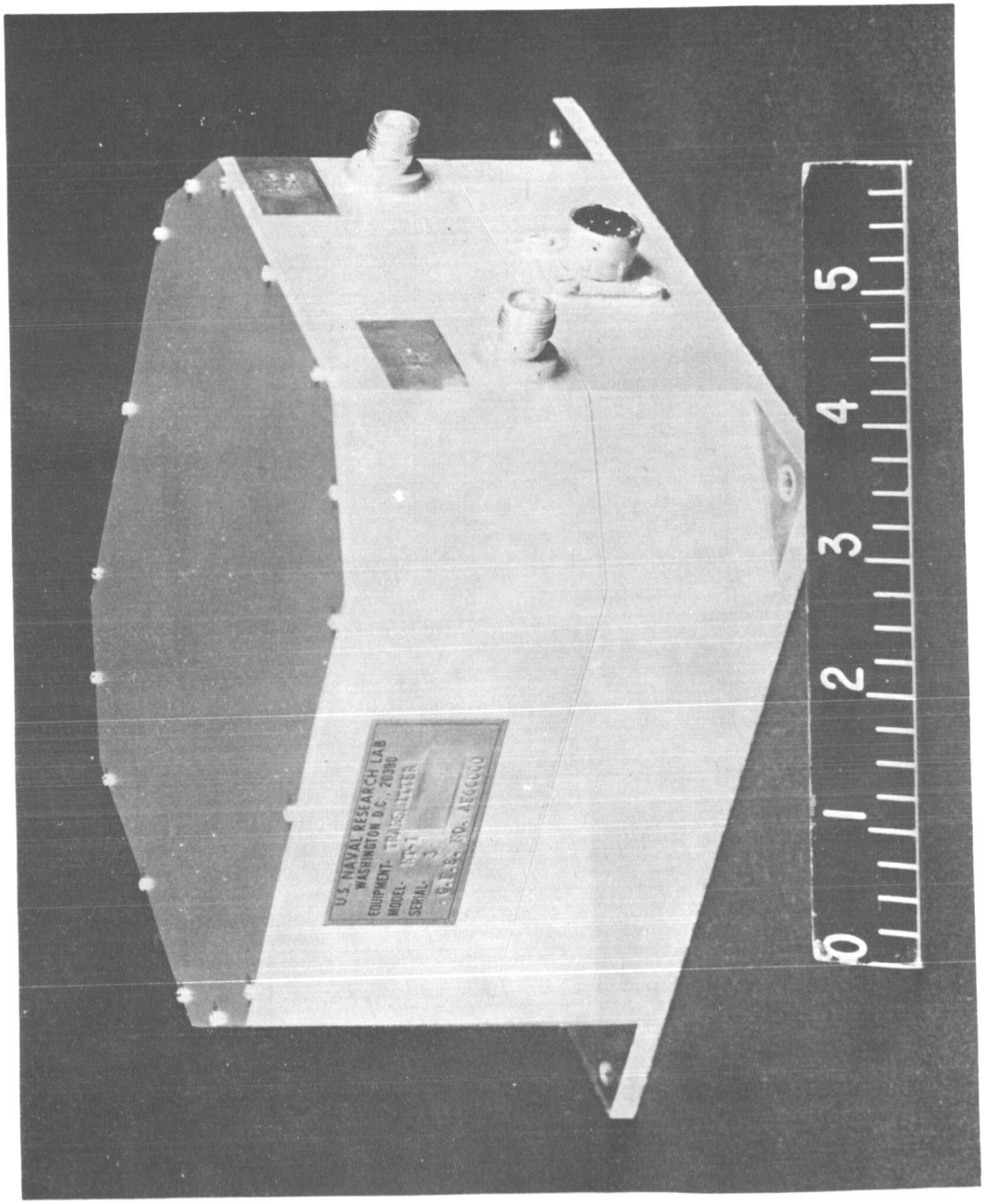

Figure 7-1.- Transmitter assembly.

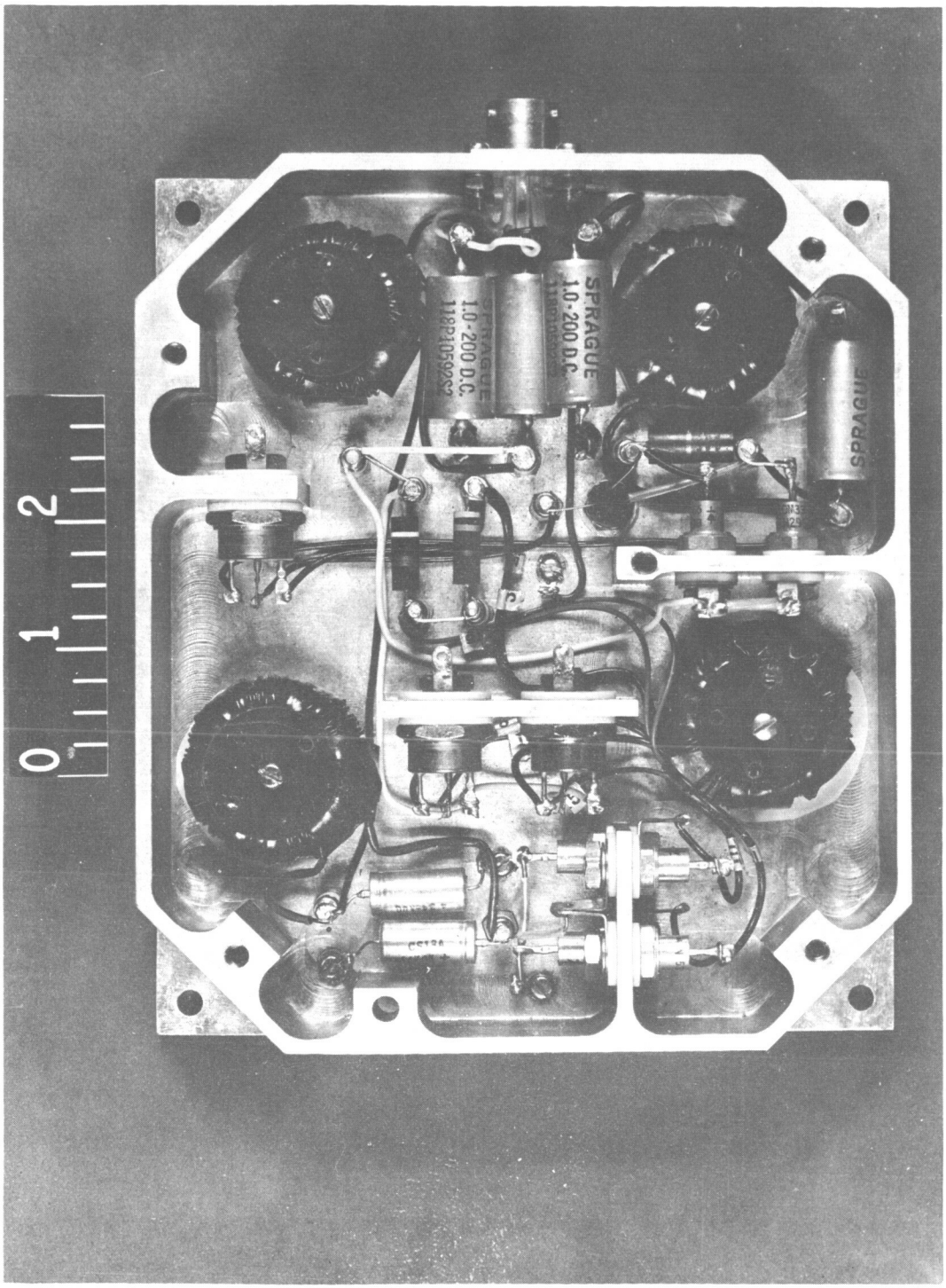

Figure 7-2.- Transmitter power supply unit.

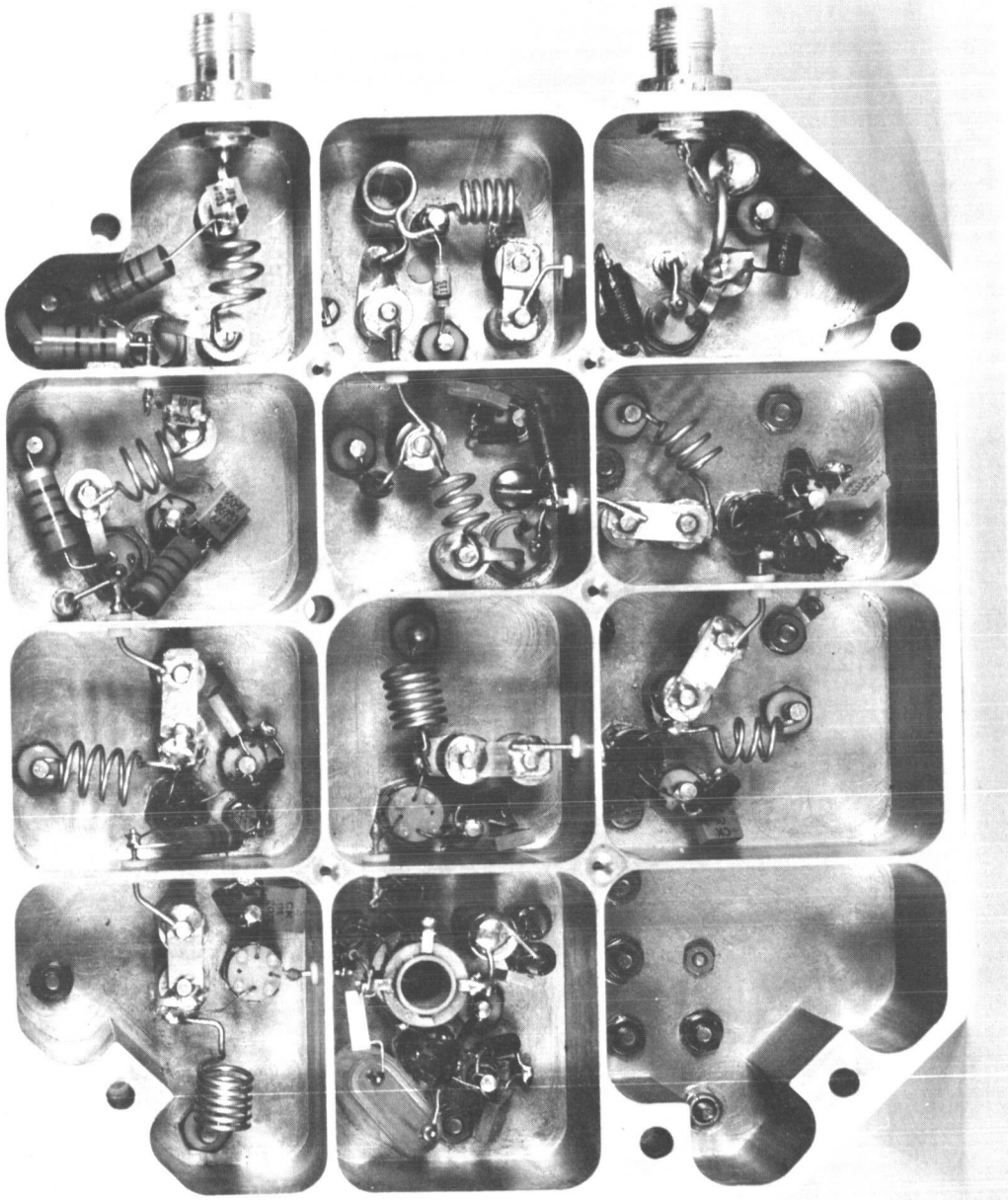

Figure 7-3.- Transmitter radio-frequency unit.

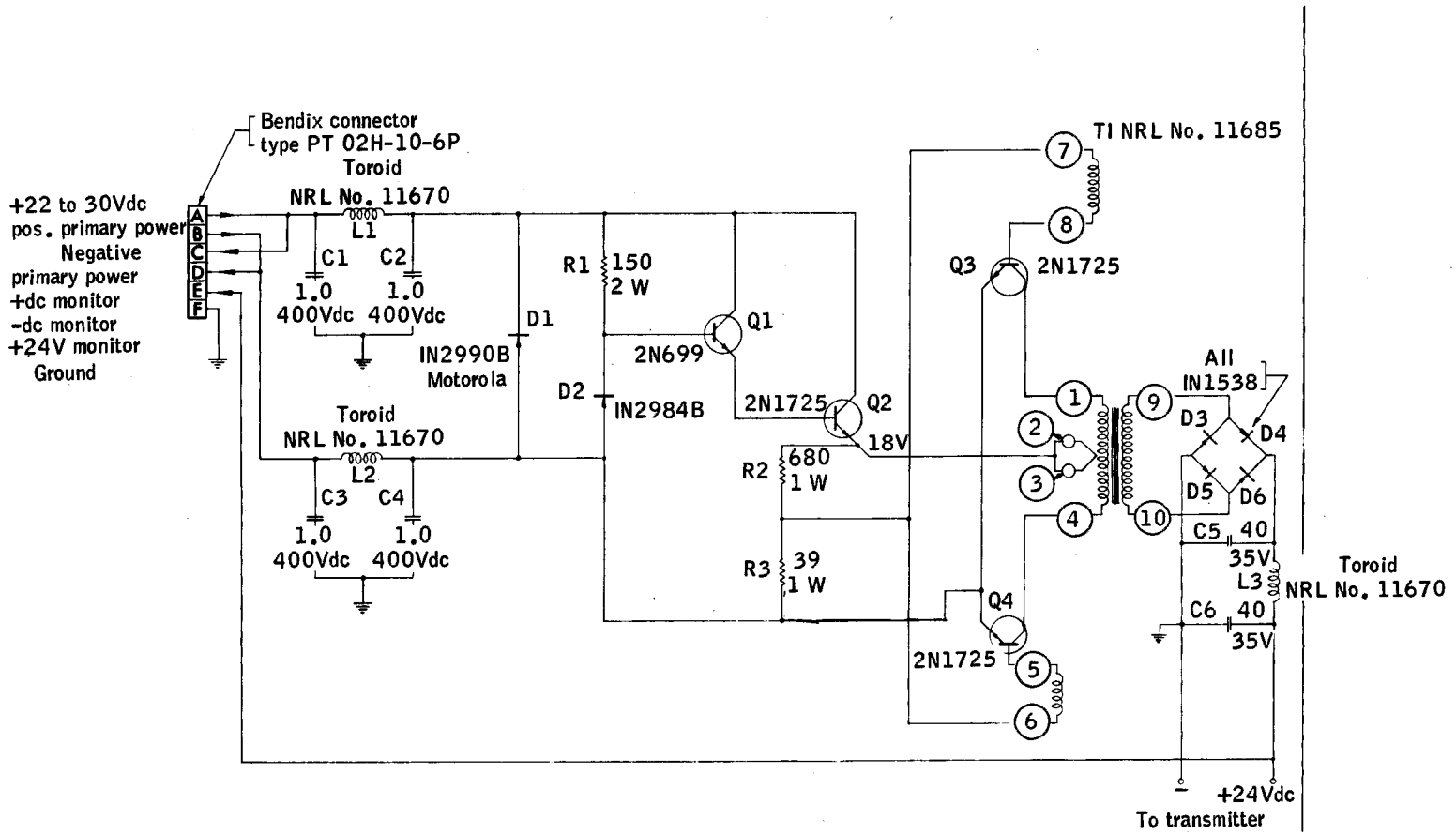

Note:
Capacitors in microfarads
Resistors in ohms

Figure 7-4.- Circuit diagram of power supply unit.

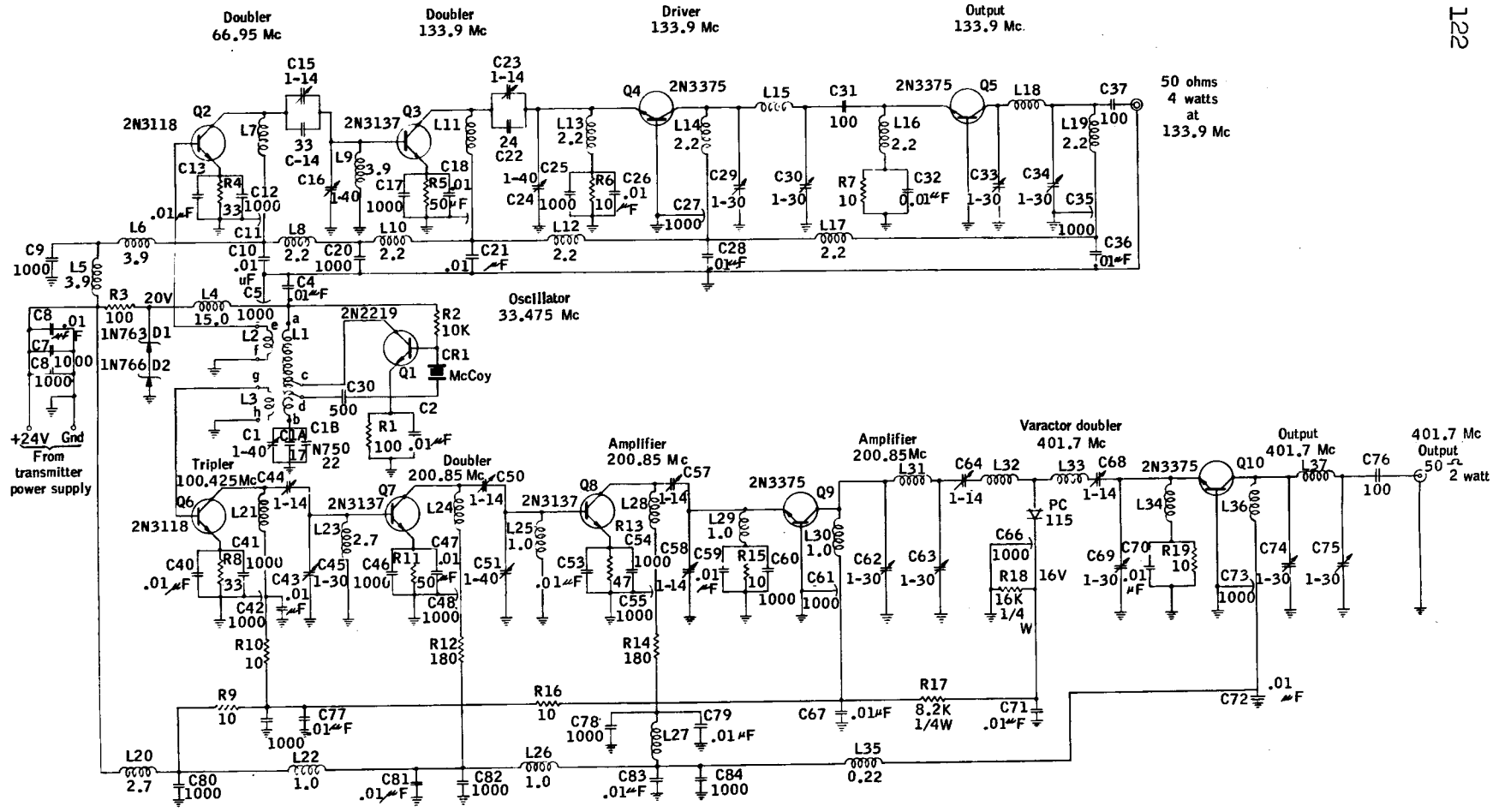

NOTE:
Capacitors in micro-microfarads, inductors in microhenries, resistors in ohms unless otherwise noted.

Figure 7-5.- Circuit diagram of radio frequency unit.

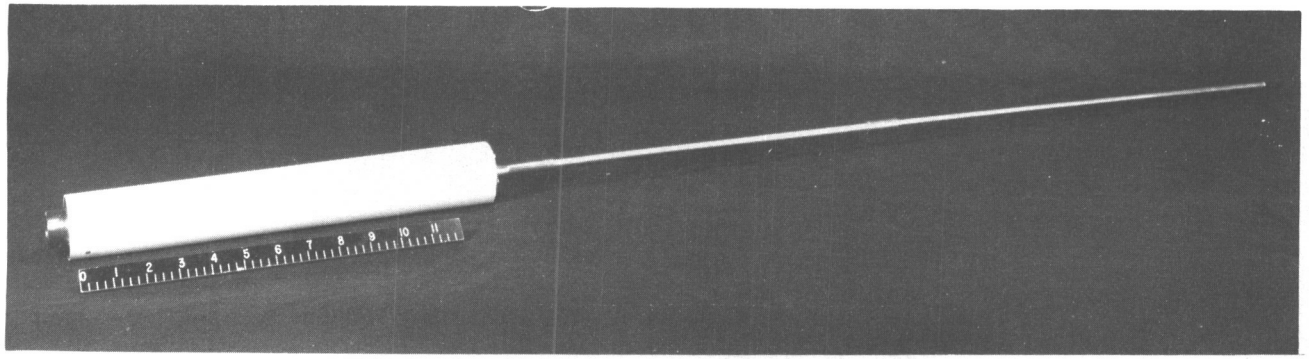

Figure 7-6.- Antenna, erected position.

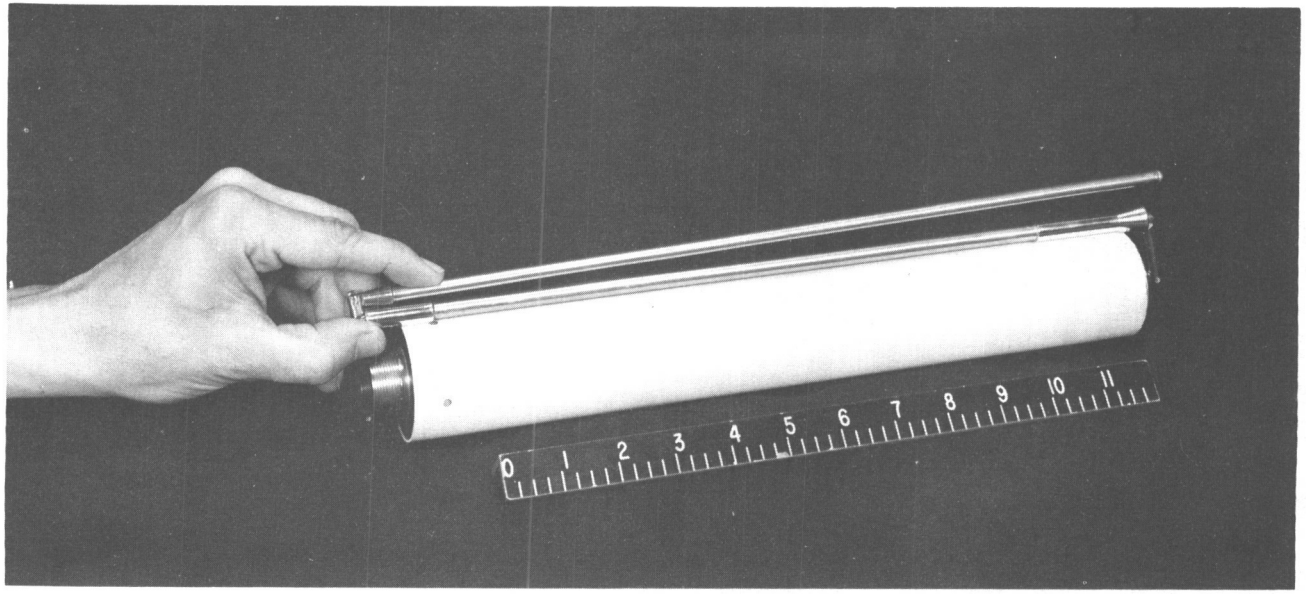

Figure 7-7.- Antenna, folded position.

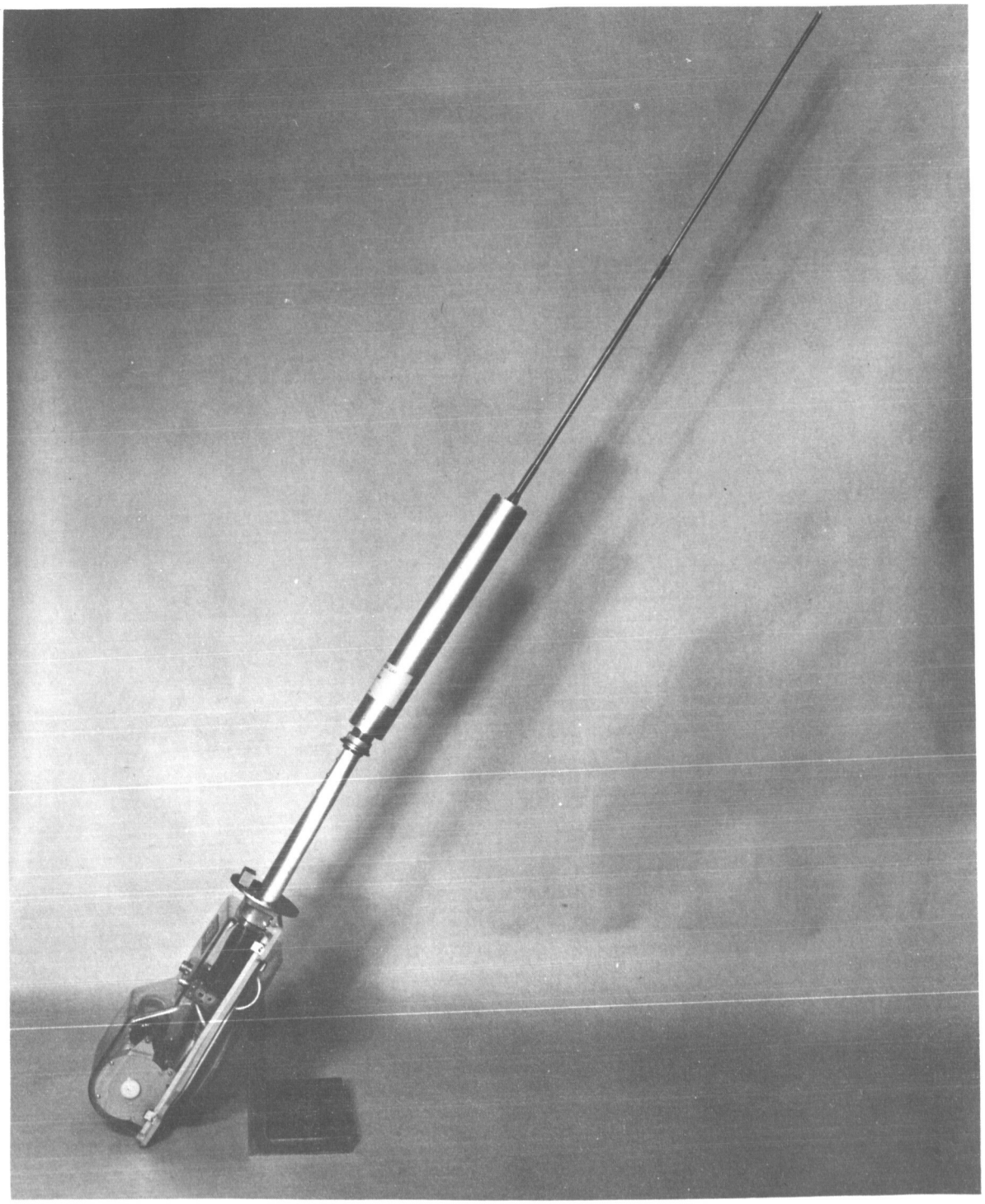

Figure 7-8.- Antenna boom assembly with antenna.

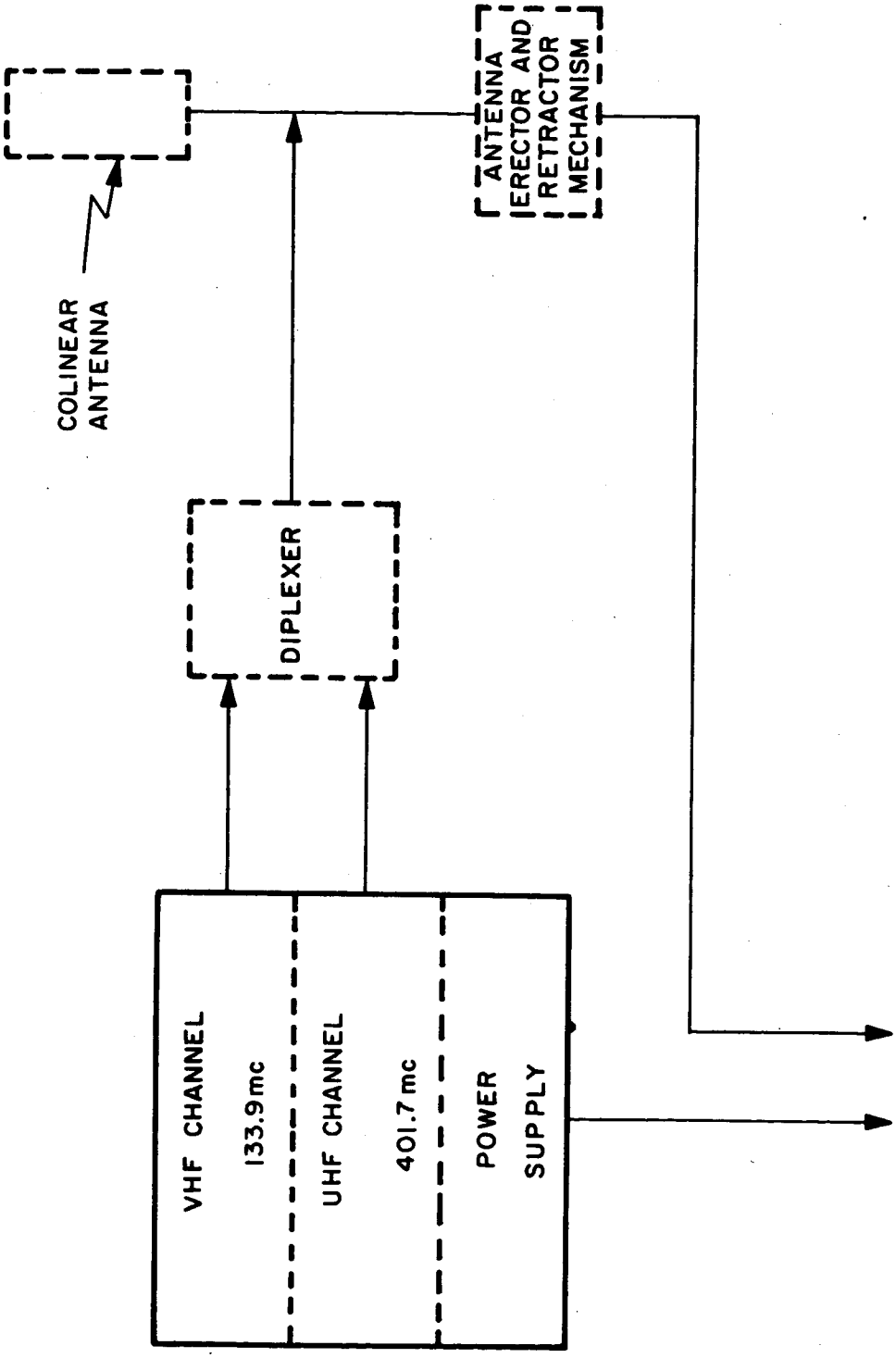

Figure 7-9.- Block diagram of transmitter system.

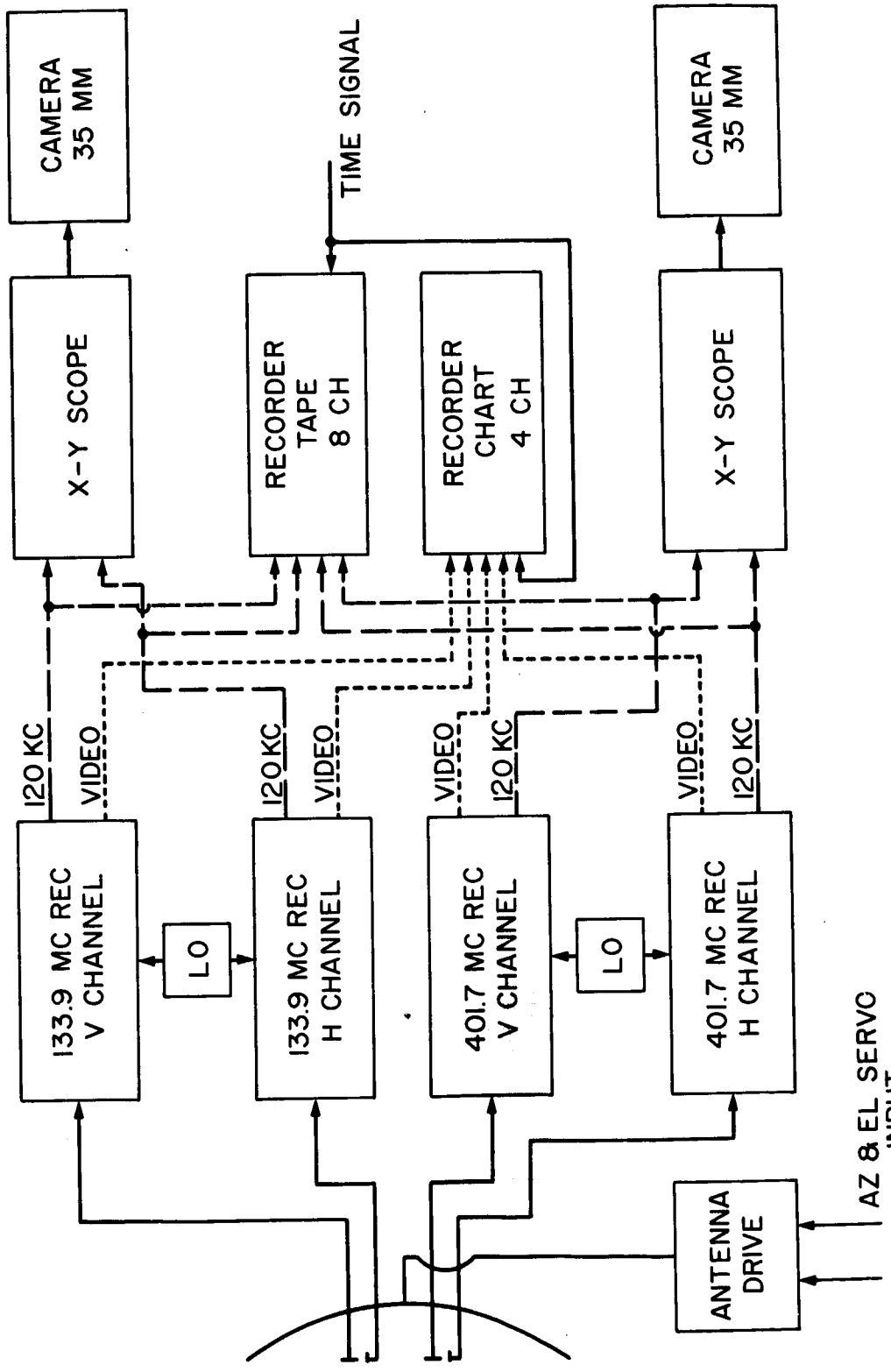

Figure 7-10. - Block diagram of receiving system.

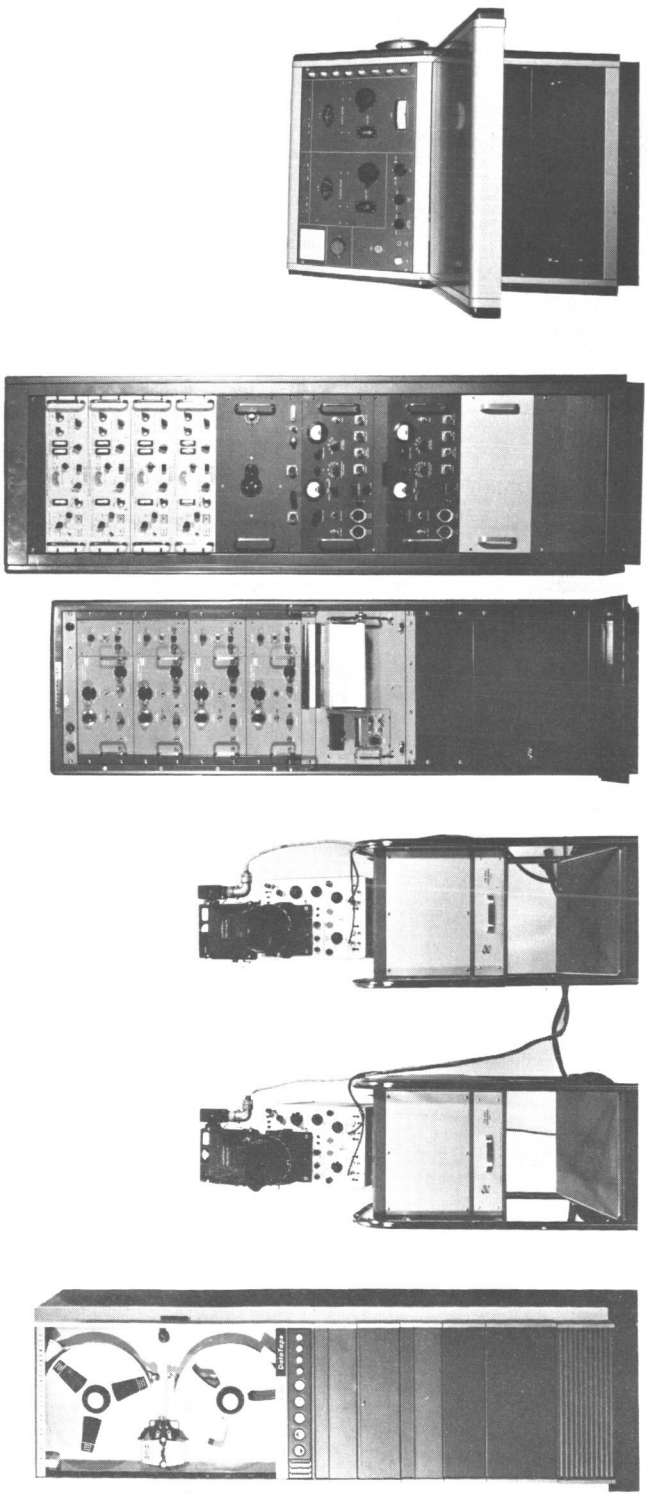

Figure 7-11.- Ground receiving equipment.